

**GENERALIZED FILTERING CONFIGURATIONS WITH
APPLICATIONS IN DIGITAL AND OPTICAL SIGNAL AND
IMAGE PROCESSING**

**A DISSERTATION
SUBMITTED TO THE DEPARTMENT OF ELECTRICAL AND ELECTRONICS
ENGINEERING
AND THE INSTITUTE OF ENGINEERING AND SCIENCE
OF BILKENT UNIVERSITY,
IN PARTIAL FULFILLMENT OF THE REQUIREMENTS
FOR THE DEGREE OF
DOCTOR OF PHILOSOPHY.**

**By
Mehmet Aiper Kutay
February 24, 1999**

THESIS
**QA
404
-K88
1999**

GENERALIZED FILTERING CONFIGURATIONS WITH
APPLICATIONS IN DIGITAL AND OPTICAL SIGNAL AND
IMAGE PROCESSING

A DISSERTATION

SUBMITTED TO THE DEPARTMENT OF ELECTRICAL AND ELECTRONICS
ENGINEERING

AND THE INSTITUTE OF ENGINEERING AND SCIENCES
OF BILKENT UNIVERSITY

IN PARTIAL FULFILLMENT OF THE REQUIREMENTS
FOR THE DEGREE OF
DOCTOR OF PHILOSOPHY

By

Mehmet Alper Kutay

February 24, 1999

WH

404

.K88

1999

E 046842

I certify that I have read this thesis and that in my opinion it is fully adequate, in scope and in quality, as a thesis for the degree of Doctor of Philosophy.


Haldun M. Özaktaş, Ph.D. (Supervisor)

I certify that I have read this thesis and that in my opinion it is fully adequate, in scope and in quality, as a thesis for the degree of Doctor of Philosophy.


Enis Çetin, Ph.D.

I certify that I have read this thesis and that in my opinion it is fully adequate, in scope and in quality, as a thesis for the degree of Doctor of Philosophy.

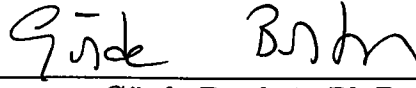

Orhan Arıkan, Ph.D.

I certify that I have read this thesis and that in my opinion it is fully adequate, in scope and in quality, as a thesis for the degree of Doctor of Philosophy.



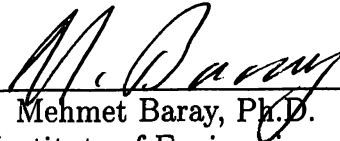
Mefharet Kocatepe, Ph.D.

I certify that I have read this thesis and that in my opinion it is fully adequate, in scope and in quality, as a thesis for the degree of Doctor of Philosophy.



Güzde Bozdağı, Ph.D.

Approved for the Institute of Engineering and Sciences:



Mehmet Baray, Ph.D.

Director of Institute of Engineering and Sciences

ABSTRACT

GENERALIZED FILTERING CONFIGURATIONS WITH APPLICATIONS IN DIGITAL AND OPTICAL SIGNAL AND IMAGE PROCESSING

Mehmet Alper Kutay

Ph. D. in Electrical and Electronics Engineering

Supervisor: Dr. Haldun M. Özaktas

February 24, 1999

In this thesis, we first give a brief summary of the fractional Fourier transform which is the generalization of the ordinary Fourier transform, discuss its importance in optical and digital signal processing and its relation to time-frequency representations. We then introduce the concept of filtering circuits in fractional Fourier domains. This concept unifies the multi-stage (repeated) and multi-channel (parallel) filtering configurations which are in turn generalizations of single domain filtering in fractional Fourier domains. We show that these filtering configurations allow a cost-accuracy trade-off by adjusting the number of stages or channels. We then consider the application of these configurations to three important problems, namely system synthesis, signal synthesis, and signal recovery, in optical and digital signal processing. In the system and signal synthesis problems, we try to synthesize a desired system characterized by its kernel, or a desired signal characterized by its second order statistics by using fractional Fourier domain filtering circuits. In the signal recovery problem, we try to recover or estimate a desired signal from its degraded version. In all of the examples we give, significant improvements in performance are obtained with respect to single domain filtering methods with only modest increases in optical or digital implementation costs. Similarly, when the proposed method is compared with the direct implementation of general linear systems, we see that significant computational savings are obtained with acceptable decreases in performance.

Keywords: Fractional Fourier transforms, optical signal processing, signal and system synthesis, signal recovery, time- or space-varying filtering

ÖZET

GENELLENMİŞ SÜZGEÇLEME KONFIGURASYONLARI VE BUNLARIN SAYISAL VE OPTİKSEL İŞARET VE GÖRÜNTÜ İŞLEMEDEKİ UYGULAMALARI

Mehmet Alper Kutay
Elektrik ve Elektronik Mühendisliği Doktora
Tez Yöneticisi: Dr. Haldun M. Özaktaş
24 Şubat 1999

Bu tezde ilk olarak bilinen Fourier dönüşümünün bir genellemesi olan kesirli Fourier dönüşümünün kısa bir özeti verildi ve bu dönüşümün optiksel ve sayısal işaret işlemedeki önemi ve zaman-frekans gösterimleri ile olan bağlantısı üzerinde duruldu. Daha sonra kesirli Fourier domenlerinde süzgeçleme devreleri kavramı ortaya konuldu. Bu kavram tek aşamalı süzgeçleme yönteminin genellemesi olan çokaşamalı ve çokkanallı süzgeçleme konfigürasyonlarını bir çatı altında birleştirmekte ve herhangi bir uygulamada doğruluk maliyet değiş-tokuşu yapma olanağı sağlamaktadır. Bu süzgeçleme devre konfigürasyonlarının optiksel ve sayısal işaret işlemedeki çok önemli üç problem olan sistem sentezi, işaret sentezi ve işaret iyileştirmedeki uygulamaları üzerinde duruldu. Sistem ve işaret sentezi uygulamalarında çekirdek fonksiyonu ile tanımlanan istenen bir sistem, veya ikinci-derece istatistiksel özellikleri ile tasvir edilen istenen bir işaret kesirli Fourier domeni süzgeçleme devresi kullanılarak sentezlenmeye çalışılmıştır. İşaret elde edimi veya iyileştirilmesi uygulamasında ise bozulmuş istenen bir işaret iyileştirilmeye veya kestirilmeye çalışılmıştır. Bütün bu örneklerde, süzgeçleme devresi metodumuz tek bir bölgecikte uygulanan filtreleme metodları ile karşılaştırıldığında, optik veya nümerik uygulama konusundaki masrafları fazla artırmadan sistem performansının çok daha fazla geliştirilebileceği gösterilmiştir. Benzer olarak, önerdiğimiz metod genel doğrusal sistemler ile karşılaştırıldığında, yeterli olabilecek sistem performanslarının çok daha düşük masraf karşılığı bizim metodumuzla elde edilebileceği anlaşılmıştır.

Anahtar Kelimeler: Kesirli Fourier dönüşümü, optiksel işaret işleme, işaret ve sistem sentezi, işaret iyileştirilmesi, zaman veya mekan ile değişen süzgeçleme

ACKNOWLEDGMENTS

Many people have contributed to the development of this thesis. But above all, I would like to express my deepest gratitude to Dr. Haldun M. Özaktaş for his supervision, constructive suggestions, and encouragement throughout the development of this work. It is also my pleasure to thank our research group members Dr. Fatih Erden, Ayşegül Şahin, Çağatay Candan and Özgür Güteryüz for their valuable input and many useful discussions.

Special thanks should go to Dr. Orhan Arıkan for many useful suggestions and discussions throughout Ph.D. study.

I would like to thank Dr. Enis Çetin, Dr. Mefharet Kocatepe, and Dr. Gözde Bozdağı for reading the manuscript and commenting on the thesis.

The graduate students at the EE department provided me great support. I would also like to thank all of my friends for their suggestions and encouragement.

Finally, I want to express my sincere thanks to my dearest Bahar for her love, generosity and patience, and also to our families for their encouragement, help, and support.

Contents

1	Introduction	1
2	The Fractional Fourier Transform	5
2.1	Introduction and History	5
2.2	Definition and Properties	7
2.2.1	Eigenvalues and Spectral Expansion	10
2.2.2	Operational properties	12
2.2.3	Relation to the Wigner distribution	12
2.2.4	Fractional Fourier Domains	15
2.3	Optical And Digital Implementation	16
2.4	Discrete Fractional Fourier Transform	18
2.5	Generalization to Two-Dimensional Systems	19
2.5.1	Separable Two-Dimensional Fractional Fourier Transformation . .	19
2.5.2	Non-separable Two-Dimensional Fractional Fourier Transformation	20
3	Generalized Filtering Configurations Based on Fractional Fourier Transforms	22
3.1	Single-stage Filtering in Fractional Fourier Domains	23

3.2	Multi-Stage Filtering in Fractional Fourier Domains	27
3.3	Multi-Channel Filtering in Fractional Fourier Domains	29
3.4	Filtering Circuits	31
3.5	Discrete Formulation	32
3.5.1	Extension to the Rectangular Case	34
3.5.2	Complexity Analysis	35
3.6	Discussion	38
4	Applications in System Synthesis	43
4.1	General Linear System Synthesis	46
4.1.1	Solution of the System Synthesis Problem	50
4.1.2	Extensions	53
4.2	Examples	54
5	Applications in Signal Synthesis	58
5.1	Signal Synthesis	58
5.2	Examples	66
6	Applications in Signal Recovery	73
6.1	Signal Recovery and Restoration	73
6.2	Examples	82
7	Conclusions and Future Work	89
	Vita	101

List of Figures

1.1	Filtering configurations	2
2.1	Oblique integral projections of the Wigner distribution.	15
3.1	Filtering in a transform domain	24
3.2	Filtering in a fractional Fourier domain	26
3.3	Filtering in multiple fractional Fourier domains	28
3.4	Multi-stage filtering in fractional Fourier domains	28
3.5	Multi-channel filtering in fractional Fourier domains	30
3.6	Fractional Fourier domain filtering circuit.	31
3.7	Cost comparison of exact and approximate implementations of linear systems.	37
3.8	Cost-accuracy trade-off.	39
3.9	Short-time fractional Fourier filter	42
4.1	Reverse perfect shuffle interconnection architecture. (After [13])	56
5.1	Mutual intensity synthesis problem	60
5.2	The expansion coefficients in GSM beam and corresponding mutual intensity function	68
5.3	Synthesized mutual intensity functions	69

5.4	Normalized error versus number of filters	70
5.5	The expansion coefficients of the desired GSM beam and corresponding mutual intensity function	71
5.6	The expansion coefficients of the given and desired GSM beams	71
5.7	The mutual intensity functions of the desired and synthesized GSM beams	72
6.1	Observation model for the degraded signal	74
6.2	Pre-compensation filter configuration.	75
6.3	Post-compensation filter configuration.	75
6.4	Image restoration with pre-compensation filter configuration	83
6.5	Image restoration with post-compensation filter configuration	84
6.6	Normalized error versus number of filters	85
6.7	The filtering circuit used in image restoration	85
6.8	Restoration of a signal corrupted by additive chirp noise	86
6.9	Denoising example	87
6.10	Wigner distribution of a signal with quadratic instantaneous frequency .	88
6.11	Denoising of a signal with quadratic instantaneous frequency	88

Chapter 1

Introduction

In many applications in signal processing and optical information processing, it is desired to implement linear systems. Linear systems are easy to handle and can describe many phenomenon in real life to a good approximation. A general linear system is characterized by the relation,

$$g(u) = \int H(u, u')f(u') du', \quad (1.1)$$

where $H(u, u')$ is called the kernel of the system. Equation 1.1 can be discretized as

$$g_k = \sum_{n=0}^{N-1} H_{kn}f_n. \quad (1.2)$$

The last equation, which is simply a matrix-vector multiplication, may either represent a system which is inherently discrete or may constitute an approximation of its continuous version. Digital implementation of such general linear systems takes $O(N^2)$ time. Common single-stage optical implementations, such as optical matrix-vector multiplier architectures or multi-facet architectures [1, 2] require an optical system whose space-bandwidth product is $O(N^2)$.

A widely known sub-class of general linear systems is linear shift-invariant or convolution type systems which are characterized by kernels of the special form $H(u, u') = h(u - u')$ or $H_{kn} = h_{k-n}$. Ordinary Fourier transformation is a very important operator in the analysis of such systems because these systems correspond to multiplication with a filter function in the Fourier domain. Their digital implementation takes $O(N \log N)$ time (by using the FFT algorithm) and their optical implementation

requires an optical system whose space-bandwidth product is $O(N)$. This efficiency in the implementation of such systems leads them to play an important role in digital signal processing and optical information processing. In most of the signal restoration (deblurring, denoising), reconstruction and enhancement problems the operators involved are approximated by shift-invariant systems [3, 4, 5]. These approximations are sometimes justified and the use of convolution type systems is fully adequate. However in other cases, their use is either totally inappropriate or at best a crude approximation which is employed only because of their significantly lower digital or optical implementation cost. This is not surprising given the fact that shift-invariant systems are a much more restrictive class than general linear systems, which is evident upon noting that general linear systems have N^2 degrees of freedom whereas shift-invariant systems have only N .

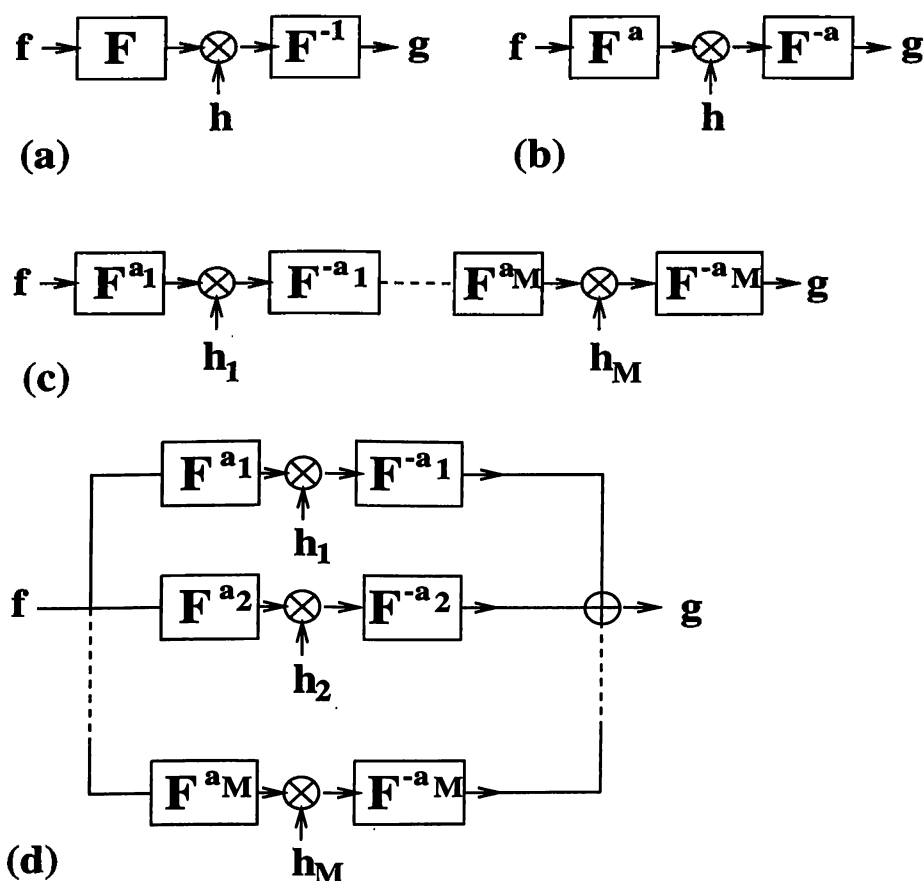


Figure 1.1: Single-stage filtering in the Fourier domain (a), and the a th order fractional Fourier domain (b). Repeated (multi-stage or series) filtering in fractional Fourier domains (c). Multi-channel (parallel) filtering in fractional Fourier domains (d).

We may think of shift-invariant systems and general linear systems as representing two extremes in a cost-accuracy tradeoff: the general systems have $O(N^2)$ degrees of freedom and can be implemented with $O(N^2)$ cost and, shift-invariant systems have $O(N)$ degrees of freedom and can be implemented with $O(N \log N)$ cost. Sometimes use of shift-invariant systems may be inadequate, but at the same time use of general linear systems may be overkill and prohibitively costly. In such situations where both extremes are unacceptable, or simply when we desire greater flexibility in trading off between cost and accuracy, it would be desirable to be able to interpolate between these two extremes. There may be many ways of achieving this. One such way is the use of filtering in fractional Fourier domains [6]. Common single-stage Fourier-domain filtering is shown in Fig. 1.1 (a). Fig. 1.1 (b) depicts single-stage filtering in the α th order fractional Fourier domain. In this configuration the Fourier transform blocks in Fig. 1.1 (a) are simply replaced by the fractional Fourier transform blocks. It has been shown that in some cases this configuration enables significant improvements. More detailed discussion with applications are given in [7, 8, 9, 10, 11, 12]. A generalization of the single-stage fractional Fourier domain filtering is the repeated or multi-stage filtering in fractional Fourier domains and this configuration is shown in Fig. 1.1 (c). In this configuration M single stage fractional Fourier domain filters (Fig. 1.1 (b)) are combined in series so that the output of this configuration is obtained by applying M single fractional Fourier domain filters consecutively to the input. The input is first transformed into the a_1 th domain where it is multiplied by a filter $h_1(u)$. The result is then transformed back into the original domain. This process is repeated M times. This configuration was first proposed in [6] and explored in detail in [13, 14, 15, 16]. A dual configuration is the multi-channel filtering in fractional Fourier domains which is shown in Fig. 1.1 (d). This configuration was first suggested by Orhan Arıkan. In this thesis, the multi-channel filtering configuration will be discussed in detail and a further generalization, filtering circuits in fractional Fourier domains will be introduced. Applications of these filtering circuits in digital signal and optical information processing will be given.

The fractional Fourier transform is the generalization of the ordinary Fourier transform. Given this, every property and application of the common Fourier transform becomes a special case of that of the fractional transform. A comprehensive discussion with some properties and its relation to well-known physical, optical and signal processing concepts are summarized in a chapter [17] and in more detail in a forthcoming book [18].

Overview

We here summarize what is achieved in this thesis. One of the most important property of the fractional Fourier transform is its relation to the Wigner distribution and ambiguity function. We have shown that this property generalizes to certain other time-frequency distributions belonging to the so-called Cohen class [19].

In order to successfully apply the transform to digital signal processing applications, we need to calculate the transform digitally. We have developed an efficient algorithm ($O(N \log N)$) for the computation of the fractional Fourier transform [20]. This algorithm also leads to a definition for the discrete fractional Fourier transform. However, this definition does not satisfy exactly some of the essential properties of the discrete transform. Thus we have proposed a discrete fractional definition by finding the a th power of the discrete Fourier transform (DFT) matrix and showed that this definition is fully analogous to the continuous definition [21, 22, 23].

As a main application of the transform in signal processing, we have first introduced the concept of filtering in a single fractional Fourier domain [7, 8, 10]. We then applied the algorithm to image restoration problems and discussed some of the issues that do not exist for one-dimensional signals [12]. We improved the performance of the image restoration algorithm by using the non-separable definition of the transform [24].

The idea of single-domain filtering has been further generalized to multi-stage (repeated) filtering in fractional domains [13, 14, 15]. Recently we have proposed a dual configuration which is the multi-channel filtering [25, 26, 27, 28]. In this thesis we unify all these filtering configurations and discuss their applications under three main headings: system synthesis, signal synthesis and signal recovery.

The outline of the thesis is as follows. In chapter 2, we introduce the fractional Fourier transformation. We define it mathematically, discuss some of its properties including its relationship with the Wigner distribution and quadratic-phase systems, and generalize its definition to two-dimensions. We will also discuss the discrete fractional Fourier transformation. Then in chapter 3, we introduce the concept of filtering circuits in fractional Fourier domains. We first overview the single and multi-stage (repeated) fractional Fourier domain filtering configurations and then discuss in detail multi-channel (parallel) filtering configuration and unify all these configurations under the concept of filtering circuits in fractional Fourier domains. In chapters 4, 5 and 6 we will give applications of filtering circuits in fractional Fourier domains with some simulation examples. Finally, conclusions and future work in this field are discussed in Chapter 7.

Chapter 2

The Fractional Fourier Transform

The filtering circuits concept introduced in this thesis depends mainly on the fractional Fourier transformation. In this chapter we introduce this transform and discuss some of its properties that motivate the applications in signal processing. We will also discuss the discrete fractional Fourier transform. Most of the material in this chapter is adopted from [17].

2.1 Introduction and History

The fractional Fourier transform is a generalization of the ordinary Fourier transform with an order parameter a . Mathematically, the a th order fractional Fourier transform is the a th power of the Fourier transform operator. The $a = 1$ st order fractional transform is the ordinary Fourier transform. The ordinary frequency domain is merely a special case of a continuum of fractional Fourier domains that will be introduced later. Every property and application of the common Fourier transform becomes a special case of that of the fractional transform. In every area in which Fourier transforms and frequency domain concepts are used, there exists the potential for generalization and improvement by using the fractional transform. For instance, the theory of optimal Wiener filtering in the ordinary Fourier domain can be generalized to optimal filtering in fractional domains, resulting in smaller mean-square errors at practically no additional cost [8, 11, 12].

In essence, the a th order fractional Fourier transform interpolates between a function

$f(u)$ and its Fourier transform $F(\mu)$. The 0th order transform is simply the function itself, whereas the 1st order transform is its Fourier transform. The 0.5th transform is something in between, such that the same operation that takes us from the original function to its 0.5th transform will take us from its 0.5th transform to its ordinary Fourier transform. More generally, index additivity is satisfied: The a_2 th transform of the a_1 th transform is equal to the $(a_2 + a_1)$ th transform. The -1 th transform is the inverse Fourier transform, and the $-a$ th transform is the inverse of the a th transform.

Early papers related to the fractional Fourier transform include [29, 30, 31, 32]. Of importance are two separate streams of mathematical papers which appeared throughout the eighties [33, 34, 35, 36]. However, the number of publications exploded only after the introduction of the transform to the optics and signal processing communities [37, 38, 39, 40, 42]. Not all of these authors were aware of each other or building on the work of those preceding them, nor is the transform always immediately recognizable in some of these works.

The fractional Fourier transform (or essentially equivalent transforms) appear in many contexts, although it has not always been recognized as being the fractional power of the Fourier transform and thus referred to as the fractional Fourier transform. For instance, the Green's function of the quantum-mechanical harmonic oscillator is the kernel of the fractional Fourier transform. Also, the fractional Fourier transform is a special case of the more general linear canonical transform [43]. This transform has been studied in many contexts, but again the particular special case which is the fractional Fourier transform has usually not been recognized as such.

The above does not represent a complete list of known historical references. For a more complete list and also a more comprehensive treatment of the fractional Fourier transform and its relation to phase-space distributions, we refer the reader to [17] and a forthcoming book [18].

Given the widespread use of the ordinary Fourier transform in science and engineering, it is important to recognize this integral transform as the generalization of the Fourier transform. Indeed, it has been this recognition which has inspired most of the many recent applications. Replacing the ordinary Fourier transform with the fractional Fourier transform (which is more general and includes the ordinary Fourier transform as its special case) adds an additional degree of freedom to the problem, represented by the order parameter a . This in turn may allow either a more general formulation of the problem (as in the optical propagation) or improvements based on

the possibility of optimizing over a (as in the optimal Wiener filtering example).

The fractional Fourier transform has been found to have several applications in the area known as *analog optical information processing*, or *Fourier optics*. This transform allows a reformulation of this area in a way much more general than that found in standard texts on the subject. It has also led to generalizations of the notions of space (or time) and frequency domains, which are central concepts in *signal processing*, leading to many applications in this area.

More specifically, some applications which have already been investigated or suggested include diffraction theory [41, 44, 45, 46, 47], optical beam propagation and spherical mirror resonators (lasers) [48, 49], propagation in graded index media [37, 38, 39, 50, 51, 52], Fourier optics [45, 53, 54, 55, 56], statistical optics [57, 58], optical systems design [59, 60], quantum optics [61, 62], radar, phase retrieval [63], tomography [64, 65, 66], signal detection, correlation and pattern recognition [51, 67, 68, 69, 70], space- or time-variant filtering [6, 8, 11, 12, 13, 15, 25, 71, 72, 73, 74], signal recovery, restoration and enhancement [8, 14, 15, 16, 26, 27, 28, 75], multiplexing and data compression [6], study of space- or time-frequency distributions [19, 42, 65, 76], and solution of differential equations [33, 34]. These are only a fraction of the possible applications.

2.2 Definition and Properties

The a th order fractional Fourier transform of the function $f(u)$ will most often be denoted by $f_a(u)$ or equivalently $\mathcal{F}^a f(u)$. The transform is defined as a linear integral transform with kernel $K_a(u, u')$:

$$f_a(u) = \mathcal{F}^a[f(u)] = \int K_a(u, u')f(u') du'. \quad (2.1)$$

The kernel will be given explicitly below. All integrals are from minus to plus infinity unless otherwise stated. We prefer to use the same dummy variable u both for the original function in the space (or time) domain, and its fractional Fourier transform. This is in contrast to the conventional practice associated with the ordinary Fourier transform, where a different symbol, say μ , denotes the argument of the Fourier transform $F(\mu)$:

$$F(\mu) = \int f(u)e^{-i2\pi\mu u} du, \quad (2.2)$$

$$f(u) = \int F(\mu) e^{i2\pi\mu u} d\mu. \quad (2.3)$$

When it is desirable to distinguish the argument of the transformed function from that of the original function, we will let u_a denote the argument of the a th order fractional Fourier transform: $f_a(u_a) = (\mathcal{F}^a[f(u)])(u_a)$. With this convention, u_0 corresponds to u , the space (or time) coordinate, u_1 corresponds to the spatial (or temporal) frequency coordinate μ , and $u_2 = -u_0$, $u_3 = -u_1$.

We will refer to $\mathcal{F}^a[\cdot]$, or simply \mathcal{F}^a , as the a th order fractional Fourier transform operator. This operator transforms a function $f(u)$ into its fractional Fourier transform $f_a(u)$. f is a finite energy signal and $f(u)$ is a finite energy function which are well behaved in the sense usually presumed in physical applications.

After introducing the notation, we now define the a th order fractional Fourier transform $f_a(u)$ through the following linear integral transform:

$$f_a(u) = \int K_a(u, u') f(u') du', \quad (2.4)$$

$$K_a(u, u') = A_\phi \exp \left[i\pi (\cot \phi u^2 - 2 \csc \phi uu' + \cot \phi u'^2) \right],$$

where

$$\phi = \frac{a\pi}{2}, \quad (2.5)$$

$$A_\phi = \sqrt{1 - i \cot \phi}. \quad (2.6)$$

The square root is defined such that the argument of the result lies in the interval $(-\pi/2, \pi/2]$. The kernel is not strictly defined when a is an even integer. However, it is possible to show that as a approaches an even integer, the kernel behaves like a delta function under the integral sign. Thus, consistent with the limiting behavior of the above kernel for values of a approaching even integers, we define $K_{4j}(u, u') = \delta(u - u')$ and $K_{4j\pm 2}(u, u') = \delta(u + u')$, where j is an arbitrary integer. Generally speaking, the fractional Fourier transform of $f(u)$ exists under the same conditions under which its Fourier transform exists [34, 42].

We first examine the case when a is equal to an integer j . We note that by definition \mathcal{F}^{4j} and $\mathcal{F}^{4j\pm 2}$ correspond to the identity operator \mathcal{I} and the parity operator \mathcal{P} respectively (that is, $f_{4j}(u) = f(u)$ and $f_{4j\pm 2}(u) = f(-u)$). For $a = 1$ we find $\phi = \pi/2$, $A_\phi = 1$, and

$$f_1(u) = \int \exp(-i2\pi uu') f(u') du'. \quad (2.7)$$

We see that $f_1(u)$ is equal to the ordinary Fourier transform of $f(u)$, which was previously denoted by the conventional upper case $F(u)$. Likewise, it is possible to see that $f_{-1}(u)$ is the ordinary inverse Fourier transform of $f(u)$. Our definition of the fractional Fourier transform is consistent with defining integer powers of the Fourier transform through repeated application (that is, $\mathcal{F}^2 = \mathcal{F}\mathcal{F}$, $\mathcal{F}^3 = \mathcal{F}\mathcal{F}^2$, and so on). Since $\phi = a\pi/2$ appears in equation 2.4 only in the argument of trigonometric functions, the definition is periodic in a (or ϕ) with period 4 (or 2π). Thus it is sufficient to limit attention to the interval $a \in [-2, 2)$. These facts can be restated in operator notation:

$$\mathcal{F}^0 = \mathcal{I}, \quad (2.8)$$

$$\mathcal{F}^1 = \mathcal{F}, \quad (2.9)$$

$$\mathcal{F}^2 = \mathcal{P}, \quad (2.10)$$

$$\mathcal{F}^3 = \mathcal{F}\mathcal{P} = \mathcal{P}\mathcal{F}, \quad (2.11)$$

$$\mathcal{F}^4 = \mathcal{F}^0 = \mathcal{I}, \quad (2.12)$$

$$\mathcal{F}^{4j+a} = \mathcal{F}^{4j'+a}, \quad (2.13)$$

where j, j' are arbitrary integers.

Let us now examine the behavior of the kernel for small $|a| > 0$:

$$K_a(u, u') = \frac{e^{-i\pi \text{sgn}(\phi)/4}}{\sqrt{|\phi|}} \exp[i\pi(u - u')^2/\phi]. \quad (2.14)$$

Now, using the well known limit

$$\delta(u) = \lim_{c \rightarrow 0} e^{-i\pi/4} \sqrt{\frac{1}{c}} e^{i\pi u^2/c}, \quad (2.15)$$

the kernel is seen to approach $\delta(u - u')$ as a approaches 0. Thus defining the kernel $K_a(u, u')$ to be precisely $\delta(u - u')$ at $a = 0$ maintains continuity of the transform with respect to a . A similar discussion is possible when a approaches other integer multiples of 2. A more rigorous discussion of continuity with respect to a may be found in [34].

We now discuss the index additivity property:

$$\mathcal{F}^{a_1} \mathcal{F}^{a_2} f(u) = \mathcal{F}^{a_1+a_2} f(u) = \mathcal{F}^{a_2} \mathcal{F}^{a_1} f(u), \quad (2.16)$$

or in operator notation

$$\mathcal{F}^{a_1} \mathcal{F}^{a_2} = \mathcal{F}^{a_1+a_2} = \mathcal{F}^{a_2} \mathcal{F}^{a_1}. \quad (2.17)$$

This can be proved by repeated application of equation 2.4, and amounts to showing

$$\int K_{a_2}(u, u'')K_{a_1}(u'', u') du'' = K_{a_1+a_2}(u, u') \quad (2.18)$$

by direct integration, which can be accomplished by using standard Gaussian integrals [17].

The index additivity property is of central importance. Indeed, without it, \mathcal{F}^a would not actually be the a th power of \mathcal{F} . For instance, the 0.2nd fractional Fourier transform of the 0.5th transform is the 0.7th Fourier transform. Repeated application leads to statements such as, for instance, the 1.3th transform of the 2.1st transform of the 1.4th transform is the 4.8th transform (which is the same as the 0.8th transform). Transforms of different orders commute with each other so that their order can be freely interchanged. From the index additivity property, we deduce that the inverse of the a th order fractional Fourier transform operator $(\mathcal{F}^a)^{-1}$ is simply equal to the operator \mathcal{F}^{-a} (because $\mathcal{F}^{-a}\mathcal{F}^a = \mathcal{I}$). This can also be shown by directly demonstrating that

$$\int K_a(u, u'')K_{-a}(u'', u') du = \delta(u - u'), \quad (2.19)$$

so that $K_a^{-1}(u, u') = K_{-a}(u, u')$. Thus we see that we can freely manipulate the order parameter a as if it denoted a power of the Fourier transform operator \mathcal{F} .

Fractional Fourier transforms constitute a one-parameter family of transforms. This family is a subfamily of the more general family of linear canonical transforms which have three parameters [43]. As all linear canonical transforms do, fractional Fourier transforms satisfy the associativity property and they are unitary, as we can directly see by examining the kernel of the inverse transform obtained by replacing a with $-a$:

$$K_a^{-1}(u, u') = K_{-a}(u, u') = K_a^*(u, u') = K_a^*(u', u). \quad (2.20)$$

The kernel $K_a(u, u')$ is symmetric and unitary, but not Hermitian. Unitarity implies that the fractional Fourier transform can be interpreted as a transformation from one orthogonal basis to another, and that inner products and norms are not changed under the transformation.

2.2.1 Eigenvalues and Spectral Expansion

The eigenvalues and eigenfunctions of the ordinary Fourier transform are well known and they are the Hermite-Gaussian functions $\psi_n(u)$. The eigenvalues may be expressed

as $\exp(-in\pi/2)$ and are given by $1, -i, -1, i, 1, -i, \dots$ for $n = 0, 1, 2, 3, 4, 5, \dots$. Thus the eigenvalue equation for the ordinary Fourier transform may be written as

$$\mathcal{F}\psi_n(u) = e^{-in\pi/2}\psi_n(u), \quad (2.21)$$

where the Hermite-Gaussian functions are more explicitly given by

$$\psi_n(u) = A_n H_n(\sqrt{2\pi} u) e^{-\pi u^2}, \quad (2.22)$$

$$A_n = 2^{1/4} / \sqrt{2^n n!}, \quad (2.23)$$

for $n = 0, 1, 2, 3, 4, 5, \dots$. Here $H_n(u)$ are the Hermite polynomials. The particular scale factors which appear in this equation are a direct consequence of the way we have defined the Fourier transform with 2π in the exponent.

The a th order fractional Fourier transform shares the same eigenfunctions as the Fourier transform, but its eigenvalues are the a th power of the eigenvalues of the ordinary Fourier transform:

$$\mathcal{F}^a \psi_n(u) = e^{-ian\pi/2} \psi_n(u). \quad (2.24)$$

This result can be established directly from equation 2.4.

Function $FN(\mathcal{A})$ of an operator (or matrix) \mathcal{A} with eigenvalues λ_n will have the same eigenfunctions as \mathcal{A} and that its eigenvalues will be $FN(\lambda_n)$. The above eigenvalue equation is particularly satisfying in this light since \mathcal{F}^a as we have defined it, is indeed seen to correspond to the a th power of the Fourier transform operator ($FN(\cdot) = (\cdot)^a$). However, it should be noted that the definition of the a th power function is ambiguous, and our definition of the fractional Fourier transform through equation 2.4 is associated with a particular way of resolving the ambiguity associated with the a th power function (equation 2.24). Other definitions of the transform also deserving to be called the fractional power of the Fourier transform are possible. The particular definition we are considering is the one that has been most studied and that has led to the greatest number of interesting applications.

Knowledge of the complete set of eigenvalues and eigenfunctions of a linear operator is sufficient to completely characterize the operator. In fact, in some works, the fractional Fourier transform has been defined through its eigenvalue equation [33, 37, 38, 39]. It is possible to show that the kernel of the fractional Fourier transform $K_a(u, u')$ can be decomposed as

$$K_a(u, u') = \sum_{n=0}^{\infty} e^{-ian\pi/2} \psi_n(u) \psi_n(u'). \quad (2.25)$$

This is the spectral decomposition of the kernel of the fractional Fourier transform. The kernel given in equation 2.25 can be shown to be identical to that given in equation 2.4 directly by using an identity known as Mehler's formula:

$$\sum_{n=0}^{\infty} \frac{e^{in\phi}}{2^n n! \sqrt{\pi}} H_n(u) H_n(u') = \frac{1}{\sqrt{\pi} \sqrt{1 - \exp(2i\phi)}} \exp \left[\frac{2uu'e^{i\phi} - e^{2i\phi}(u^2 + u'^2)}{1 - e^{2i\phi}} \right]. \quad (2.26)$$

Several properties of the fractional Fourier transform immediately follow from equation 2.24. In particular the special cases $a = 0$, $a = 1$, and the index additivity property are deduced easily.

2.2.2 Operational properties

Various operational properties of the transform are given below [33, 34, 38, 42]. Most of these are most readily derived or verified by using equation 2.4 or the symmetry properties of the kernel.

$$\begin{aligned} \mathcal{F}^a[f(-u)](u) &= \mathcal{F}^a[f(u)](-u) \\ \mathcal{F}^a[f(ku)](u) &= |k|^{-1} \sqrt{\frac{1 - i \cot \phi}{1 - ik^{-2} \cot \phi}} e^{i\pi u^2 \cot \phi (1 - \cos^2 \phi' / \cos^2 \phi)} \mathcal{F}^{a'}[f(u)](u \sin \phi' / k \sin \phi) \\ \mathcal{F}^a[f(u - \xi)](u) &= e^{i\pi \xi^2 \sin \phi \cos \phi} e^{-i2\pi u \xi \sin \phi} \mathcal{F}^a[f(u)](u - \xi \cos \phi) \\ \mathcal{F}^a[e^{i2\pi \xi u} f(u)](u) &= e^{-i\pi \xi^2 \sin \phi \cos \phi} e^{i2\pi u \xi \cos \phi} \mathcal{F}^a[f(u)](u - \xi \sin \phi) \\ \mathcal{F}^a[uf(u)](u) &= \cos \phi u \mathcal{F}^a[f(u)](u) - \sin \phi (i2\pi)^{-1} \frac{d\mathcal{F}^a[f(u)](u)}{du} \\ \mathcal{F}^a[(i2\pi)^{-1} df(u)/du](u) &= \sin \phi u \mathcal{F}^a[f(u)](u) + \cos \phi (i2\pi)^{-1} \frac{d\mathcal{F}^a[f(u)]}{du} \\ \mathcal{F}^a \left[\int_{u_0}^u f(u') du' \right] (u) &= \sec \phi e^{-i\pi u^2 \tan \phi} \int_{u_0}^u \mathcal{F}^a[f(u)](u') e^{i\pi u'^2 \tan \phi} du' \end{aligned}$$

In the above ξ is an arbitrary real number, k is a real number ($k \neq 0, \pm\infty$), and n is an integer. $\phi' = \arctan(k^2 \tan \phi)$, where ϕ' is taken to be in the same quadrant as ϕ .

2.2.3 Relation to the Wigner distribution

The direct and simple relationship of the fractional Fourier transform to the Wigner distribution, as well as to certain other phase-space distributions is perhaps its most important and elegant property [81, 40, 42, 6].

Here we will define and briefly discuss some of the most important properties of the Wigner distribution. The Wigner distribution $W_f(u, \mu)$ of a function $f(u)$ is defined as

$$W_f(u, \mu) = \int f(u + u'/2) f^*(u - u'/2) e^{-2\pi i \mu u'} du'. \quad (2.27)$$

$W_f(u, \mu)$ can also be expressed in terms of $F(\mu)$, or indeed as a function of any fractional transform of $f(u)$. Some of its most important properties are

$$|f(u)|^2 = \int W(u, \mu) d\mu, \quad (2.28)$$

$$|F(\mu)|^2 = \int W(u, \mu) du, \quad (2.29)$$

$$\text{En}[f(u)] = \int W(u, \mu) du d\mu, \quad (2.30)$$

$\text{En}[f(u)]$ is the total energy of the signal $f(u)$. Roughly speaking, $W(x, \nu)$ can be interpreted as a function that indicates the distribution of the signal energy over space and frequency. The Wigner distribution of $F(u)$ (the Fourier transform of $f(u)$), is a ninety degree rotated version of the Wigner distribution of $f(u)$. More on the Wigner distribution and other such distributions and representations may be found in [77, 78, 79, 80].

Now, if $W_f(u, \mu)$ denotes the Wigner distribution of $f(u)$, then the Wigner distribution of the a th fractional Fourier transform of $f(u)$, denoted by $W_{f_a}(u, \mu)$, is given by

$$W_{f_a}(u, \mu) = W_f(u \cos \phi - \mu \sin \phi, u \sin \phi + \mu \cos \phi), \quad (2.31)$$

so that the Wigner distribution of $W_{f_a}(u, \mu)$ is obtained from $W_f(u, \mu)$ by rotating it clockwise by an angle ϕ . Let us define \mathcal{R}_ϕ to be the operator which rotates a function of (u, μ) by angle ϕ in the conventional counterclockwise direction. Then we can write

$$W_{f_a}(u, \mu) = \mathcal{R}_{-\phi} W_f(u, \mu). \quad (2.32)$$

This elegant and fundamental property underlies an important number of the applications of the fractional Fourier transform. In fact, some authors have defined the transform as that operation which corresponds to rotation of the Wigner distribution of a function [40].

A corollary of the above result follows easily [81, 65, 6]. Let us recall equations 2.28 and 2.29 which state that the integral projection of $W_f(u, \mu)$ onto the u axis is the magnitude square of the u -domain representation of the signal and that the integral

projection of $W_f(u, \mu)$ onto the μ axis is the magnitude square of the μ -domain representation of the signal. Now, let us rewrite the first of these equations for $f_a(u)$, the a th order fractional Fourier transform of $f(u)$:

$$\int W_{f_a}(u, \mu) d\mu = |f_a(u)|^2. \quad (2.33)$$

Since $W_{f_a}(u, \mu)$ is simply $W_f(u, \mu)$ clockwise rotated by angle ϕ , the integral projection of $W_{f_a}(u, \mu)$ onto the u axis is identical to the integral projection of $W_f(u, \mu)$ onto an axis making angle ϕ with the u axis. This new axis making angle $\phi = a\pi/2$ with the u axis is referred to as the u_a axis. Let \mathcal{RAD}_ϕ denote the *Radon transform* operator, which maps a two-dimensional function of (u, μ) , to its integral projection onto an axis making angle ϕ with the u axis. Thus the above can be written as

$$\mathcal{RAD}_\phi W_f(u, \mu) = |f_a(u)|^2. \quad (2.34)$$

In conclusion, the integral projection of the Wigner distribution of a function onto the u_a axis is equal to the magnitude square of the a th order fractional Fourier transform of the function (Fig. 2.1). Equations 2.28 and 2.29 are special cases with $a = 0$ and $a = 1$. Wood and Barry discussed what they referred to as the “Radon-Wigner transform” without realizing its relation to the fractional Fourier transform (Wood and Barry 1994a, b). The above discussion demonstrates that the Radon-Wigner transform is simply the magnitude squared of the fractional Fourier transform.

The Wigner distribution is not the only time-frequency representation satisfying the rotation property (equation 2.32). The ambiguity function also satisfies this property because the ambiguity function is the two-dimensional Fourier transform of the Wigner distribution, and the two-dimensional Fourier transform of the rotated version of a function is the rotated version of the two-dimensional Fourier transform of the original function [6, 42]. Almeida (1994) showed that the rotation property also holds for the spectrogram. We have further shown that the rotation property generalizes to certain other time-frequency distributions belonging to the so-called Cohen class, whose members can be obtained from the Wigner distribution by convolving it with a kernel characterizing that distribution. The distributions for which the rotation property holds are those which have a rotationally symmetric kernel [19].

Thus, fractional Fourier transformation corresponds to rotation of many phase-space representations. This not only confirms the important role this transform plays in the study of such representations, but also supports the notion of referring to the axis making

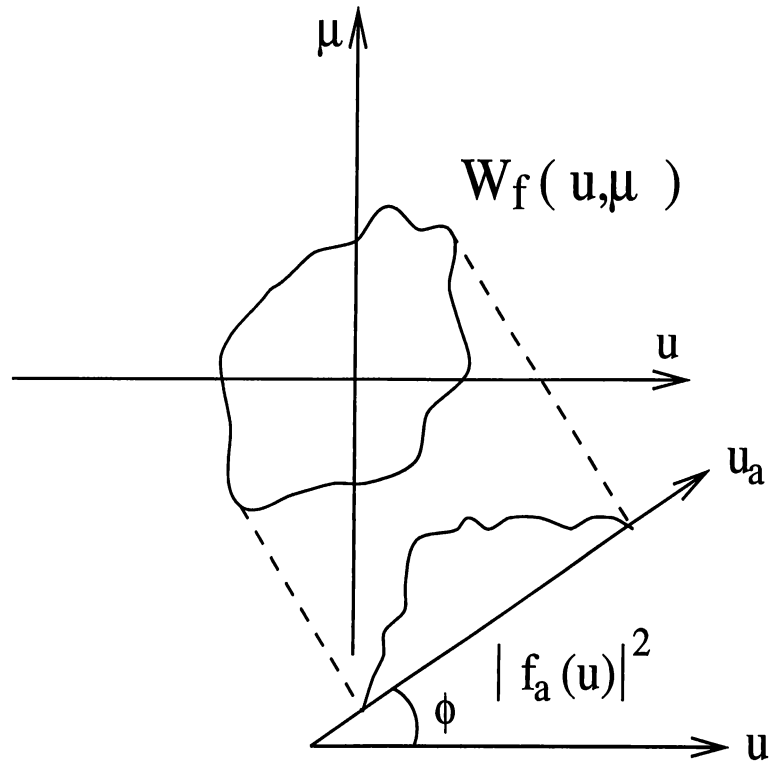


Figure 2.1: Oblique integral projections of the Wigner distribution.

angle $\phi = a\pi/2$ with the u axis as the *ath fractional Fourier domain* [82]. Despite this generalization, the only distribution which satisfies a relation of the form of equation 2.34 is the Wigner distribution [81].

2.2.4 Fractional Fourier Domains

Equations 2.32 and 2.34 immediately lead to the interpretation of oblique axes in phase space as fractional Fourier domains. Just as the projection of the Wigner distribution onto the space domain gives the magnitude square of the space-domain representation of the signal, and the projection of the Wigner distribution onto the frequency domain gives the magnitude square of the frequency-domain representation of the signal (equations 2.28 and 2.29), the projection on the axis making angle $\phi = a\pi/2$ with the u axis gives the magnitude square of the *ath* fractional Fourier-domain representation of the signal (equation 2.34). When we need to be explicit we will use the variable u_a as the coordinate variable in the *ath* domain, so that the representation

of the signal f in the a th order fractional Fourier domain will be written as $f_a(u_a)$. We immediately recognize that the 0th and 1st domains are the ordinary space and frequency domains and that the 2nd and 3rd domains correspond to the negated space and frequency domains ($u_0 = u$, $u_1 = \mu$, $u_2 = -u$, $u_3 = -\mu$). The representation of the signal in the a' th domain is related to its representation in the a th domain through an $(a' - a)$ th order fractional Fourier transformation:

$$f_{a'}(u_{a'}) = \int K_{a'-a}(u_{a'}, u_a) f_a(u_a) du_a. \quad (2.35)$$

When $(a' - a)$ is an integer, this corresponds to a forward or inverse Fourier integral.

2.3 Optical And Digital Implementation

Fractional Fourier transformation can easily be realized optically [40, 83, 84, 85], which leads to many applications in optical signal processing as given in section 2.1. In addition to this, the digital implementation of fractional Fourier transformation also exists. In [20], we have presented a fast algorithm that calculates fractional Fourier transform in $O(N \log N)$ time. Here we briefly discuss this algorithm.

The defining equation (equation 2.4) can be put in the form

$$f_a(u) = A_\phi e^{i\pi \cot \phi u^2} \int e^{-i2\pi \csc \phi uu'} \left[e^{i\pi \cot \phi u'^2} f(u') \right] du'. \quad (2.36)$$

We assume that the representations $f_a(u_a)$ of the signal f in all fractional Fourier domains are approximately confined to the interval $[-\Delta u/2, \Delta u/2]$ (that is, a sufficiently large percentage of the signal energy is confined to these intervals). This assumption is equivalent to assuming that the Wigner distribution of $f(u)$ is approximately confined within a circle of diameter Δu (by virtue of equation 2.34). Again, this means that a sufficiently large percentage of the energy of the signal is contained in that circle. We can ensure that this assumption is valid for any signal by choosing Δu sufficiently large. Under this assumption, and initially limiting the order a to the interval $0.5 \leq |a| \leq 1.5$, the modulated function $e^{i\pi \alpha u'^2} f(u')$ may be assumed to be approximately band-limited to $\pm \Delta u$ in the frequency domain. Thus $e^{i\pi \alpha u'^2} f(u')$ can be represented by Shannon's interpolation formula

$$e^{i\pi \alpha u'^2} f(u') = \sum_{n=-N}^{N-1} e^{i\pi \cot \phi \left(\frac{n}{2\Delta u}\right)^2} f\left(\frac{n}{2\Delta u}\right) \text{sinc} \left[2\Delta u \left(u' - \frac{n}{2\Delta u} \right) \right], \quad (2.37)$$

where $N = (\Delta u)^2$. The summation goes from $-N$ to $N - 1$ since $f(u')$ is assumed to be zero outside $[-\Delta u/2, \Delta u/2]$. By using equation 2.37 and equation 2.36, and changing the order of integration and summation we obtain

$$f_a(u) = A_\phi e^{i\pi \cot \phi u^2} \sum_{n=-N}^{N-1} e^{i\pi \cot \phi (\frac{n}{2\Delta u})^2} f\left(\frac{n}{2\Delta u}\right) \int e^{-i2\pi \csc \phi u u'} \text{sinc}\left[2\Delta u \left(u' - \frac{n}{2\Delta u}\right)\right] du'. \quad (2.38)$$

By recognizing the integral to be equal to $(1/2\Delta u)e^{-i2\pi \csc \phi u \frac{n}{2\Delta u}} \text{rect}(\csc \phi u/2\Delta u)$, we can write

$$f_a(u) = \frac{A_\phi}{2\Delta u} \sum_{n=-N}^{N-1} e^{i\pi \cot \phi u^2} e^{-i2\pi \csc \phi u \frac{n}{2\Delta u}} e^{i\pi \cot \phi (\frac{n}{2\Delta u})^2} f\left(\frac{n}{2\Delta u}\right), \quad (2.39)$$

since $\text{rect}(\csc u/2\Delta u) = 1$ in the interval $|u| \leq \Delta u/2$. Then, the samples of $f_a(u)$ are given by

$$f_a\left(\frac{m}{2\Delta u}\right) = \frac{A_\phi}{2\Delta u} \sum_{n=-N}^{N-1} e^{i\pi \left(\cot \phi (\frac{m}{2\Delta u})^2 - 2 \csc \phi \frac{mn}{(2\Delta u)^2} + \cot \phi (\frac{n}{2\Delta u})^2\right)} f\left(\frac{n}{2\Delta u}\right), \quad (2.40)$$

which is a finite summation allowing us to obtain the samples of the fractional transform $f_a(u)$ in terms of the samples of the original function $f(u)$. Direct computation of equation 2.40 would require $O(N^2)$ operations. A fast ($O(N \log N)$) algorithm can be obtained by putting equation 2.40 into the following form:

$$f_a\left(\frac{m}{2\Delta u}\right) = \frac{A_\phi}{2\Delta u} e^{i\pi(\cot \phi - \csc \phi)(\frac{m}{2\Delta u})^2} \sum_{n=-N}^{N-1} e^{i\pi \csc \phi (\frac{m-n}{2\Delta u})^2} e^{i\pi(\cot \phi - \csc \phi)(\frac{n}{2\Delta u})^2} f\left(\frac{n}{2\Delta u}\right). \quad (2.41)$$

We now recognize that the summation is the convolution of $e^{i\pi \csc \phi (\frac{n}{2\Delta u})^2}$ and the chirp modulated function $f(\cdot)$. The convolution can be computed in $O(N \log N)$ time by using the fast Fourier transform (FFT). The output samples are then obtained by a final chirp modulation. Hence the overall complexity is $O(N \log N)$.

We had limited ourselves to $0.5 \leq |a| \leq 1.5$ in deriving the above algorithm. Using the index additivity property of the fractional Fourier transform we can extend this range to all values of a easily. For instance, for the range $0 \leq a \leq 0.5$, we can write

$$\mathcal{F}^a = \mathcal{F}^{a-1+1} = \mathcal{F}^{a-1} \mathcal{F}^1. \quad (2.42)$$

Since $0.5 \leq |a-1| \leq 1$, we can use the above algorithm in conjunction with the ordinary Fourier transform to compute $f_a(u)$. The overall complexity remains at $O(N \log N)$.

In the above algorithm, given the input vector (which is assumed to correspond to the samples of a continuous signal taken at the Nyquist rate), we first interpolate the vector

by two. To preserve duality and symmetry between the time and frequency domains, we also pad zeros to increase the length by an additional factor of two. This step not only increases the robustness of the algorithm by further oversampling the signal in the frequency domain, but also allows to obtain symmetric signals both in time and frequency domains. (Interpolation by two in the time domain results in zero-padding in the frequency domain, while zero padding in the time domain results in interpolation by two in the frequency domain. Thus if we both pad zeros and interpolate, we also get an interpolated and zero-padded signal in the frequency domain.)

2.4 Discrete Fractional Fourier Transform

The digital computation algorithm proposed in [20] suggests a definition for the discrete fractional Fourier transform (matrix) since it maps the samples of input function to the samples of the fractional Fourier transform of the function:

$$\mathbf{f}_a = \mathbf{F}^a \mathbf{f} \quad (2.43)$$

Here \mathbf{f}_a and \mathbf{f} are the $N \times 1$ vectors whose elements are the samples of $f_a(u)$ and $f(u)$ respectively, and \mathbf{F}^a is the $N \times N$ discrete fractional Fourier transform matrix. The elements of \mathbf{F}^a can be easily found from this algorithm using equation 2.40. Although this matrix approximately calculates the fractional Fourier transform, it fails to satisfy exactly some basic requirements of the consistent discrete fractional Fourier transformation, such as unitarity, index additivity and reducing to DFT (discrete Fourier Transform) matrix for $a = 1$. On the other hand, in most of the digital signal processing applications we use these properties in formulating and solving the problems. Thus, we need a consistent discrete fractional Fourier transform matrix.

In section 2.2.1, we show how the continuous fractional Fourier transform kernel may be decomposed in terms of the eigenvalues and eigenfunctions of the ordinary Fourier transform (equation 2.25). A dual equation can be used to define the discrete fractional Fourier transformation if the eigenvectors of DFT matrix corresponding to Hermite-Gaussian functions are known (the eigenvalues of the DFT matrix are same as the eigenvalues of the ordinary Fourier transform). In [21, 22], this idea has been discussed thoroughly and a discrete fractional Fourier transform is defined. This definition satisfies all the requirements for the discrete fractional Fourier transform, but its efficient implementation is not known yet and it is an open problem.

In the next chapters where we introduce the concept of filtering circuits in fractional Fourier domains, we will use this definition of the fractional Fourier transform while formulating and solving the problems because it satisfies exactly the unitarity and index additivity. On the other hand, since it is shown that for most of the digital signals, the output of this definition deviates only slightly from the output of the digital computation algorithm of [20], this algorithm will be used in order to implement efficiently those filtering circuits in a given application.

2.5 Generalization to Two-Dimensional Systems

Up to here, we considered only the one-dimensional definition of the fractional Fourier transformation. Here, we will generalize the definition of the fractional Fourier transform to two-dimensions. The following subsections explain two ways of generalizing the definition to two-dimensional systems.

2.5.1 Separable Two-Dimensional Fractional Fourier Transformation

The natural extension of the fractional Fourier transform to two and higher dimensions is

$$\begin{aligned} f_{\mathbf{a}}(\mathbf{q}) &= f_{a_u, a_v}(u, v) = \mathcal{F}^{\mathbf{a}} f(\mathbf{q}) = \mathcal{F}^{a_u, a_v} f(u, v) \\ &= \int \int K_{a_u, a_v}(u, v; u', v') f(u', v') du' dv', \\ K_{a_u, a_v}(u, v; u', v') &= K_{a_u}(u, u') K_{a_v}(v, v') \end{aligned} \quad (2.44)$$

for two dimensions and similarly for higher dimensions. Here $\mathbf{q} = u\hat{\mathbf{u}} + v\hat{\mathbf{v}}$ and $\mathbf{a} = a_u\hat{\mathbf{u}} + a_v\hat{\mathbf{v}}$ where $\hat{\mathbf{u}}$ and $\hat{\mathbf{v}}$ are unit vectors in the u and v directions. $K_a(u, u')$ is the one-dimensional kernel defined in equation 2.4. A comprehensive discussion of the separable 2-D fractional Fourier transformation may be found in [86]. Notice that different transform orders a_u and a_v are allowed in the two dimensions, although some authors have defined higher dimensional transforms with only a single order parameter. The effect of a one-dimensional fractional Fourier transform (say in the u direction) on a two-dimensional function is interpreted in the obvious manner by treating the other

dimension (in this case v) as a parameter. Denoting such one-dimensional transforms as $\mathcal{F}^{a_u \hat{u}}$ and $\mathcal{F}^{a_v \hat{v}}$, it becomes possible to write

$$\mathcal{F}^{\mathbf{a}} = \mathcal{F}^{a_u \hat{u}} \mathcal{F}^{a_v \hat{v}} = \mathcal{F}^{a_v \hat{v}} \mathcal{F}^{a_u \hat{u}}, \quad (2.45)$$

constituting a concise statement of the separability of the two-dimensional transform. Notice that the notation we have introduced makes these equations compatible with the index additivity property, so that it is possible to deduce identities such as $\mathcal{F}^{0.7\hat{u}} \mathcal{F}^{0.5\hat{u}-0.3\hat{v}} \mathcal{F}^{0.2\hat{v}} \mathcal{F}^{0.8\hat{u}+0.1\hat{v}} = \mathcal{F}^{2.0\hat{u}} = \mathcal{P}_u$, where \mathcal{P}_u is the parity operator in the u dimension.

Most of the results and properties presented for the one-dimensional case are easily generalized to two and higher dimensions by virtue of separability as embodied by equation 2.45.

2.5.2 Non-separable Two-Dimensional Fractional Fourier Transformation

When the definition of Fourier transformation is generalized to two-dimensional systems, new properties like affine property also starts to be observed. The affine property is stated in [100] as a theorem which says that: If $f(u, v)$ has two-dimensional Fourier transform $F(u, v)$, then $f(au + bv, cu + dv)$ has two-dimensional Fourier transform

$$G(u, v) = \frac{1}{\Delta} F\left(\frac{du - cv}{\Delta}, \frac{-bu + av}{\Delta}\right) \quad (2.46)$$

where $\Delta = ad - bc$. We may also look for a similar property for the two-dimensional fractional Fourier transformation. The separable fractional Fourier transformation in equation 2.44 does not have such a property. Starting with this motivation, in [86] a new two-dimensional fractional Fourier transformation definition which satisfies the affine property is introduced. In [86] the non-separable fractional Fourier transform is given as

$$\mathcal{F}_{\theta_1, \theta_2}^{a_u, a_v} \{f(\mathbf{q})\} = \int_{-\infty}^{\infty} B_{\theta_1, \theta_2}^{a_u, a_v}(\mathbf{q}, \mathbf{q}'') f(\mathbf{q}'') d\mathbf{q}'' \quad (2.47)$$

where

$$B_{\theta_1, \theta_2}^{a_u, a_v}(\mathbf{q}, \mathbf{q}'') = K_q \exp[i\pi(\mathbf{q}^T \mathbf{A} \mathbf{q} + 2\mathbf{q}^T \mathbf{B} \mathbf{q}'' + \mathbf{q}''^T \mathbf{C} \mathbf{q}'')] \quad (2.48)$$

with

$$K_q = K_{u'} K_{v'}, \quad \mathbf{r} = \begin{bmatrix} u & v \end{bmatrix}^T, \quad \mathbf{q}'' = \begin{bmatrix} u'' & v'' \end{bmatrix}^T,$$

$$\mathbf{A} = \begin{bmatrix} \cot \phi_{u'} & 0 \\ 0 & \cot \phi_{v'} \end{bmatrix},$$

$$\mathbf{B} = \begin{bmatrix} -\frac{\cos \theta_2 \csc \phi_{u'}}{\cos(\theta_1 - \theta_2)} & \frac{\sin \theta_1 \csc \phi_{u'}}{\cos(\theta_1 - \theta_2)} \\ -\frac{\sin \theta_2 \csc \phi_{v'}}{\cos(\theta_1 - \theta_2)} & -\frac{\cos \theta_1 \csc \phi_{v'}}{\cos(\theta_1 - \theta_2)} \end{bmatrix},$$

$$\mathbf{C} = \begin{bmatrix} \frac{\cos^2 \theta_2}{\cos^2(\theta_1 - \theta_2)} \cot \phi_{u'} + \frac{\sin^2 \theta_2}{\cos^2(\theta_1 - \theta_2)} \cot \phi_{v'} & -\frac{\sin \theta_1 \cos \theta_2}{\cos^2(\theta_1 - \theta_2)} \cot \phi_{u'} + \frac{\sin \theta_2 \cos \theta_1}{\cos^2(\theta_1 - \theta_2)} \cot \phi_{v'} \\ -\frac{\sin \theta_1 \cos \theta_2}{\cos^2(\theta_1 - \theta_2)} \cot \phi_{u'} + \frac{\sin \theta_2 \cos \theta_1}{\cos^2(\theta_1 - \theta_2)} \cot \phi_{v'} & \frac{\cos^2 \theta_1}{\cos^2(\theta_1 - \theta_2)} \cot \phi_{v'} + \frac{\sin^2 \theta_1}{\cos^2(\theta_1 - \theta_2)} \cot \phi_{u'} \end{bmatrix}.$$

In [86] a thorough analysis of optical realization of both separable and non-separable two-dimensional fractional Fourier transformation is also presented.

With this non-separable two-dimensional fractional Fourier transform definition, we have generalized single stage fractional Fourier domain filtering to obtain further improvements in image restoration applications. The results of this work are reported in [24].

Chapter 3

Generalized Filtering Configurations Based on Fractional Fourier Transforms

In this chapter, we introduce the concept of filtering circuits in fractional Fourier domains. This configuration includes the multi-stage (repeated) and multi-channel (parallel) filtering configurations which are generalizations of the single domain filtering configuration.

Single-stage and multi-stage filtering in fractional Fourier domains have been discussed in detail in [7, 10, 11, 12, 13, 14, 15]. In this chapter, we will introduce and discuss in detail the multi-channel filtering configuration, propose some possible extensions for all of the configurations and unify all these configurations under the concept of filtering circuits.

In the next sections, we will first review single-stage and multi-stage filtering configurations. Then we will introduce the multi-channel configuration.

3.1 Single-stage Filtering in Fractional Fourier Domains

In chapter 1, we discussed time-invariant systems as the subclass of the general linear systems. Time-invariant systems (Fig. 1.1 (a)) may also be interpreted as a special case of single-stage transform domain filtering which is in turn a sub-class of general linear systems. General single-stage transform domain filtering configuration is shown in Fig. 3.1 (a). According to this configuration, the output is obtained by multiplying the input with a filter function h in the transform domain. The overall system is characterized by:

$$\mathcal{T} = \mathcal{S}^{-1} \Lambda \mathcal{S} \quad (3.1)$$

where \mathcal{S} is a transform and Λ corresponds to a multiplication with the filter function h . \mathcal{T} can be implemented efficiently if the transform \mathcal{S} has efficient implementation. The time-invariant system is a special case with the transform \mathcal{S} equals to the ordinary Fourier transform (Fig. 3.1 (b)). Other special case may be obtained by using the identity transform ($\mathcal{S} = \mathcal{I}$) and in this case we have the time or space domain filtering for which the output is obtained by simply masking the input with a window function h (Fig. 3.1 (c)).

If we choose the transform in (3.1) as the fractional Fourier transform ($\mathcal{S} = \mathcal{F}^a$), we obtain the single-stage fractional Fourier domain filter (Fig. 3.1 (d)). In this case the overall system is given by:

$$\mathcal{T}_{ss} = \mathcal{F}^{-a} \Lambda \mathcal{F}^a \quad (3.2)$$

This configuration interpolates between the time-domain and frequency domain filtering configurations and enables significant improvements in signal restoration and denoising as discussed below [7, 10, 12].

As a simple application of the single-stage fractional Fourier domain filtering we consider the signal or image restoration problem. In many signal processing applications, signals which we wish to recover are degraded by a known distortion and/or by noise. Then the problem is to reduce or eliminate these degradations. Appropriate solutions to such problems depend on the observation model and the objectives, as well as the prior knowledge available about the desired signal, degradation process and noise. A commonly used observation model is

$$x_{\text{obs}} = \mathcal{G}x + n, \quad (3.3)$$

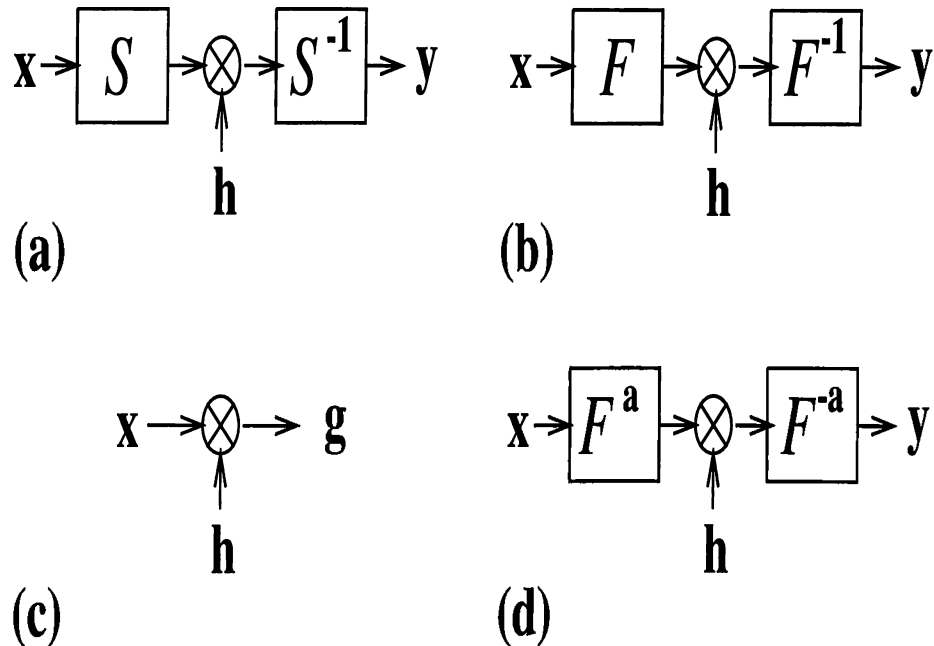


Figure 3.1: (a) Single-stage transform domain filtering, (b) Fourier domain filtering, (c) time (space) domain filtering, (d) fractional Fourier domain filtering.

where \mathcal{G} is the linear system that degrades the desired signal (may be an image) x , and n is an additive noise term. The problem is to find an estimation operator represented by the kernel \mathcal{H} , such that the estimated signal

$$x_{\text{est}} = \mathcal{H}x_{\text{obs}} \quad (3.4)$$

minimizes the mean square error defined as:

$$\sigma_e^2 = E \left[\|x_{\text{est}} - x\|^2 \right], \quad (3.5)$$

where $\|\cdot\|^2$ denotes a norm and $E[\cdot]$ denotes an ensemble average. The classical Wiener filter provides the solution to the above problem when the degradation is time-invariant and the input and noise processes are stationary. The Wiener filter is time-invariant, and can thus be implemented effectively with a multiplicative filter in the conventional Fourier domain with the fast Fourier transform algorithm. For an arbitrary degradation model or non-stationary processes, the classical Wiener filter cannot often provide a satisfactory result. In this case, the optimum recovery operator is in general time-varying and has no fast implementation. However we can use the single-stage fractional Fourier domain filter to improve the performance. This filtering configuration has been studied in detail in [8, 10] for 1-D signals and in [12] for 2-D signals and images.

To understand the basic motivation for filtering in fractional Fourier domains, consider Fig. 3.2, where the Wigner distributions of a desired signal and an undesired distortion are superimposed. We observe that they overlap in both the 0th and 1st domains, but they do not overlap in the 0.5th domain (consider the projections onto the $u_0 = u$, $u_1 = \mu$, and $u_{0.5}$ axes). Although we cannot eliminate the distortions in the space or frequency domains, we can eliminate them easily by using a simple amplitude mask in the 0.5th domain.

We now discuss the optimal filtering problem mathematically. The estimated (filtered) signal x_{est} is expressed as

$$x_{\text{est}} = \mathcal{T}_{\text{ss}} x_{\text{obs}}, \quad (3.6)$$

$$\mathcal{T}_{\text{ss}} = \mathcal{F}^{-a} \Lambda \mathcal{F}^a, \quad (3.7)$$

According to equation 3.7, we first take the a th order fractional Fourier transform of the observed signal x_{obs} , then multiply the transformed signal with the filter h and take the inverse a th order fractional Fourier transform of the resulting signal to obtain our estimate. Since the fractional Fourier transform has efficient digital and optical implementations, the cost of fractional Fourier domain filtering is approximately the same as the cost of ordinary Fourier domain filtering. With the above form of the estimation operator, the problem is to find the optimum multiplicative filter function h_{opt} that minimizes the mean-square error defined in equation 3.5.

For a given transform order a , h_{opt} can be found analytically using the orthogonality principle or the calculus of variations [8, 10, 12]:

$$h_{\text{opt}}(u) = \frac{\int \int K_a(u_a, u) K_{-a}(u_a, u') R_{x_{\text{obs}}} (u, u') du' du}{\int \int K_a(u_a, u) K_{-a}(u_a, u') R_{x_{\text{obs}} x_{\text{obs}}} (u, u') du' du}, \quad (3.8)$$

where the stochastic auto- and cross-correlation functions $R_{x_{\text{obs}} x_{\text{obs}}} (u, u')$ and $R_{x_{\text{obs}}} (u, u')$ can be computed from the correlation functions $R_{xx} (u, u')$ and $R_{nn} (u, u')$ (which are assumed to be known).

The above formulation gives the solution for 1-D signals. The problem and the solution can be generalized to 2-D signals and images by using both separable and non-separable definitions of the fractional Fourier transform [12, 24]. When applied to 2-D signals and images, some form of windowing is necessary before the fractional Fourier transform stages to reduce the boundary artifacts [12].

Fractional Fourier domain filtering is particularly advantageous when the distortion or noise is of a chirped nature. Such situations are encountered in many real-life

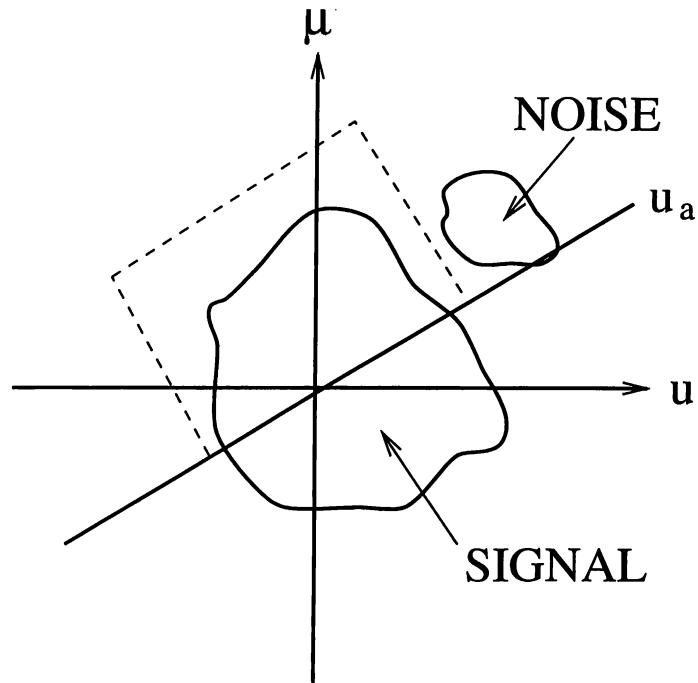


Figure 3.2: Filtering in fractional Fourier domain as observed in the space- (or time-) frequency plane.

applications. For instance, a major problem in the reconstruction from holograms is the elimination of twin-image noise. Since this noise is essentially a modulated chirp signal, it can be dealt with fractional Fourier domain filtering. Another example is the correction of the effects of point or line defects found on lenses or filters in optical systems, which appear at the output plane in the form of chirp artifacts. Another application arises in synthetic aperture radar which employs chirps as transmitted pulses, so that the measurements are related to the terrain reflectivity function through a chirp convolution. This process results in chirp type disturbances caused by moving objects in the terrain, which should be removed if high resolution imaging is to be achieved. Fractional Fourier domain filtering has also been applied to restoration of images blurred by space-varying point spread function or atmospheric turbulence [12]. These type of degradations are typical in astronomical and underwater imaging [87].

3.2 Multi-Stage Filtering in Fractional Fourier Domains

In the previous section we overviewed the single stage filtering in fractional Fourier domains. This filtering configuration has been shown to improve the performance as compared to ordinary Fourier filtering in cases where the time- or space varying systems are involved. We can also find situations where single fractional Fourier domain filtering is insufficient.

As a simple example consider the Fig. 3.3, where the Wigner distributions of a desired signal and an undesired distortion are superimposed. This figure is similar to Fig. 3.2, but in this case we cannot find a single fractional Fourier domain where the noise can easily be separated from the signal. (If we consider the projections onto any oblique axis, we see that the signal and undesired distortion overlap in all of the fractional Fourier domains.) However, by introducing the concept of multiple fractional Fourier domain filters, we can eliminate the noise from the signal as follows. We can first go to the domain represented by ϕ_1 and eliminate the corresponding part of noise (marked as **1** in the figure) by simple unit amplitude mask, then we can go to the domain represented by ϕ_2 and eliminate the corresponding part (marked as **2** in the figure) and finally we can go to the domain represented by ϕ_3 and eliminate the rest of the noise (marked as **3** in the figure).

The above example illustrates a situation where using multiple fractional Fourier domain filters may be beneficial. There are three different ways of generalizing the single-domain fractional Fourier filter to multiple domains. One generalization is the multi-stage or repeated filtering in fractional Fourier domains which has been discussed in [13, 14, 15]. The other two ways are the multi-channel and the filtering circuits configurations which will be discussed in this thesis.

In the multi-stage filtering configuration shown in Fig. 3.4 M single stage fractional Fourier domain filters are combined in series [13, 14, 15, 16]. The input is first transformed into the a_1 th domain where it is multiplied by a filter h_1 . The result is then transformed back into the original domain. This process is repeated M times consecutively. (Notice that this amounts to sequentially visiting the domains a_1, a_2, a_3 , etc. and applying a filter in each.) It has been shown in [14] that, by modifying the filters h_k appropriately, the repeated configuration can be reduced to one involving

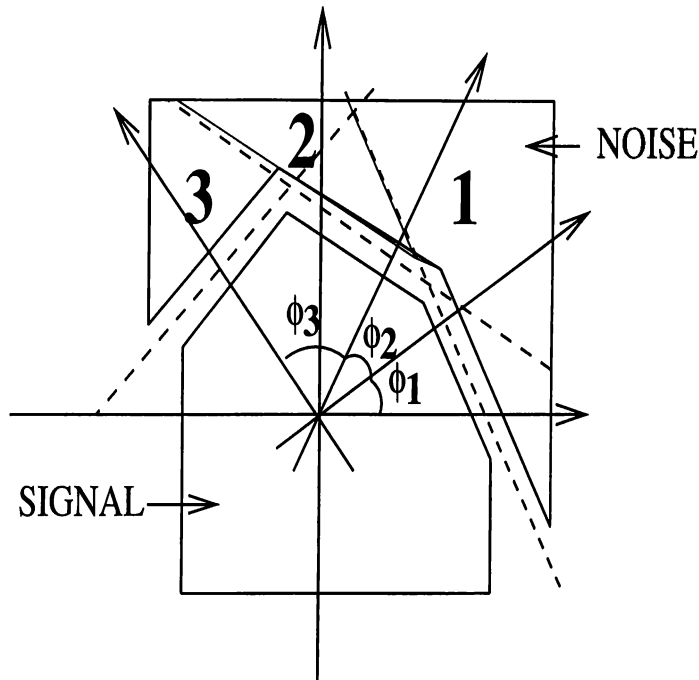


Figure 3.3: Filtering in multiple fractional Fourier domains as observed in the space- (or time-) frequency plane.

only ordinary Fourier transforms. However, the modified filters often exhibit oscillatory behavior so that this reduction is not necessarily beneficial in practice. Another point with this configuration is that the back transform of stage k with order a_k , may be combined with the forward transform of stage $k + 1$ with order a_{k+1} , resulting in a single transform of order $a_{k+1} - a_k$. Thus the system consists of multiplicative filters sandwiched between fractional transform stages of order $a'_k = a_{k+1} - a_k$.

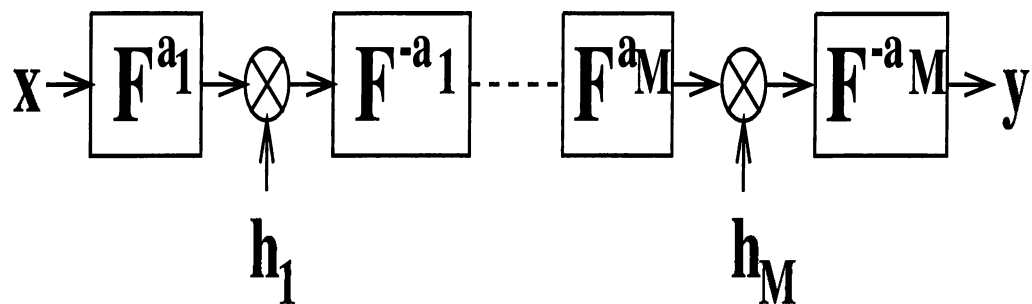


Figure 3.4: Multi-stage filtering in fractional Fourier domains

Let Λ_k denote the operator corresponding to multiplication by the filter function h_k . Then, the overall operator \mathcal{T}_{ms} corresponding to the multi-stage configuration is given

by,

$$\begin{aligned}\mathcal{T}_{\text{ms}} &= \prod_{k=1}^M \mathcal{F}^{-a_k} \Lambda_k \mathcal{F}^{a_k} \\ &= \mathcal{F}^{-a_M} \Lambda_M \dots \mathcal{F}^{a_2 - a_1} \Lambda_1 \mathcal{F}^{a_1}\end{aligned}\tag{3.9}$$

where \mathcal{F}^{a_k} represents the a_k th order fractional Fourier transform operator.

Different applications and interpretations of this filtering configuration has been given and discussed in [13, 14, 15]. Namely, this filtering configuration may be applied to the synthesis of a desired linear transformation kernel, signal restoration and denoising and beam shaping in optics. In the synthesis problem the aim is to synthesize a desired linear transformation kernel \mathcal{T}_d in the form of \mathcal{T}_{ms} . The problem is then to find the optimal filters h_k and domains a_k such that \mathcal{T}_{ms} is as close to \mathcal{T}_d as possible. The criteria of closeness may be a norm between two kernels.

In the signal restoration application, we consider a problem similar to the one discussed in section 3.1. In this case our estimation operator is in the form of \mathcal{T}_{ms} ,

$$x_{\text{est}} = \mathcal{T}_{\text{ms}} x_{\text{obs}}.$$

The problem is then to find the optimal filters h_k and domains a_k so that x_{est} is as close to x as possible. Again the criteria may be a norm.

Regardless of which of the above applications we take, the problem of determining the optimal filter coefficients is difficult for this configuration, since the overall kernel \mathcal{T}_{ms} depends nonlinearly on the filter coefficients h_k . Nevertheless an iterative approach has been successfully applied [13, 15].

We should finally note that when we set $M = 1$, the multi-stage configuration exactly corresponds to the single-stage filtering of previous section.

3.3 Multi-Channel Filtering in Fractional Fourier Domains

A dual configuration to the multi-stage filtering is the multi-channel filtering which we will discuss now. In this configuration we combine the M single stage fractional Fourier domain filters in parallel (Fig. 3.5). The input is first divided into M channels. Then

for each channel k , the input is transformed to the a_k th domain, multiplied with a filter h_k , and then transformed back. The output is obtained by summing the results of each channel.

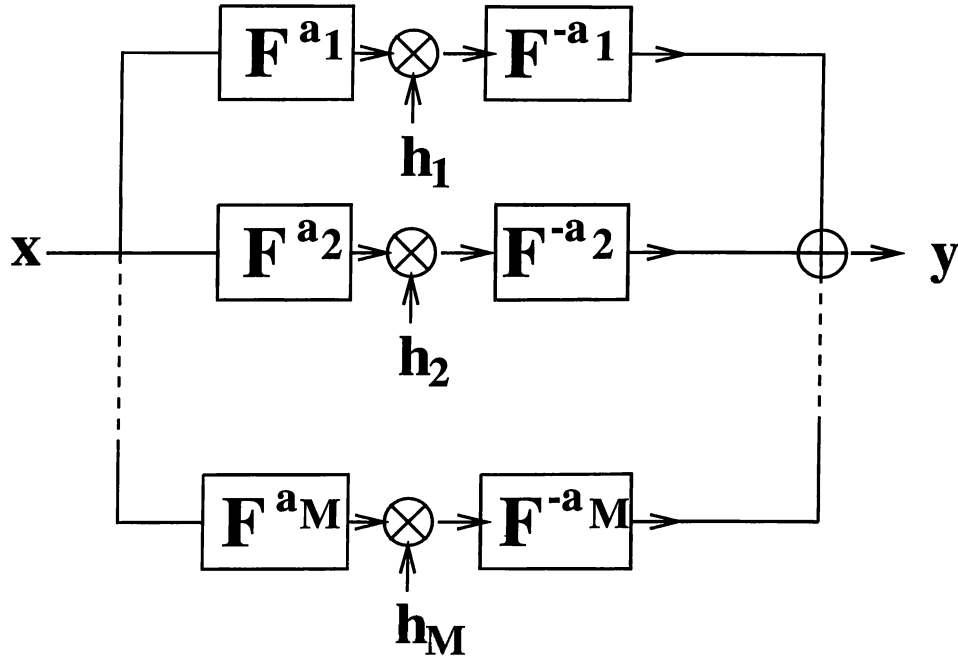


Figure 3.5: Multi-channel filtering in fractional Fourier domains

Again let Λ_k denote the operator corresponding to multiplication by the filter function h_k . Then, the overall operator \mathcal{T}_{mc} corresponding to the multi-channel configuration is given by,

$$\begin{aligned} \mathcal{T}_{\text{mc}} &= \sum_{k=1}^M \mathcal{F}^{-a_k} \Lambda_k \mathcal{F}^{a_k} \\ &= \mathcal{F}^{-a_1} \Lambda_1 \mathcal{F}^{a_1} + \dots + \mathcal{F}^{-a_M} \Lambda_M \mathcal{F}^{a_M} \end{aligned} \quad (3.10)$$

where \mathcal{F}^{a_k} represents the a_k th order fractional Fourier transform operator.

We note that in a more general configuration each channel may be of the form $\mathcal{F}^{a'_k} \Lambda_k \mathcal{F}^{a_k}$ where a_k and a'_k are arbitrary and do not necessarily satisfy $a'_k = -a_k$. In fact, there is no reason not to consider other parametric transforms with fast algorithms.

Different applications and interpretations of this filtering configuration will be given

in chapters 4, 5 and 6. Here we only state that each application discussed for the multi-stage case is also a potential application for this configuration. Finally, we note that $M = 1$ corresponds to the single-stage filtering.

3.4 Filtering Circuits

In the previous sections, we used M single-stage fractional Fourier domain filters as *building blocks* to construct the multi-stage and multi-channel configurations in fractional domains. For the multi-stage case, they are combined in series. For the multi-channel case on the other hand, they are combined in parallel. In analogy to circuit theory, we can generalize these configurations further to filtering circuits in fractional Fourier domains. An example of such filtering circuit is shown in Fig. 3.6.

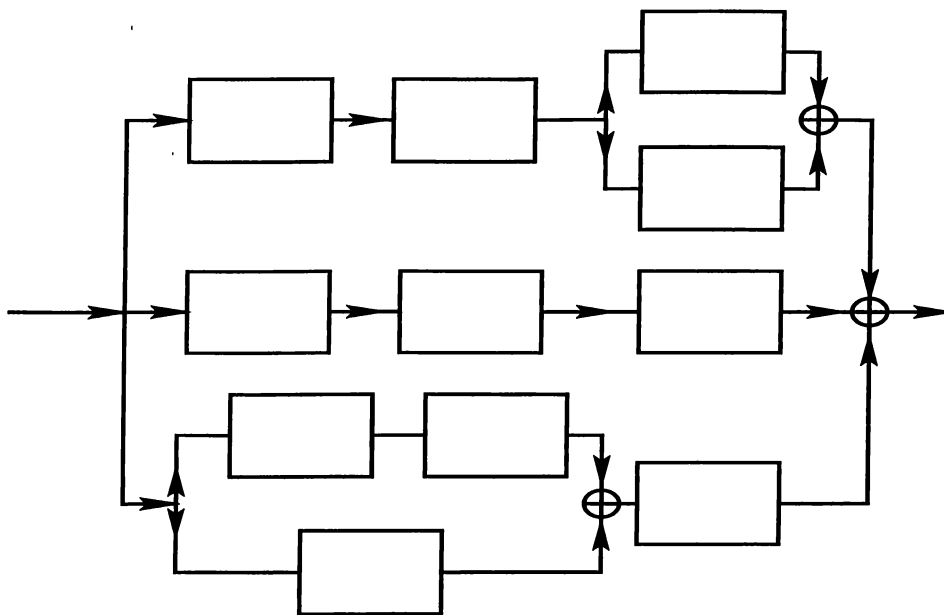


Figure 3.6: An example of filtering circuit in fractional Fourier domains. Each block corresponds to a single-stage filtering in fractional Fourier domain (Fig. 3.1 (d)) with different orders and filter functions.

The multi-channel and multi-stage configurations become the special cases of filtering circuit configurations. Mathematically we can represent the overall system \mathcal{T}_{fc} as

$$\mathcal{T}_{fc} = FC(\mathcal{T}_{ss}) \quad (3.11)$$

where $FC(\cdot)$ is the function representing the filter configuration.

This representation unifies all the configurations we have discussed so far. It can be used in all of the applications suggested for other filters. However the optimal choice of the structure (number of channels and stages) and filters and orders in that structure in a given application seems difficult and requires further research.

One way of obtaining the structure in a given application may be the use of Wigner distributions (as in Fig. 3.3). Interpreting the signal and noise regions may yield a suitable structure.

3.5 Discrete Formulation

Up to now, the configurations have been discussed in a general framework which apply to both discrete and continuous time. To benefit from the insights of linear algebra and to simplify the notation, we will work with the discrete form of the configurations in this section. The continuous formulation is completely analogous but notationally more cumbersome.

Let \mathbf{F}^{a_k} denote the discrete fractional Fourier transform matrix with order a_k [20, 21, 22] and $\mathbf{\Lambda}_k$ denotes the diagonal matrix whose diagonal elements are the elements of the filter vector $\mathbf{h}_k = [h_k[1] \ h_k[2] \ \dots \ h_k[N]]^T$:

$$\mathbf{\Lambda}_k = \begin{bmatrix} h_k[1] & 0 & \dots & \\ 0 & h_k[2] & 0 & \\ 0 & & & \\ 0 & & 0 & h_k[N] \end{bmatrix}. \quad (3.12)$$

Then the overall matrix for the single-stage, multi-stage and multi-channel configurations are given by:

$$\mathbf{T}_{\text{ss}} = \mathbf{F}^{-a} \mathbf{\Lambda} \mathbf{F}^a \quad (3.13)$$

$$\begin{aligned} \mathbf{T}_{\text{ms}} &= \prod_{k=1}^M \mathbf{F}^{-a_k} \mathbf{\Lambda}_k \mathbf{F}^{a_k} \\ &= \mathbf{F}^{-a_M} \mathbf{\Lambda}_M \dots \mathbf{F}^{a_2 - a_1} \mathbf{\Lambda}_1 \mathbf{F}^{a_1} \end{aligned} \quad (3.14)$$

$$\begin{aligned} \mathbf{T}_{\text{mc}} &= \sum_{k=1}^M \mathbf{F}^{-a_k} \mathbf{\Lambda}_k \mathbf{F}^{a_k} \\ &= \mathbf{F}^{-a_1} \mathbf{\Lambda}_1 \mathbf{F}^{a_1} + \dots + \mathbf{F}^{a_M} \mathbf{\Lambda}_M \mathbf{F}^{a_M} \end{aligned} \quad (3.15)$$

We can obtain the other forms for the representations of \mathbf{T}_{ss} and \mathbf{T}_{mc} of the single-stage and multi-channel configurations. To do this, we first identify the columns of the matrix \mathbf{F}^{-a_k} as $\mathbf{f}_{k,j}$:

$$\mathbf{F}^{-a_k} = [\mathbf{f}_{k,1} \ \mathbf{f}_{k,2} \ \dots \ \mathbf{f}_{k,N}] \quad (3.16)$$

By using the unitarity of the fractional Fourier transform, the forward matrix \mathbf{F}^{a_k} can then be written as

$$\mathbf{F}^{a_k} = \begin{bmatrix} \mathbf{f}_{k,1}^\dagger \\ \mathbf{f}_{k,2}^\dagger \\ \vdots \\ \mathbf{f}_{k,N}^\dagger \end{bmatrix}. \quad (3.17)$$

Here, $\mathbf{f}_{k,j}^\dagger$ denotes the j th row of the matrix \mathbf{F}^{a_k} and $(\cdot)^\dagger$ denotes the Hermitian conjugate.

If we plug the above forms of the forward and inverse discrete fractional Fourier matrices into equations 3.13, 3.14 and 3.15 we obtain the following forms for the matrices (\mathbf{T}_{ss} , \mathbf{T}_{ms} and \mathbf{T}_{mc}) of the filtering configurations:

$$\begin{aligned} \mathbf{T}_{\text{ss}} &= \sum_{j=1}^N h_1[j] \mathbf{f}_{1,j} \mathbf{f}_{1,j}^\dagger \\ &= \sum_{j=1}^N h_1[j] \hat{\mathbf{T}}_{1j} \end{aligned} \quad (3.18)$$

$$\begin{aligned} \mathbf{T}_{\text{ms}} &= \left(\sum_{j=1}^N h_M[j] \mathbf{f}_{M,j} \mathbf{f}_{M,j}^\dagger \right) \dots \left(\sum_{j=1}^N h_1[j] \mathbf{f}_{1,j} \mathbf{f}_{1,j}^\dagger \right) \\ &= \left(\sum_{j=1}^N h_M[j] \hat{\mathbf{T}}_{Mj} \right) \dots \left(\sum_{j=1}^N h_1[j] \hat{\mathbf{T}}_{1j} \right) \end{aligned} \quad (3.19)$$

$$\begin{aligned} \mathbf{T}_{\text{mc}} &= \sum_{k=1}^M \sum_{j=1}^N h_k[j] \mathbf{f}_{k,j} \mathbf{f}_{k,j}^\dagger \\ &= \sum_{k=1}^M \sum_{j=1}^N h_k[j] \hat{\mathbf{T}}_{kj} \end{aligned} \quad (3.20)$$

where we introduced the matrices $\hat{\mathbf{T}}_{kj} = \mathbf{f}_{k,j} \mathbf{f}_{k,j}^\dagger$.

From the above equations, it is evident now that the overall matrices of the single-stage and multi-channel configurations are linearly dependent on the filter coefficients $h_k[j]$ and the matrices $\hat{\mathbf{T}}_{kj}$ play the role of a family of “basis matrices” which are used to construct the matrices \mathbf{T}_{ss} and \mathbf{T}_{mc} . It is also evident that \mathbf{T}_{ms} depends nonlinearly on the filter coefficients.

The discrete formulation of the filter circuits can be similarly obtained. The overall system matrix \mathbf{T}_{fc} would also be dependent nonlinearly on the filter coefficients.

3.5.1 Extension to the Rectangular Case

In the previous section and in [8, 10, 13, 14, 15, 25, 26], the overall filter matrices \mathbf{T}_{ss} , \mathbf{T}_{ms} and \mathbf{T}_{mc} are assumed to be $N \times N$ matrices of full rank. In this section we will generalize these configurations to input-output relations where they may be of different length. Thus the resulting overall matrices will be rectangular.

In some applications, we may encounter situations where the signals (vectors) involved may have different lengths. For example consider the following simple system whose input and output are of lengths N_{in} and N_{out} respectively:

$$\mathbf{y} = \mathbf{H}\mathbf{x}. \quad (3.21)$$

Here \mathbf{H} , \mathbf{x} , \mathbf{y} are of dimensions $N_{out} \times N_{in}$, $N_{in} \times 1$ and $N_{out} \times 1$ respectively. In order to handle such applications we can generalize equations 3.13, 3.15 by modifying the dimensions of the diagonal matrices $\mathbf{\Lambda}_k$:

$$(\mathbf{T}_{ss})_{N_{out} \times N_{in}} = \mathbf{F}_{N_{out}}^{-a} \mathbf{\Lambda}_{N_{out} \times N_{in}} \mathbf{F}_{N_{in}}^a \quad (3.22)$$

$$(\mathbf{T}_{mc})_{N_{out} \times N_{in}} = \sum_{k=1}^M \mathbf{F}_{N_{out}}^{-a_k} (\mathbf{\Lambda}_k)_{N_{out} \times N_{in}} \mathbf{F}_{N_{in}}^{a_k} \quad (3.23)$$

where $\mathbf{F}_N^{a_k}$ is the discrete fractional Fourier matrix of dimension $N \times N$ and $(\mathbf{\Lambda}_k)_{N_{out} \times N_{in}}$ is the diagonal matrix of dimension $N_{out} \times N_{in}$:

$$(\mathbf{\Lambda}_k)_{N_{out} \times N_{in}} = \begin{bmatrix} h_k[1] & 0 & \dots & 0 \\ 0 & h_k[2] & 0 & \dots & 0 \\ 0 & & \ddots & \vdots & \\ 0 & & 0 & h_k[N] & 0 \end{bmatrix} \quad N_{out} \leq N_{in} \quad (3.24)$$

$$(\mathbf{\Lambda}_k)_{N_{out} \times N_{in}} = \begin{bmatrix} h_k[1] & 0 & \dots & & \\ 0 & h_k[2] & 0 & & \\ 0 & & \ddots & & \\ 0 & & 0 & h_k[N] & \\ 0 & & & 0 & \end{bmatrix} \quad N_{out} > N_{in} \quad (3.25)$$

where $N \equiv \min(N_{\text{in}}, N_{\text{out}})$. For the case $N_{\text{out}} \leq N_{\text{in}}$, last $N_{\text{in}} - N$ columns of the matrix $(\mathbf{\Lambda}_k)_{N_{\text{out}} \times N_{\text{in}}}$ are zero whereas the last $N_{\text{out}} - N$ rows of the matrix $(\mathbf{\Lambda}_k)_{N_{\text{out}} \times N_{\text{in}}}$ are zero if $N_{\text{out}} > N_{\text{in}}$. We here note that if $N_{\text{in}} \neq N_{\text{out}}$ there is an ambiguity in placing the elements of the filters to the diagonal. We choose to start from the upper left element of the matrix.

The generalization of the multi-stage configuration to rectangular matrices is somewhat ambiguous. The only necessary condition is to match the input and output stage dimensions. The dimensions of the other stages are not constrained and may be freely chosen. But in order to preserve the information as much as possible it is better to choose the dimensions equal or larger than $N \equiv \min(N_{\text{out}}, N_{\text{in}})$ for each stage. We may set the first $\mathbf{\Lambda}_1$ and last filter $\mathbf{\Lambda}_M$ dimensions to $N_{\text{out}} \times N_{\text{inter}}$ and $N_{\text{inter}} \times N_{\text{in}}$ respectively and take the dimensions of other stages to be equal to $N_{\text{inter}} \times N_{\text{inter}}$, or may taper dimensions gently or somehow to match from N_{in} to N_{out} . In our simulations, the results obtained from these two choices don't differ significantly. However, more conclusive statements would require further research.

We can easily generalize the alternative representations of equations 3.18 and 3.20 to the rectangular case as well:

$$(\mathbf{T}_{\text{ss}})_{N_{\text{out}} \times N_{\text{in}}} = \sum_{j=1}^N h_1[j] (\hat{\mathbf{T}}_{1j})_{N_{\text{out}} \times N_{\text{in}}} \quad (3.26)$$

$$(\mathbf{T}_{\text{mc}})_{N_{\text{out}} \times N_{\text{in}}} = \sum_{k=1}^M \sum_{j=1}^N h_k[j] (\hat{\mathbf{T}}_{kj})_{N_{\text{out}} \times N_{\text{in}}} \quad (3.27)$$

where $(\hat{\mathbf{T}}_{kj})_{N_{\text{out}} \times N_{\text{in}}}$ is again obtained by multiplying the j th column of $\mathbf{F}_{N_{\text{out}}}^{-a_k}$ with the j th row of $\mathbf{F}_{N_{\text{in}}}^{a_k}$:

$$\hat{\mathbf{T}}_{kj}[m, n] = \mathcal{F}_{N_{\text{out}}}^{-a_k}[m, j] \mathcal{F}_{N_{\text{in}}}^{a_k}[j, n] \quad m = 1, \dots, N_{\text{out}}; n = 1, \dots, N_{\text{in}}. \quad (3.28)$$

3.5.2 Complexity Analysis

In this section we consider the implementation costs of each of the filtering configurations and compare them with the implementation cost of general linear systems. The main idea is that if the approximation in implementing a general linear system with parallel or serial filtering configurations with a few number of filters (M) is an acceptable one, significant reduction of cost is possible.

Let the input be represented by N_{in} samples and the output by N_{out} samples. Digital implementation of such general linear systems will take $O(N_{\text{out}}N_{\text{in}})$ time. Common single-stage optical implementations, such as optical matrix-vector multiplier architectures or multi-facet architectures [2] require an optical system whose space-bandwidth product is $O(N_{\text{out}}N_{\text{in}})$. On the other hand, the digital implementation of shift-invariant systems takes $O(N_{\text{in}} \log N_{\text{in}} + \min(N_{\text{in}}, N_{\text{out}}) + N_{\text{out}} \log N_{\text{out}}) \approx O(N' \log N')$ time (by using the FFT), where $N' \equiv \max(N_{\text{out}}, N_{\text{in}})$. Their optical implementation requires a pair of optical systems whose space-bandwidth products are $O(N_{\text{in}})$ and $O(N_{\text{out}})$ (for instance, by using a pair of “2f” systems to take the Fourier transforms). The cost of single-stage fractional Fourier domain filtering is the same as that of shift-invariant systems which correspond to ordinary Fourier domain filtering since the fractional Fourier transform can be implemented both optically and digitally with approximately the same cost of ordinary Fourier transform.

In the above paragraph, we have implicitly assumed that all rows of the matrix representing the general linear system are linearly independent. Since the rank R of a matrix always satisfies $R \leq N \equiv \min(N_{\text{out}}, N_{\text{in}})$, this is possible only when $R = N_{\text{out}} \leq N_{\text{in}}$. In the general case, the rank R corresponds to the number of linearly independent rows. Multiplying these linearly independent rows with the input takes $O(RN_{\text{in}})$ time. Multiplication of other rows can be accomplished more easily since it is known that remaining $(N_{\text{out}} - R)$ rows are known to be linear combinations of the other R rows. Since R coefficients are sufficient to characterize these rows, multiplying them with the input takes $O((N_{\text{out}} - R)R)$ time. The total amount of time is thus

$$O(RN_{\text{in}} + (N_{\text{out}} - R)R) = O(R(N_{\text{in}} + N_{\text{out}}) - R^2). \quad (3.29)$$

We are not able to propose a simple scheme for exploiting rank information in optical implementation, so that we again take the cost of optical implementation as before.

Now we turn our attentions to the implementation costs of rectangular multi-stage and multi-channel filtering configurations. Since each of these configurations consists of M single-stage filters, the digital implementation costs are given by:

$$O(M(N_{\text{in}} \log N_{\text{in}} + N_{\text{out}} \log N_{\text{out}} + N)) \approx O(MN' \log N') \quad (3.30)$$

for the multi-channel configuration and

$$O\left(N_{\text{in}} \log N_{\text{in}} + \sum_{k=1}^M (\min(N_{k-1}, N_k) + N_k \log N_k)\right) \approx O\left(\sum_{k=0}^M \min(N_{k-1}, N_k) + N_k \log N_k\right)$$

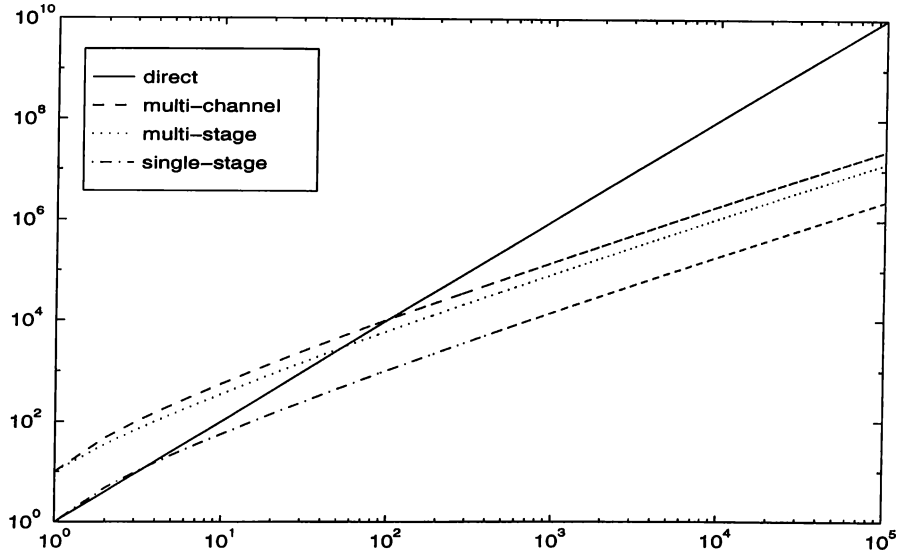


Figure 3.7: Cost comparison of exact and approximate implementations of linear systems.

$$\approx O\left(\sum_{k=0}^M N_k \log N_k\right) \quad (3.31)$$

for the multi-stage configuration. In the last equation N_k denotes the output dimension at stage k . It seems natural that $N_{\text{in}} = N_0 \leq N_1 \leq N_2 \leq \dots \leq N_{M-1} \leq N_M = N_{\text{out}}$ or $N_{\text{in}} = N_0 \geq N_1 \geq N_2 \geq \dots \geq N_{M-1} \geq N_M = N_{\text{out}}$ depending on whether $N_{\text{in}} \leq N_{\text{out}}$ or $N_{\text{in}} \geq N_{\text{out}}$. For both cases we may approximately write the cost of the multi-stage configuration as $O(MN' \log N')$. Optical costs may be similarly found. The multi-channel system requires M pairs of optical systems whose space-bandwidth products are $O(N_{\text{in}})$ and $O(N_{\text{out}})$. The multi-stage configuration on the other hand can be implemented with $M + 1$ optical systems with space-bandwidth products $O(N_k)$.

For a simple illustration, we plotted the exact costs of each filtering configuration together with the cost of a general linear system as a function of N in Fig. 3.7. In this figure, we take $M = 10$ for both the series and parallel configurations, and assume $N_{\text{out}} = N_{\text{in}} = N$ and $R = N$.

The results presented in this section have been obtained in collaboration with Hakan Özaktaş.

3.6 Discussion

In this chapter we introduced the concept of fractional Fourier domain filtering configurations in fractional Fourier domains. These filtering configurations may find applications in areas where general linear systems are used. The aim is to approximate the general linear system with these filters with small M , so that similar performances can be achieved with lower implementation cost.

Both serial and parallel filtering configurations have at most $MN + M$ degrees of freedom. As discussed, their digital implementation will take $O(MN \log N)$ time since the fractional Fourier transform can be implemented in $O(N \log N)$ time [20]. Optical implementation will require an M -stage or M -channel optical system, each with space-bandwidth product N . We see that these configurations lie (interpolate) between general linear systems and shift-invariant systems both in terms of cost and flexibility. If we choose M to be small, cost and flexibility are both low. If we choose M larger, cost and flexibility are both higher. In between, these systems give us considerable freedom in trading off efficiency and flexibility for each other, the latter which will translate into a better approximation and greater accuracy in most applications. $M = 1$ corresponds to single-stage filtering. As M approaches N , the number of degrees of freedom of the introduced filtering configurations approaches that of a general linear system.

To see the cost-accuracy trade-off better, we consider the Fig. 3.8. In this figure we have plotted both the cost and error as a function of number of filters in a given application. The cost clearly increases as M increases, and the error will decrease since we have more flexibility. If we eliminate the number of filters from both plots we obtain the cost-error plot.

The important point is that increasing M gives us greater flexibility and will allow us to realize a broader class of linear systems, or put in a different way, to better approximate a given linear system. In other words, the capabilities of an M -filter system can be characterized in two ways. First, for a given value of M , we can realize a certain subset of all linear systems *exactly* (or to some other specified degree of accuracy). As M increases, the subset in question becomes larger and larger. Second, and perhaps more useful, is to consider the problem of approximating a *given* linear system. For a given value of M , we can approximate this system with a certain degree of accuracy (or error). For instance, a shift-invariant system can be realized with perfect accuracy with $M = 1$. In general, there will be a finite accuracy for each value of M . As M is increased, the

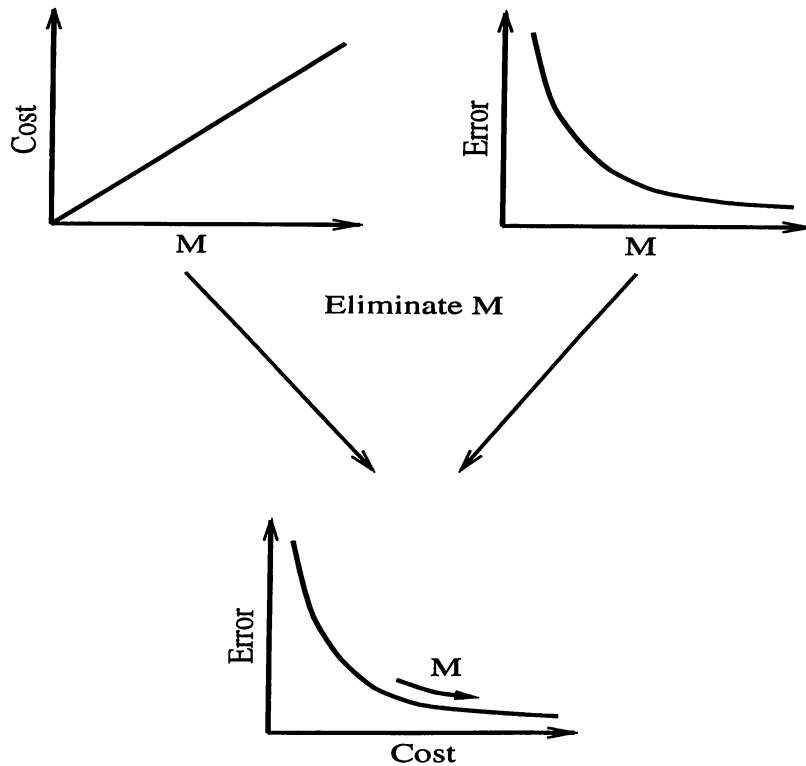


Figure 3.8: Cost-accuracy trade-off.

accuracy will usually increase (but never decrease). Thus, in the context of a particular application or problem, we can seek the minimum value of M which results in the desired accuracy, or the highest accuracy (or minimum error) that can be achieved for a given value of M . Of course, this amounts to seeking the best performance for given cost, or least cost for given performance. Such cost-performance points are referred to as *Pareto optimal* cost-performance combinations. The locus of such Pareto optimal points constitutes the cost-performance tradeoff curve. Given our particular situation, we can choose the most desirable point on this tradeoff curve. We envision this approach to be particularly useful for relatively small values of M , on the low cost, low flexibility side of the tradeoff curve. This is particularly true in analog optical systems, where attenuation and noise would limit the number of stages or channels.

Naturally, the number of stages and filters required to attain a given accuracy will be smaller for matrices exhibiting greater regularity or other more subtle forms of intrinsic structure. In such cases, direct implementation of the matrix-vector product is clearly inefficient. The regularity or structure inherent in a given matrix can be exploited on a case by case basis through ingenuity or invention; most sparse matrix algorithms and fast

transform algorithms are obtained in this manner. In contrast, our method provides a systematic way of obtaining an efficient implementation which does not require ingenuity on a case by case basis. This approach would be especially useful when the regularity or structure of the matrix is not simple or is not expressed symbolically or when we are presented with a specific matrix in numerical form for which no easily discernible regularity or structure is apparent.

A distinct circumstance in which the method may be beneficial, even when a strong intrinsic structure does not exist, is when it is sufficient to compute the matrix-vector product with limited accuracy. This may be the case when some other component or stage of the overall system limits the accuracy to a lower value anyway, or simply when the application itself demands limited accuracy.

The proposed systems can be used in a given application in one of two distinct ways, which we distinguish in detail in chapter 4. Here we only discuss briefly. **(i)** Starting with a signal restoration, recovery, reconstruction or synthesis problem, we determine the optimal linear estimation or reconstruction matrix using any models and methods considered appropriate. Or, we may simply be given a matrix \mathbf{H} to multiply input vectors \mathbf{x} with. Then, we seek the transform orders a_k and filters \mathbf{h}_k such that the resulting matrices \mathbf{T}_{ss} , \mathbf{T}_{ms} , or \mathbf{T}_{mc} (as given by (3.13), (3.14) or 3.15) is as close as possible to \mathbf{H} according to some specified criteria. **(ii)** We take (3.13), (3.14) or 3.15) as a constraint on the form of the linear estimation or reconstruction matrix to be employed. Given a specific optimization criteria, such as minimum mean-square error, we find the optimal values of a_k and \mathbf{h}_k such that the given criteria is optimized. We will say more about these approaches in the next chapter.

The repeated and multi-channel configurations may be based on other transforms with fast algorithms, instead of the fractional Fourier transform. For instance, the three-parameter family of linear canonical transforms may be used in place of the fractional Fourier transform [88]. Concentrating on (3.15), the essential idea is to approximate a general linear operator as a linear combination of operators with fast algorithms. If an acceptable approximation can be found with a value of M which is not too large, the computational burden can be significantly reduced.

For instance, the singular value decomposition (SVD) leads to a similar approximation if we keep only the M largest singular values and discard the others: $\mathbf{y} = \left[\sum_{k=1}^M \lambda_k \mathbf{U}_k \right] \mathbf{x}$. Since \mathbf{U}_k is of outer-product form, its implementation takes only $O(N)$ time for an overall implementation time of $O(MN)$. The similarity between equation 3.15

and SVD lead us to a concept of fractional Fourier domain decomposition (FFDD) [89] which we will discuss in chapter 4.

The multi-channel configuration may also be used for windowed fractional Fourier transform applications. In this case we modify the configuration as in Fig. 3.9 so that for each channel or branch we first multiply the input with a window function \mathbf{W}_k to select the appropriate time-slot or local region. Here the matrix \mathbf{W}_k is a diagonal matrix with the window function on the main diagonal. The window function may be different for each channel or it may be same and only slided to the appropriate time slot. This modified multi-channel structure corresponds to filtering different time-slots of input in different fractional Fourier domains. The overall operator corresponding to this configuration is given by

$$\begin{aligned}\mathcal{T}_{\text{wmc}} &= \sum_{k=1}^M \mathcal{F}^{-a_k} \Lambda_k \mathcal{F}^{a_k} \mathcal{W}_k \\ &= \mathcal{F}^{-a_1} \Lambda_1 \mathcal{F}^{a_1} \mathcal{W}_1 + \dots + \mathcal{F}^{a_M} \Lambda_M \mathcal{F}^{a_M} \mathcal{W}_M\end{aligned}\quad (3.32)$$

and in discrete time

$$\begin{aligned}\mathbf{T}_{\text{wmc}} &= \sum_{k=1}^M \mathbf{F}^{-a_k} \Lambda_k \mathbf{F}^{a_k} \mathbf{W}_k, \\ &= \sum_{k=1}^M \sum_{j=1}^N h_k[j] \mathbf{f}_{k,j} \mathbf{f}_{k,j}^\dagger \mathbf{W}_k, \\ &= \sum_{k=1}^M \sum_{j=1}^N h_k[j] \hat{\mathbf{T}}_{kj} \mathbf{W}_k\end{aligned}\quad (3.33)$$

where $\hat{\mathbf{T}}_{kj} = \mathbf{f}_{k,j} \mathbf{f}_{k,j}^\dagger$ as before.

Up to this point, we have discussed the filtering circuits for one-dimensional signals. Generalization to two dimensions is easy if we use the separable definition of the fractional Fourier transformation. Generalization using non-separable definition is also possible but requires more care.

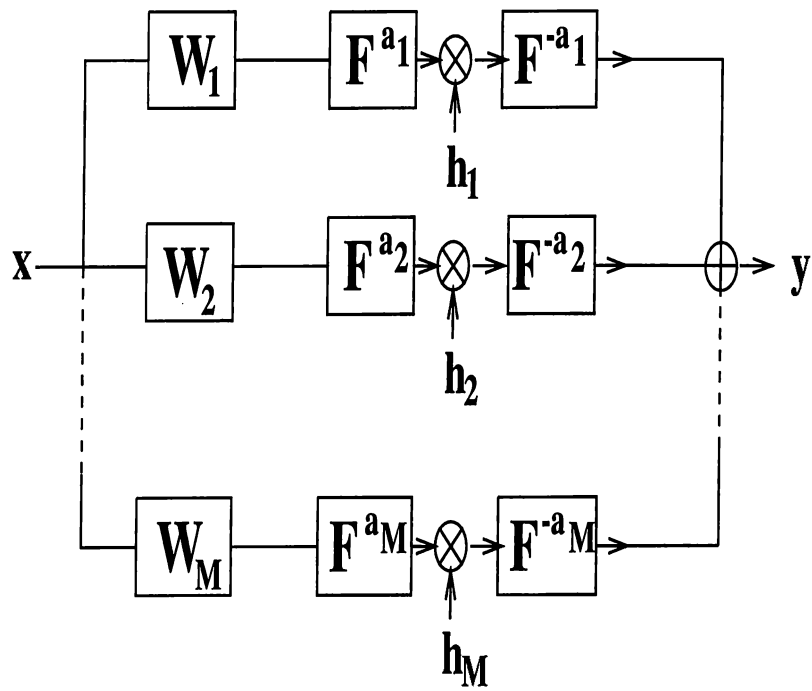


Figure 3.9: Short-time fractional Fourier filter

Chapter 4

Applications in System Synthesis

The filtering circuits concept discussed in the previous chapter may find many applications in signal and optical information processing. In this and the next chapters we will discuss some of the possible applications. To gain useful insight, we will divide application areas into three groups: system synthesis, signal synthesis and signal recovery.

In the synthesis applications our aim is to synthesize a desired input or output signal, or a desired system. We will apply the concept of fractional Fourier domain filtering to obtain the desired input-output relation or a desired signal. We will consider the signal synthesis problem in the next chapter. Here we discuss in some detail the problem of synthesizing a given desired system in the form of a filtering circuit.

The problem of approximately synthesizing a general linear system arises when we want to implement that system efficiently. If we can approximately synthesize a system in terms of a few number of other systems with efficient implementation algorithms, then we can reduce the cost considerably. In section 4.1 we will discuss this idea in detail, overview some existing methods and propose our method of synthesizing a general linear system in the form of fractional Fourier domain filters. We will also give simulation examples showing the effectiveness of the proposed filtering configurations.

Before going into the details of the system synthesis applications, we will first discuss the different solution methods that can be used in both signal and system synthesis, and signal recovery applications.

Distinct Approaches in Applications

Here we will distinguish two distinct approaches which can be pursued for the signal synthesis and signal recovery applications to be discussed in the next chapters: (i) Starting with a signal restoration, recovery, reconstruction or synthesis problem, we determine the optimal linear estimation or reconstruction matrix using any models and methods considered appropriate. Or, we may simply be given a matrix \mathbf{H} to multiply input vectors \mathbf{x} with. Then, we seek the transform orders a_k and filters \mathbf{h}_k such that the resulting matrices \mathbf{T}_{ss} , \mathbf{T}_{ms} , or \mathbf{T}_{mc} (as given by (3.13), (3.14) or 3.15) is as close as possible to \mathbf{H} according to some specified criteria. This approach is nothing but the system synthesis we will discuss in this chapter. (ii) We take (3.13), (3.14) or 3.15) as a constraint on the form of the linear estimation, reconstruction or synthesis matrix to be employed. Given a specific optimization criteria, such as minimum mean-square error, we find the optimal values of a_k and \mathbf{h}_k such that the given criteria is optimized.

We will briefly discuss these two approaches below.

Approach (i) : Kernel Synthesis

In this approach, given a matrix \mathbf{H} with dimensions $N_{\text{out}} \times N_{\text{in}}$ to multiply input vectors \mathbf{x} with, we seek the transform orders a_k and filters \mathbf{h}_k such that the resulting matrices \mathbf{T}_{ss} , \mathbf{T}_{ms} , or \mathbf{T}_{mc} (as given by (3.13), (3.14) or 3.15) is as close as possible to \mathbf{H} according to some specified criteria. The desired matrix \mathbf{H} may represent the optimum general linear estimation or reconstruction matrix that is found by other standard or fast techniques. This problem is in fact the system synthesis problem discussed below in section 4.1. Thus we can also reduce the signal synthesis, signal recovery or reconstruction problems to be discussed in the next chapters to a system synthesis problem by first finding the optimal general linear system.

Approach (ii) : Kernel Constraint

In this approach, we restrict the linear transformation between the input and output signals to the filtering configurations whose kernels are given by equations 3.13, 3.14, and 3.15. That is, we take these equations as constraints on the form of the linear transformations to be employed in a given application. We then search for the optimum filter profiles. This approach may be applied to both signal synthesis and signal restoration problems. However, the reader may also find different applications where significant improvements in performance is obtained when the linear transformation between the input and output signals is formed as one of the filtering operations discussed

in chapter 3.

The formulation and application of this approach depends highly on a given application. So this approach will be discussed in more detail in later sections when specific applications are discussed. We also refer the reader to section 3.1 for an example application.

Although for both of the approaches (i) and (ii), the aim is to approximate a linear system by these configurations, the criteria used in each approximation is different. In approach (i), determination of the optimal general linear system (determination of the solution) is decoupled from determination of the filters and transform orders (implementation of the solution), whereas these are tightly coupled in approach (ii). However, we conjecture that this approach is more restrictive than approach (ii), for which a better tradeoff curve can be obtained. An interesting problem which remains open is to explore the relation between the filtering configurations obtained from these two approaches.

The single stage and multi-stage filtering configurations possess analytic solutions for both of the approaches in the applications we consider. The problem can be reduced to a least-squares problem that can be solved using linear-algebra methods. We refer the reader to section 4.1.1 for an example. However solving these equations may require excessive memory and time. The multi-stage configuration, on the other hand, leads to a non-linear set of equations that may be solved using iterative approaches. Below we will discuss a sub-optimal method that can be used to obtain the filter coefficients for both of the approaches and for all of the configurations we propose.

Matching Pursuit Algorithm

We have to solve linear or non-linear equations in order to find the optimal filter coefficients in the both of the approaches above. These equations may become large and require high implementation cost when the signal sizes involved are large. A fast but approximate method that can be used for the solution of both approaches is the matching pursuit algorithm. This algorithm is an iterative algorithm and tries to find the optimal orders and filter coefficients one at a time.

In a given application, we start with a single-stage filtering problem (which is relatively easy compared to the other configurations) and find the optimal order and filter coefficients. We then modify the problem with this known single-stage filter, and apply the algorithm once again. We go on with this procedure until the number of filters

M is reached.

For example we consider the signal restoration problem of section 3.1 with multi-channel filtering configuration. The estimate is given by:

$$\mathbf{x}_{\text{est}} = \mathbf{T}_{\text{mc}}\mathbf{x}_{\text{obs}}$$

To solve the optimal orders and filters with matching pursuit algorithm we first find the optimal single-stage filter $\mathbf{T}_{\text{ss,opt}}$ as in section 3.1. We then find the error signal $\mathbf{e} = \mathbf{x} - \mathbf{T}_{\text{ss,opt}}\mathbf{x}_{\text{obs}}$ and try to estimate \mathbf{e} from \mathbf{x}_{obs} by another single-stage filter:

$$\min E \left[\|\mathbf{e} - \mathbf{T}_{\text{ss}}\mathbf{x}_{\text{obs}}\|^2 \right]$$

We then update the error by using this optimal single stage-filter and try to estimate it yet by another single-stage filter. We go on with this process until the number of filters M is reached.

This method can also be used in kernel synthesis approach that will be discussed in section 4.1.1. We will comment on this when we discuss kernel synthesis in detail.

The matching pursuit algorithm in general does not yield the optimal filter coefficients and fractional orders that can be achieved by chosen number of filters and configuration. It finds a sub-optimal solution. Its main advantage is that the solution can be obtained efficiently in an iterative manner.

4.1 General Linear System Synthesis

In a system synthesis problem, we want to synthesize a desired system, i.e. a specific input-output relation. This problem arises especially when the direct implementation of this desired system is costly and we can satisfy ourselves by an approximate but efficiently implementable system. Direct optical implementation of general linear systems requires optical components with space-bandwidth products of the order of N^2 . Similarly digital implementation of such systems requires $O(N^2)$ multiplications. If we can approximate the desired system by synthesizing or decomposing it with other systems with efficient implementations, we can reduce the cost considerably. This problem is in fact a well known problem and is also related with the signal compression problem. For instance, $N_{\text{out}} \times N_{\text{in}}$ matrix may both represent an image or a system acting on one-dimensional

signals. Thus the decomposition of this matrix may be interpreted both as a two-dimensional image (signal) representation, or a decomposition of a linear operator which represents a system that acts on one-dimensional signals. When interpreted as signal representations, these synthesis or decompositions may be used for data compression and when interpreted as an operator decomposition they may lead to the fast implementation of that operator.

The singular-value decomposition (SVD) and unitary transform domain representations are the most widely known and used decompositions. In this thesis we introduce the synthesis or decomposition in the form of fractional Fourier domain filters. We will also discuss below the *fractional Fourier domain decomposition* (FFDD). The FFDD is a matrix decomposition which has some different interpretations in addition to similarities as compared with the above existing decompositions. We will first review these two important class of existing decompositions and then discuss the FFDD. Our discussion will be based on matrices which can be interpreted both as an image (signal) or a linear operator characterizing a system. Generalization to higher dimensions is possible but excluded from consideration here.

The singular-value decomposition (SVD) plays a fundamental role in signal and system analysis, representation, and processing with many applications in diverse areas. The SVD of an arbitrary $N_{\text{out}} \times N_{\text{in}}$ complex matrix \mathbf{H} is

$$\mathbf{H}_{N_{\text{out}} \times N_{\text{in}}} = \mathbf{U}_{N_{\text{out}} \times N_{\text{in}}} \mathbf{\Sigma}_{N_{\text{out}} \times N_{\text{in}}} \mathbf{V}_{N_{\text{in}} \times N_{\text{in}}}^{\dagger}, \quad (4.1)$$

where \mathbf{U} and \mathbf{V} are unitary matrices whose columns are the eigenvectors of $\mathbf{H}\mathbf{H}^{\dagger}$ and $\mathbf{H}^{\dagger}\mathbf{H}$ respectively. The superscript \dagger denotes Hermitian transpose. $\mathbf{\Sigma}$ is a diagonal matrix whose elements σ_j (the singular values) are the nonnegative square roots of the eigenvalues of $\mathbf{H}\mathbf{H}^{\dagger}$ and $\mathbf{H}^{\dagger}\mathbf{H}$. The number of strictly positive singular values is equal to the rank R of \mathbf{H} . The SVD can also be written in the form of an outer-product (or spectral) expansion

$$\mathbf{H} = \sum_{j=1}^R \sigma_j \mathbf{u}_j \mathbf{v}_j^{\dagger} \quad (4.2)$$

where \mathbf{u}_j and \mathbf{v}_j are the columns of \mathbf{U} and \mathbf{V} . It is common to assume that the σ_j are ordered in decreasing value. Equation 4.2 can also be interpreted as an expansion of the matrix \mathbf{H} in terms of basis matrices of an outer-product form $\mathbf{u}_j \mathbf{v}_j^{\dagger}$. Each outer-product matrix can be implemented with a cost of $O(N)$.

It is well known that the least-squares rank R' approximation of the matrix \mathbf{H} is obtained by keeping the largest R' eigenvalues in equation 4.2. Thus if some or most of

the eigenvalues of \mathbf{H} can be discarded, we can reduce the cost of direct implementation considerably. Interpreted as a two-dimensional signal, this case also corresponds to data compression.

Another decomposition is the transform domain representation. The transform domain representation of an arbitrary $N_{\text{out}} \times N_{\text{in}}$ complex matrix \mathbf{H} is given by:

$$\mathbf{H}_{N_{\text{out}} \times N_{\text{in}}} = \mathbf{P}_{N_{\text{out}} \times N_{\text{out}}}^{-1} \hat{\mathbf{H}}_{N_{\text{out}} \times N_{\text{in}}} (\mathbf{P}_{N_{\text{in}} \times N_{\text{in}}}^{-1})^T, \quad (4.3)$$

$$= \sum_{k=1}^{N_{\text{out}}} \sum_{j=1}^{N_{\text{in}}} \hat{H}_{kj} \mathbf{p}_k \mathbf{p}_j^T, \quad (4.4)$$

where \mathbf{P} is a unitary fast transform, \mathbf{p}_k are the columns of \mathbf{P}^{-1} , and $\hat{\mathbf{H}}_{N_{\text{out}} \times N_{\text{in}}}$ is the representation of $\mathbf{H}_{N_{\text{out}} \times N_{\text{in}}}$ in the transform domain. For instance, if $\mathbf{P} = \mathbf{F}$ is the discrete Fourier transform matrix (DFT matrix), equation 4.4 then corresponds to the ordinary Fourier domain representation of $\mathbf{H}_{N_{\text{out}} \times N_{\text{in}}}$.

If most of the components of $\hat{\mathbf{H}}$ can be discarded, equation 4.4 may also lead to fast implementation of \mathbf{H} . However it would need to be truncated quite severely to lead to a satisfactory fast implementation. On the other hand, we can force $\hat{\mathbf{H}}$ to be a diagonal matrix for fast implementation. However, this would correspond merely to the *single-domain* version of the scheme we will present below.

In this thesis we propose to approximate a given arbitrary $N_{\text{out}} \times N_{\text{in}}$ matrix in the form of fractional Fourier domain filtering configurations given by equations 3.18, 3.19 and 3.20. The problem of approximating a given arbitrary matrix in the form of equation 3.19 was introduced previously in [13]. Here we will discuss the multi-channel configuration keeping in mind that for $M = 1$ it reduces to the single-stage configuration.

We first define the fractional Fourier domain decomposition (FFDD) of a matrix \mathbf{H} as [89]

$$\mathbf{H}_{N_{\text{out}} \times N_{\text{in}}} = \sum_{k=1}^{N'} \mathbf{F}_{N_{\text{out}}}^{-a_k} [\mathbf{\Lambda}_k]_{N_{\text{out}} \times N_{\text{in}}} (\mathbf{F}_{N_{\text{in}}}^{-a_k})^\dagger, \quad (4.5)$$

$$= \sum_{k=1}^{N'} \sum_{j=1}^N h_k[j] (\hat{\mathbf{T}}_{kj})_{N_{\text{out}} \times N_{\text{in}}} \quad (4.6)$$

where $\mathbf{\Lambda}_1, \mathbf{\Lambda}_2, \dots, \mathbf{\Lambda}_{N'}$ are diagonal matrices each of whose $N = \min(N_{\text{out}}, N_{\text{in}})$ elements correspond to filter coefficients as discussed, $(\hat{\mathbf{T}}_{kj})_{N_{\text{out}} \times N_{\text{in}}}$ is as given by (3.28), and $N' = \max(N_{\text{out}}, N_{\text{in}})$. When \mathbf{H} is Hermitian (skew-Hermitian), filters \mathbf{h}_k are real (imaginary).

We also note that $(\mathbf{F}_{N_{\text{in}}}^{-a_k})^\dagger = \mathbf{F}_{N_{\text{in}}}^{a_k}$. Equation 4.6 is simply an expansion of \mathbf{H} in terms of the *basis matrices* $\hat{\mathbf{T}}_{kj}$, $1 \leq k \leq N'$, $1 \leq j \leq N$, where the $h_k[j]$ serve as the weighting coefficients of the expansion.

Comparing and contrasting the FFDD with the SVD will help gain insight into the FFDD. If we compare one term on the right-hand side of equation 4.6 with the right-hand side of equation 4.1, we see that they are similar in that they both consist of 3 terms of corresponding dimensionality, the first and third being unitary matrices and the second being a diagonal matrix. But whereas the columns of \mathbf{U} and \mathbf{V} constitute orthonormal bases specific to \mathbf{H} , the columns of $\mathbf{F}_{N_{\text{out}}}^{-a_k}$ and $\mathbf{F}_{N_{\text{in}}}^{-a_k}$ constitute orthonormal bases for the a_k th fractional Fourier domain. Customization of the decomposition is achieved through the coefficients $h_k[j]$ (and perhaps also the orders a_k). Also to a certain extent, the inner summation in equation 4.6 resembles the outer-product form of the SVD given in equation 4.2. The $N_{\text{out}} \times N_{\text{in}}$ matrices $(\hat{\mathbf{T}}_{kj})_{N_{\text{out}} \times N_{\text{in}}}$ are of unit rank since they are the outer product of vectors.

We can also compare the FFDD with the transform domain representation. Although the equations 4.6 and 4.4 look very similar, the expansion we are proposing *cannot* be written in the form of (4.3) for any choices of a_k and $h_k[j]$. In equation 4.4, the two summations correspond to the two dimensions, constituting an expansion in terms of the separable basis images $\mathbf{p}_k \mathbf{p}_j^T$. On the other hand, in equation 4.6, one of the summations runs over filter coefficients whereas the other runs over different fractional domains. Whereas there is only a single fixed transform in question in the previous approach, here we have a summation over a series of fractional Fourier transforms with the parameters a_k , providing a much more flexible means of approximating a given matrix.

We now turn to the problem of approximating a system in the form of a multi-channel fractional Fourier domain filter. If we can approximate a given matrix \mathbf{H} by keeping a moderate number of $h_k[j]$ in equation 4.6, we may reduce the implementation cost considerably as discussed previously in sections 3.6. Below we will discuss how filter coefficients $h_k[j]$ can be found in order to approximate the matrix \mathbf{H} in the least squares sense. We will then give some examples to illustrate the applications.

Some of the results presented in this section have been obtained in collaboration with Hakan Özaktas.

4.1.1 Solution of the System Synthesis Problem

In this section we will show how the optimal filter coefficients of a given fractional Fourier filtering configuration may be found. We define the problem again: Given a matrix \mathbf{H} with dimensions $N_{\text{out}} \times N_{\text{in}}$ to multiply input vectors \mathbf{x} with, we seek the transform orders a_k and filters \mathbf{h}_k such that the resulting matrices \mathbf{T}_{ss} , \mathbf{T}_{ms} , or \mathbf{T}_{mc} (as given by (3.13), (3.14) or 3.15) is as close as possible to \mathbf{H} according to some specified criteria. The criteria of the closeness between the desired matrix and the filter configuration matrix is taken as Frobenious norm:

$$\sigma_e^2 = \|\mathbf{H} - \mathbf{T}\|_F^2, \quad (4.7)$$

For matrices the Frobenious norm is defined as

$$\|\mathbf{H} - \mathbf{T}\|_F^2 = \sum_{m=1}^{N_{\text{out}}} \sum_{n=1}^{N_{\text{in}}} |H(m, n) - T(m, n)|^2 \quad (4.8)$$

The problem is then to find the optimal filters and domains such that the resulting matrix $\mathbf{T} \in (\mathbf{T}_{\text{ss}}, \mathbf{T}_{\text{ms}}, \mathbf{T}_{\text{mc}})$ minimizes σ_e^2 .

Let us consider first the single-stage configuration. If we plug the form of \mathbf{T}_{ss} (equation 3.22) in (4.7), the problem is

$$\min \|\mathbf{H} - \mathbf{F}_{N_{\text{out}}}^{-a} \mathbf{\Lambda}_{N_{\text{out}} \times N_{\text{in}}} \mathbf{F}_{N_{\text{in}}}^a\|_F^2. \quad (4.9)$$

Since the fractional Fourier transform matrices are unitary, the above is equivalent to

$$\min \|\mathbf{F}_{N_{\text{out}}}^a \mathbf{H} \mathbf{F}_{N_{\text{in}}}^{-a} - \mathbf{\Lambda}_{N_{\text{out}} \times N_{\text{in}}}\|_F^2 \quad (4.10)$$

Minimizing the above expression can be achieved by maximizing the diagonal of the matrix $\mathbf{F}_{N_{\text{out}}}^a \mathbf{H} \mathbf{F}_{N_{\text{in}}}^{-a}$ by varying the order a and recognizing the corresponding filter coefficients $h[k]$ as the diagonal elements.

In the multi-stage case, the overall kernel \mathbf{T}_{ms} depends nonlinearly on the filter coefficients $h_k[j]$ as evident from equation 3.19. The solution of the optimization problem arising in this case is difficult. Nevertheless an iterative approach has been successfully applied to this problem [13, 14, 15].

In the multi-channel case, given the domains a_k , the problem can be exactly posed as a least-squares optimization problem leading to an associated set of normal equations which can be solved with other standard techniques. To see this, we first plug the form

of \mathbf{T}_{mc} (equation 3.27) into (4.7) to define the problem as

$$\min \|\mathbf{H} - \sum_{k=1}^M \sum_{j=1}^N h_k[j] (\hat{\mathbf{T}}_{kj})_{N_{\text{out}} \times N_{\text{in}}}\|_F^2. \quad (4.11)$$

It is necessary to first “vectorize” the above equation in order to interpret it as a least-squares problem. Let $\underline{\mathbf{H}}$, $\underline{\mathbf{T}}_{\text{mc}}$, and $\hat{\underline{\mathbf{T}}}_{kj}$ denote the $N_{\text{out}}N_{\text{in}} \times 1$ vectors obtained by stacking the columns of \mathbf{H} , \mathbf{T}_{mc} and $\hat{\mathbf{T}}_{kj}$ on top of each other. Finally, let $\underline{\mathbf{h}}$ denote the $MN \times 1$ vector obtained by stacking the M column filter vectors $\mathbf{h}_1, \mathbf{h}_2, \dots, \mathbf{h}_M$ on top of each other (here $N = \min(N_{\text{out}}, N_{\text{in}})$ as defined in the previous chapter). With these conventions, we obtain

$$\underline{\mathbf{T}}_{\text{mc}}[p] = \sum_{q=1}^{MN} \hat{\underline{\mathbf{T}}}_q[p] \underline{\mathbf{h}}[q] \quad p = 1, 2, \dots, N_{\text{out}}N_{\text{in}}, \quad (4.12)$$

where the indice q in this case follows a row ordering over the two indices kj , i. e. $q \equiv (kj)$ when $q = N * (k - 1) + j$ $k = 1, \dots, M$ $j = 1, \dots, N$. This equation can also be written in matrix form as

$$\underline{\mathbf{T}}_{\text{mc}} = [\hat{\underline{\mathbf{T}}}_1 \hat{\underline{\mathbf{T}}}_2 \dots \hat{\underline{\mathbf{T}}}_{MN}] \underline{\mathbf{h}} \equiv \hat{\underline{\mathbf{T}}} \underline{\mathbf{h}}, \quad (4.13)$$

where the new $N_{\text{out}}N_{\text{in}} \times MN$ matrix $\hat{\underline{\mathbf{T}}}$ has been defined.

Now, we are finally able to state our problem in standard form as follows: Minimize the mean-square difference $\|\underline{\mathbf{H}} - \underline{\mathbf{T}}_{\text{mc}}\|^2$ between the desired $\underline{\mathbf{H}}$ and $\underline{\mathbf{T}}_{\text{mc}} = \hat{\underline{\mathbf{T}}} \underline{\mathbf{h}}$. This is a standard least squares problem and can be solved in a number of ways. The filter vector $\underline{\mathbf{h}}$ which minimizes $\|\underline{\mathbf{H}} - \hat{\underline{\mathbf{T}}} \underline{\mathbf{h}}\|^2$ is known to satisfy the so-called normal equations associated with the least squares problem:

$$\hat{\underline{\mathbf{T}}}^\dagger \underline{\mathbf{H}} = \hat{\underline{\mathbf{T}}}^\dagger \hat{\underline{\mathbf{T}}} \underline{\mathbf{h}}, \quad (4.14)$$

where $\hat{\underline{\mathbf{T}}}^\dagger$ is the Hermitian transpose of $\hat{\underline{\mathbf{T}}}$.

The solution to above problem can be interpreted as projecting the vector $\underline{\mathbf{H}}$ onto the column space of the matrix $\hat{\underline{\mathbf{T}}}$. This projection can be computed easily and efficiently when the columns of $\hat{\underline{\mathbf{T}}}$ are orthonormal. The filter coefficients in this case can be obtained by simply taking an inner product of the columns of $\hat{\underline{\mathbf{T}}}$ with $\underline{\mathbf{H}}$. When the columns of $\hat{\underline{\mathbf{T}}}$ are not orthonormal, the problem may be an ill-posed problem and some form of regularization may be needed.

When $M = 1$, the multi-channel configuration reduces to the single-stage filtering configuration. In this case the columns of the matrix $\hat{\underline{\mathbf{T}}}$ becomes orthonormal so that

it has an inverse and $\hat{\mathbf{T}}^\dagger \hat{\mathbf{T}}$ is the identity matrix. The solution of equation 4.14 can then be shown to correspond to the solution given for single-stage filtering. The inner product can also be computed efficiently since the columns of $\hat{\mathbf{T}}$ are related to the columns of the fractional Fourier transform matrix and the fractional Fourier transform can be implemented efficiently. When $M > 1$, the columns of the matrix $\hat{\mathbf{T}}$ are no longer orthonormal and solving the problem requires high computation and storage. In this case, we can find a biorthonormal set to the columns of $\hat{\mathbf{T}}$ in order to compute the projections efficiently. However, the problem of finding the biorthonormal set requires at least the same cost as finding the direct solution. This method can be justified when the orders in the multi-channel configuration is set a priori and the same values will be used for several kernel synthesis problems.

In the above formulation, the fractional orders are assumed to be given. The problem of choosing the optimal orders can be solved with further optimization, but it is in general costly and difficult. When this synthesis problem is to be applied to several desired matrices with no regular relation between them, a practical approach may be to choose the orders uniformly from the interval $(-1, 1]$ so that $a_k = -1 + 2k/M \quad k = 1, \dots, M$. This choice also improves the condition number of $\hat{\mathbf{T}}$ since from the continuity of the fractional Fourier transform, the problem becomes more ill-posed (singular values of the matrix $\hat{\mathbf{T}}$ becomes smaller) when the orders a_k are close to each other.

An interesting case is obtained when the number of filters is taken to be exactly $N' = \max(N_{\text{in}}, N_{\text{out}})$. In this case $\hat{\mathbf{T}}$ becomes a square matrix of dimensions $N_{\text{in}}N_{\text{out}} \times N_{\text{in}}N_{\text{out}}$ and the number of filter coefficients ($N_{\text{in}}N_{\text{out}}$) matches the number of elements of \mathbf{H} . The question that arises is whether the desired matrix can be synthesized exactly. The answer depends on the rank of $\hat{\mathbf{T}}$. In the case it is full rank, we can find the filter coefficients and thus any desired matrix \mathbf{H} can be synthesized with N' -channel filter structure. Unfortunately, the simulations showed that it is not full rank and thus not every \mathbf{H} can be synthesized.

On page 45 we mentioned that the matching pursuit algorithm may also be used in finding an approximate solution of the kernel synthesis problem. In this case, this method corresponds to projecting \mathbf{H} onto the columns of $\hat{\mathbf{T}}$ one by one and after each projection subtracting the part of the vector that lies along that column. This method would give the exact result if the columns of $\hat{\mathbf{T}}$ were orthogonal.

4.1.2 Extensions

In the applications to be discussed, we will encounter problems which correspond to the extensions of the problem described in the previous section. In this section we will briefly give the solutions to these problems.

Consider the problem of minimizing

$$\sigma_e^2 = \|\mathbf{H} - \mathbf{T}\mathbf{G}\|_F^2, \quad (4.15)$$

where \mathbf{T} is in the form of a fractional Fourier domain filtering system i.e. $\mathbf{T} \in (\mathbf{T}_{ss}, \mathbf{T}_{mc}, \mathbf{T}_{ms})$, \mathbf{H} is the desired kernel, and \mathbf{G} is the given kernel pre-multiplying the fractional Fourier domain filtering system. This problem is very similar to the problem as defined by equation 4.7.

We first note that as before the single-stage problem is the special case of the multi-channel problem with $M = 1$. Here we don't consider the multi-stage problem either, since we can easily generalize the iterative solution algorithm given in [13]. For the multi-channel configuration, we can proceed along the same steps as before. Given the domains a_k , the above problem can be exactly posed as a least-squares optimization problem leading to an associated set of normal equations which can be solved with other standard techniques, just like in section 4.1.1. In fact, we can solve the problem by slightly modifying the method discussed there. We can rewrite equation 4.15, by plugging the form of \mathbf{T}_{mc} in equation 3.27,

$$\begin{aligned} \min \|\mathbf{H} - (\sum_{k=1}^M \sum_{j=1}^N h_k[j] \hat{\mathbf{T}}_{kj})\mathbf{G}\|_F^2 \\ \min \|\mathbf{H} - \sum_{k=1}^M h_k[j] \sum_{j=1}^N \hat{\mathbf{T}}_{kj}\mathbf{G}\|_F^2 \\ \min \|\mathbf{G}_d - \sum_{k=1}^M \sum_{j=1}^N h_k[j] \hat{\mathbf{T}}'_{kj}\|_F^2 \end{aligned} \quad (4.16)$$

where we have defined the matrix $\hat{\mathbf{T}}'_{kj} = \hat{\mathbf{T}}_{kj}\mathbf{G}$. Now we can follow the steps given in section 4.1.1 by just replacing the matrix $\hat{\mathbf{T}}_{kj}$ with $\hat{\mathbf{T}}'_{kj}$. The filter coefficients may be found by solving the following equation:

$$\hat{\mathbf{T}}'^{\dagger} \underline{\mathbf{G}}_d = \hat{\mathbf{T}}'^{\dagger} \hat{\mathbf{T}}' \underline{\mathbf{h}}, \quad (4.17)$$

where $\hat{\mathbf{T}}' = [\hat{\mathbf{T}}'_1 \hat{\mathbf{T}}'_2 \dots \hat{\mathbf{T}}'_{MN}]$ and the underlines denote the column vectors obtained from the corresponding matrices by column ordering as in section 4.1.1.

Another extension is the following problem of minimizing the following:

$$\sigma_e^2 = \|\mathbf{H} - \mathbf{G}\mathbf{T}\|_F^2. \quad (4.18)$$

Exactly the same method applies in this case. We just replace $\hat{\mathbf{T}}_{kj}$ with $\hat{\mathbf{T}}''_{kj} = \mathbf{G}\hat{\mathbf{T}}_{kj}$ in the solution given in section 4.1.1. The filter coefficients may then be found by solving the following equation:

$$\hat{\mathbf{T}}''^\dagger \underline{\mathbf{G}}_d = \hat{\mathbf{T}}''^\dagger \hat{\mathbf{T}}'' \underline{\mathbf{h}}, \quad (4.19)$$

where $\hat{\mathbf{T}}'' = [\hat{\mathbf{T}}''_1 \hat{\mathbf{T}}''_2 \dots \hat{\mathbf{T}}''_{MN}]$ and underlines denote the column vectors obtained from the corresponding matrices by column ordering as in section 4.1.1.

Lastly, we consider the solution for the windowed fractional Fourier transform configuration introduced at the end of section 3.6. The problem is then minimizing the error,

$$\sigma_e^2 = \|\mathbf{H} - \mathbf{T}_{\text{wmc}}\|_F^2. \quad (4.20)$$

where \mathbf{T}_{wmc} is as defined in equation 3.33. We can proceed as in section 4.1.1 and plug the expression of \mathbf{T}_{wmc} into the equation 4.20:

$$\sigma_e^2 = \|\mathbf{H} - \sum_{k=1}^M \sum_{j=1}^N h_k[j] \hat{\mathbf{T}}_{kj} \mathbf{W}_k\|_F^2 \quad (4.21)$$

We can then go on as before by replacing $\hat{\mathbf{T}}_{kj}$ with $\hat{\mathbf{T}}_{kj} \mathbf{W}_k$ in the solution given in section 4.1.1 and find the optimal filter coefficients for given a_k s.

4.2 Examples

Some application examples of the system synthesis problem will be given in chapters 5 and 6 where we will first find the general optimal linear system in a given application (signal recovery, signal synthesis) and then try to synthesize it as a fractional Fourier domain filtering configuration. In this section we will give few examples illustrating the applications of the system synthesis problem. These examples were first studied in [13] for multi-stage (repeated) filtering configuration.

We first consider the problem of synthesizing the Hadamard transform which is one of the standard unitary transformations in signal processing. Its definition and properties may be found in [4]. Here, we synthesize this transformation with our fractional Fourier

domain filtering configurations, and for $N = 128$ we find the normalized errors, defined as

$$\epsilon_H = \frac{\|\mathbf{T} - \mathbf{H}\|_F^2}{\|\mathbf{H}\|_F^2} \quad \mathbf{T} \in (\mathbf{T}_{ss}, \mathbf{T}_{ms}, \mathbf{T}_{mc}), \quad (4.22)$$

to be 48% with single-stage filtering, 4% with the multi-stage (repeated) filtering with five filters and 8% with the multi-channel filtering with seven filters. (We choose $a_k = 0 + (k - 1)/6$ $k = 1, 2, \dots, 7$ as the fractional Fourier domain orders.) We see that the multi-channel configuration is not suitable for the synthesis of this transform and the multi-stage configuration yields better performance. Lower error figures could be obtained if we optimized over the fractional orders.

In the second example, the problem of realizing one-to-one interconnection patterns between N input and N output channels is considered [1, 2], and will try to implement these interconnection patterns with the filtering configurations introduced in this thesis. Some of the methods of realizing such interconnections have been discussed in [1, 2], and the conclusion is reached that the multistage architectures based on regular patterns such as the perfect shuffle or Banyan are most favorable. Here we will investigate the use of fractional Fourier domain filtering configurations. Our method not only provides a systematic way of designing such systems, but the implementation of such systems may be more convenient and/or cheaper since the present approach is based on the use of conventional spatial filters rather than microoptical elements.

Any one-to-one interconnection architecture between N input and N output channels is characterized by its associated $N \times N$ permutation matrix. In such a matrix every row and column has only one nonzero element which is equal to one. We synthesize the interconnection architectures by synthesizing their associated permutation matrices.

As an example, the reverse perfect shuffle architecture shown in Fig. 4.1 is considered (after [13]). This interconnection pattern can be synthesized exactly by using 6 filters in multi-stage filtering configuration and with an error of 1% by using 6 filters in multi-channel configuration ($a_k = k/6$ $k = 1, 2, \dots, 6$). We have also considered a large number of interconnection patterns which do not exhibit any obvious regularity. In all cases, these patterns could be realized with a moderate number of filters. Conventional multistage permutation network architectures can realize arbitrary permutations in $O(\log N)$ stages. Extensive numerical experimentation on many different arbitrary permutation matrices indicates that the proposed method is also able to realize these in a similar number of filters. Although it is not difficult to achieve the desired architecture with a moderate number of stages, in most cases it is possible to get away

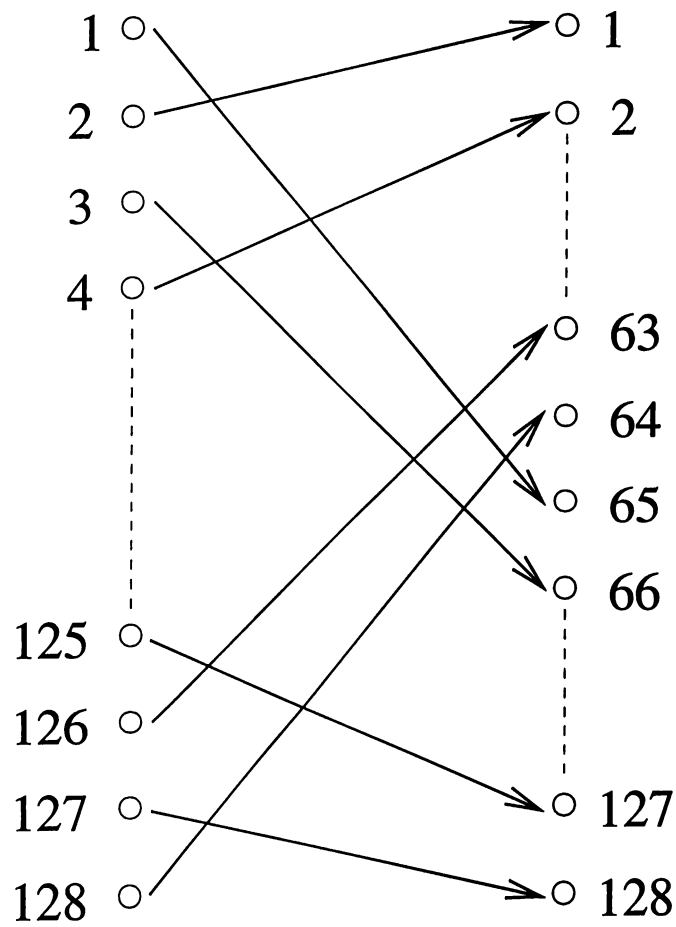


Figure 4.1: Reverse perfect shuffle interconnection architecture. (After [13])

with an even smaller number of stages, since due to the digital nature of such systems a considerable deviation can be tolerated while still retaining an acceptable eye pattern.

It may have been possible to come up with an optical setup with a comparable or even fewer number of stages through ingenuity and invention. Our approach, on the other hand, provides a systematic way of obtaining such an implementation. This would be of great utility especially in those cases where the structure of the transformation matrix is not simple or even when we are confronted with a matrix supplied in numerical form for which no easily discernible structure is apparent.

Chapter 5

Applications in Signal Synthesis

We discussed the application of the proposed filtering circuits to system synthesis in the previous chapter. There given a desired system, we wanted to synthesize it in the form of fractional Fourier transform filtering circuits. In this chapter our aim is to synthesize a desired input or output signal by using the concept of fractional Fourier domain filtering.

One important application of the signal synthesis problem arises in optics where we want to synthesize a desired optical wave, from a given optical wave both of which are characterized by their statistical properties. These statistical properties are in general in the form of second-order statistics and as discussed below this leads to non-linear quadratic equations in most of the cases. We will propose a method which reduces these non-linear equations to linear ones and hence enables us to find an analytic solution. We will discuss this method in detail and also comment on the drawbacks. We will also give some simulation examples showing the effectiveness of the proposed filtering configurations in this problem.

5.1 Signal Synthesis

In some applications we want to synthesize a signal from another signal by designing a system that maps the signal we have to the desired one. The problem of obtaining a specific output \mathbf{x}_{out} corresponding to a specific input \mathbf{x}_{in} is not an interesting problem if \mathbf{x}_{in} has all nonzero entries because we may recover \mathbf{x}_{out} from \mathbf{x}_{in} by using only a single

multiplicative filter \mathbf{h} . However, in the event that some of the entries of \mathbf{x}_{in} are zero, the problem is no longer trivial. A number of iterative algorithms have been proposed for this problem. We may also want to obtain an output \mathbf{x}_{out} that is obtained in a specific manner from the input, i. e. we can specify the input-output relation. However, for an arbitrary input, this problem reduces to the system synthesis problem discussed in detail in section 4.1. If some information is available about the input (in some statistical form), and we again want to synthesize an input-output relation that is effective for that input, the problem may be written as:

$$\min E [\|\mathbf{H}\mathbf{x} - \mathbf{T}\mathbf{x}\|^2] \quad (5.1)$$

where $\mathbf{T} \in (\mathbf{T}_{ss}, \mathbf{T}_{ms}, \mathbf{T}_{mc})$. This problem, although having a different physical interpretation, is very similar mathematically to the problems we will introduce in section 6.1 and may be solved using approach (ii), by directly putting the form of \mathbf{T} and optimizing over the filter coefficients (and possibly the orders). Another synthesis problem is to synthesize an input in order to have a desired output. Again although having a different interpretation, this problem is mathematically identical to the problem of signal recovery where we have an output which may be interpreted as the desired signal and we try to recover the input which may be interpreted as the signal to be synthesized.

Many synthesis problems also arise in optics. One important problem is to synthesize arbitrarily specified mutual intensity distributions from a given source with a given mutual intensity distribution. The systems required to achieve this goal can be efficiently constructed in the form of generalized fractional-Fourier-domain filtering configurations.

The mutual intensity of a quasi-monochromatic optical field is defined as the spatial autocorrelation of the field [95]:

$$R_x(u_1, u_2) = E[x(u_1)x^*(u_2)] \quad (5.2)$$

where $x(u_1)$ represents the complex amplitude of the optical field at $u = u_1$. It has been shown that the propagation of mutual intensity through quadratic-phase systems [91] can be expressed as a double fractional Fourier transform [57, 49, 52]. Quadratic-phase systems include systems consisting of arbitrary concatenations of thin lenses and sections of free space [45, 47]. Single-stage fractional Fourier domain filtering has already been used to synthesize mutual intensity distributions in [58]. In this thesis we will generalize the formulation to filtering circuits so that it becomes more transparent and straightforward. Furthermore, it allows the optimal form of the required filters to be calculated in a much more computationally efficient manner.

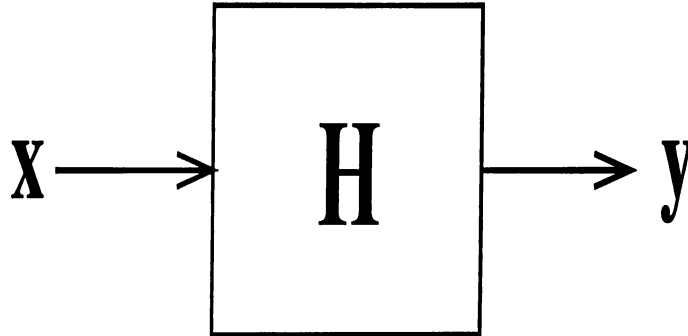


Figure 5.1: Mutual intensity synthesis problem

The basic problem we deal with is symbolically depicted in Fig. 5.1. We assume we have a quasi-monochromatic light source with given mutual intensity $R_x(u, u')$. We wish to design the system $h(u, u')$, possibly subject to certain constraints, such that the output mutual intensity $R_y(u, u')$ satisfies as closely as possible the given specifications. One-dimensional notation is employed for simplicity, although it is possible to generalize the results to two dimensional problems.

Once the optimal kernel $h(u, u')$ is determined, there remains the problem of implementing it. One way of implementing such general linear systems is to employ matrix-vector product architectures or multi-facet architectures [97]. However, these approaches are not space-bandwidth efficient. If the input has a space-bandwidth product of N (that is, if it can be represented by a vector of length N), these systems require an optical system with space-bandwidth product N^2 in order to realize an arbitrary linear system. To alleviate this inefficiency, we can incorporate the space-bandwidth efficient filtering configurations in fractional Fourier domains discussed in chapter 3. Once, the general linear synthesis kernel $h(u, u')$ is somehow obtained, we can employ approach (i) to synthesize the optimal kernel $h(u, u')$ with these configurations. We can also employ approach (ii) by taking the form of these filtering configurations as a constraint on $h(u, u')$ and by optimizing over the free parameters of these configurations.

Referring to Fig. 5.1, the output field $y(u)$ is related to the input field $x(u)$ through the relation

$$y(u) = \int_{-\infty}^{\infty} H(u, u')x(u') du', \quad (5.3)$$

which can be discretized as

$$y(m) = \sum_{n=1}^N H(m, n)x(n), \quad (5.4)$$

$$\mathbf{y} = \mathbf{H}\mathbf{x}, \quad (5.5)$$

where N is the space-bandwidth product of the signals. For simplicity in notation, we will assume that the dimensions of the input and the output optical fields are same although the discussion and the solutions we will provide may easily be generalized to the rectangular case where the input and the output dimensions of the optical system differ. The mutual intensity is the autocorrelation of the field:

$$R_x(u_1, u_2) = E[x(u_1)x^*(u_2)], \quad (5.6)$$

and similar for $y(u)$. Here $E[\cdot]$ represents the expectation value. In discrete form this becomes

$$R_x(m, n) = E[x(m)x^*(n)], \quad (5.7)$$

$$\mathbf{R}_x = E[\mathbf{x}\mathbf{x}^\dagger], \quad (5.8)$$

where \dagger denotes the Hermitian transpose or conjugate or adjoint, and a similar definition holds for \mathbf{R}_y .

It is easy to show that the output mutual intensity is related to the input mutual intensity through the relation

$$R_y(u_1, u_2) = \int_{-\infty}^{\infty} \int_{-\infty}^{\infty} H(u_1, u'_1) H^*(u_2, u'_2) R_x(u'_1, u'_2) du'_1 du'_2 \quad (5.9)$$

Although we could directly discretize this relation, we will instead multiply both sides of equation 5.5 with their Hermitian conjugates and take the expectation value:

$$E[\mathbf{y}\mathbf{y}^\dagger] = E[(\mathbf{H}\mathbf{x})(\mathbf{H}\mathbf{x})^\dagger] = \mathbf{H}E[\mathbf{x}\mathbf{x}^\dagger]\mathbf{H}^\dagger, \quad (5.10)$$

$$\mathbf{R}_y = \mathbf{H}\mathbf{R}_x\mathbf{H}^\dagger. \quad (5.11)$$

Since the right-hand-side of the last equation is quadratic in the elements of \mathbf{H} , it is desirable to introduce a representation for the mutual intensity which makes this equation linear in \mathbf{H} . As a direct consequence of its definition (equation 5.8), the mutual intensity matrix is known to be Hermitian symmetric and positive semi-definite, as all autocorrelation matrices are. Such matrices can always be expressed in the form $\mathbf{R}_x = \tilde{\mathbf{R}}_x \tilde{\mathbf{R}}_x^\dagger$, in fact in several different ways. Since \mathbf{R}_x is Hermitian symmetric, it can be diagonalized by a unitary matrix \mathbf{U} whose columns are the eigenvectors of \mathbf{R}_x :

$$\mathbf{R}_x = \mathbf{U}\mathbf{D}\mathbf{U}^\dagger \quad (5.12)$$

where \mathbf{D} is the diagonal matrix of real eigenvalues. For a positive semi-definite matrix, the eigenvalues are always greater than or equal to 0. The above representation is just the singular value decomposition of the matrix \mathbf{R}_x . It can also be written as

$$\mathbf{R}_x = \sum_{k=1}^R \lambda_k \mathbf{u}_k \mathbf{u}_k^\dagger \quad (5.13)$$

where \mathbf{u}_k is the k th column of \mathbf{U} , λ_k is the eigenvalue corresponding to \mathbf{u}_k , and R is the number of non-zero eigenvalues. This representation is also known as the *coherent mode representation* in optics [98] since each term in equation 5.13 corresponds to a coherent mode of light [96]. The number of non-zero eigenvalues determines the rank of \mathbf{D} and hence the rank of the mutual intensity function \mathbf{R}_x . The rank is closely related to the coherence degree of the light since it represents the number of coherent modes. For example, for fully coherent light the rank is 1 so that mutual intensity function can be represented by a single coherent mode and the mutual intensity matrix is of an outer product form. For the other limit which is incoherent light, the rank is N and the mutual intensity matrix corresponds to a diagonal matrix. (We should here note that not all full rank mutual intensity functions represent incoherent light.) In between, the light is partially coherent and $1 \leq r \leq N$.

If we plug 5.13 in 5.11, we obtain

$$\mathbf{R}_y = \sum_{k=1}^R \lambda_k \mathbf{v}_k \mathbf{v}_k^\dagger \quad (5.14)$$

where $\mathbf{v}_k = \mathbf{H}\mathbf{u}_k$. Here we should note that this equation does *not* correspond to the coherent mode representation for \mathbf{R}_y unless \mathbf{H} is unitary. In this representation \mathbf{v}_k do not in general form an orthonormal set and λ_k does not correspond to the eigenvalues of \mathbf{R}_y . In [98], with some specific approximations and for unitary \mathbf{H} this representation is used for solving inverse source problems in optics.

To solve the synthesis problem defined in the previous section we first define $\mathbf{D}^{1/2}$ to be the diagonal matrix whose elements are equal to the non-negative square roots of the eigenvalues of \mathbf{D} (equation 5.12), in the same order. Then we can write $\mathbf{D} = \mathbf{D}^{1/2}\mathbf{U}^\dagger\mathbf{U}\mathbf{D}^{1/2}$ since $\mathbf{U}^\dagger\mathbf{U}$ is equal to the identity matrix. It follows that

$$\mathbf{R}_x = \mathbf{U}\mathbf{D}\mathbf{U}^\dagger = (\mathbf{U}\mathbf{D}^{1/2}\mathbf{U}^\dagger)(\mathbf{U}\mathbf{D}^{1/2}\mathbf{U}^\dagger) = \tilde{\mathbf{R}}_x\tilde{\mathbf{R}}_x = \tilde{\mathbf{R}}_x\tilde{\mathbf{R}}_x^\dagger, \quad (5.15)$$

where we have defined $\tilde{\mathbf{R}}_x = \tilde{\mathbf{R}}_x^\dagger \equiv \mathbf{U}\mathbf{D}^{1/2}\mathbf{U}^\dagger$. Thus the mutual intensity matrix \mathbf{R}_x is related to the positive semi-definite square root representation $\tilde{\mathbf{R}}_x$ through the relation

$$\mathbf{R}_x = \tilde{\mathbf{R}}_x\tilde{\mathbf{R}}_x = \tilde{\mathbf{R}}_x\tilde{\mathbf{R}}_x^\dagger. \quad (5.16)$$

Using the above representation both for \mathbf{R}_x and \mathbf{R}_y , equation 5.11 can now be written as,

$$\mathbf{R}_y = \mathbf{H}\mathbf{R}_x\mathbf{H}^\dagger, \quad (5.17)$$

$$\tilde{\mathbf{R}}_y\tilde{\mathbf{R}}_y^\dagger = \mathbf{H}\mathbf{R}_x\mathbf{R}_x^\dagger\mathbf{H}^\dagger. \quad (5.18)$$

One solution of this equation is

$$\tilde{\mathbf{R}}_y = \mathbf{H}\tilde{\mathbf{R}}_x. \quad (5.19)$$

In order to synthesize this desired matrix \mathbf{H} we can first find it by standard techniques such as pseudo-inverse and least-squares methods [93] and then we may synthesize it in the form of fractional Fourier domain filtering configurations using approach (i) described in section 4.1.1. Or we may employ approach (ii) by directly plugging the form and finding the optimal filter coefficients and orders as in section 6.1. For instance, in the multi-channel configuration the problem is to find the optimal filter coefficients which minimizes the error:

$$\begin{aligned} \sigma_e^2 &= \|\tilde{\mathbf{R}}_y - \mathbf{T}_{mc}\tilde{\mathbf{R}}_x\|_F^2 \\ &= \|\tilde{\mathbf{R}}_y - \left(\sum_{k=1}^M \sum_{j=1}^N h_k[j] \hat{\mathbf{T}}_{kj}\right) \tilde{\mathbf{R}}_x\|_F^2 \end{aligned} \quad (5.20)$$

This problem is exactly the same as the one defined in section 4.1.2, and thus can be solved in the same manner.

The solution of 5.19 clearly depends on the choice of matrices $\tilde{\mathbf{R}}_x$ and $\tilde{\mathbf{R}}_y$ which are not unique. We can find other matrices $(\tilde{\mathbf{R}}_x)_2$ and $(\tilde{\mathbf{R}}_y)_2$ which satisfy equation 5.15. Since we are working with an arbitrary member of possible matrices, we are not exploiting all possible rooms for improvement. One desired matrix may be implemented more efficiently in the form of fractional Fourier domain filters than other.

Lemma 1: The rank of $\tilde{\mathbf{R}}_x^\dagger$ is equal to the rank of $\tilde{\mathbf{R}}_x$.

Lemma 2: The rank of $\tilde{\mathbf{R}}_x^\dagger\tilde{\mathbf{R}}_x$ is equal to the rank of $\tilde{\mathbf{R}}_x\tilde{\mathbf{R}}_x^\dagger$ which is equal to the rank of $\tilde{\mathbf{R}}_x$.

These two lemmas can be shown by using the SVD of the matrix $\tilde{\mathbf{R}}_x$.

Theorem 1: If \mathbf{R}_x has rank r , then the rank of $\tilde{\mathbf{R}}_x$ is also r .

Theorem 2: If \mathbf{R}_x (hence $\tilde{\mathbf{R}}_x$) has rank r , then the rank of \mathbf{R}_y (hence $\tilde{\mathbf{R}}_y$) can be at most r .

The proofs of these theorems directly follow from lemma 1 and 2 and the properties of the rank.

As already mentioned, it is possible to find many matrices $(\tilde{\mathbf{R}}_x)_p$ labeled by p which satisfy $\mathbf{R}_x = (\tilde{\mathbf{R}}_x)_p (\tilde{\mathbf{R}}_x)_p^\dagger$. $(\tilde{\mathbf{R}}_x)_p$ is necessarily of rank r . If its dimensions are $N \times M_p$, then $r \leq M_p$. The first reason for the multiplicity of such matrices is that the choice of \mathbf{U} in equation 5.12 is not unique when the eigenvalues are not distinct or the rank r is less than $N - 1$ (this in fact means that we have multiplicity for the eigenvalue 0). In this case, within the subspace associated with each degenerate eigenvalue, the choice of orthonormal basis is not unique. Secondly, we may define the matrix $\mathbf{D}_x^{1/2}$ to be the diagonal matrix whose elements are equal to the negative square-roots of the eigenvalues of \mathbf{D}_x rather than non-negative square-roots, or we may choose non-negative square-roots for some of them and negative square-roots for other. Thus an ambiguity also arises in choosing the matrix $\mathbf{D}_x^{1/2}$. And lastly, let \mathbf{V} be a possibly rectangular matrix of dimensions $M_p \times Q$ which satisfies $\mathbf{V}\mathbf{V}^\dagger = \mathbf{I}_{M_p}$. (This implies that the M_p rows of \mathbf{V} are orthonormal, which implies that $Q \geq M_p$.) Then it is easy to see that if $\mathbf{R}_x = (\tilde{\mathbf{R}}_x)_p (\tilde{\mathbf{R}}_x)_p^\dagger$ then $(\tilde{\mathbf{R}}_x)_{p'} \equiv (\tilde{\mathbf{R}}_x)_p \mathbf{V}$ also satisfies $\mathbf{R}_x = (\tilde{\mathbf{R}}_x)_{p'} (\tilde{\mathbf{R}}_x)_{p'}^\dagger$. We know that any two such matrices would satisfy a relation

$$(\tilde{\mathbf{R}}_x)_{p'} = (\tilde{\mathbf{R}}_x)_p \mathbf{M}$$

for any value of rank r since we know from the theory of SVD that $(\tilde{\mathbf{R}}_x)_{p'}$ and $(\tilde{\mathbf{R}}_x)_p$ have the same column space thus we can find such a \mathbf{M} matrix[93]. It can be further shown that if the matrices $(\tilde{\mathbf{R}}_x)_{p'}$ and $(\tilde{\mathbf{R}}_x)_p$ are of dimensions $N \times r$, then the matrix \mathbf{M} is unitary.

For the semi-definite square-root representation we require the condition $(\tilde{\mathbf{R}}_x)_p = (\tilde{\mathbf{R}}_x)_p^\dagger$ so $(\tilde{\mathbf{R}}_x)_p$ should be of dimensions $N \times N$. The non-uniqueness of this representation also stems from the degenerate eigenvalues and from the fact that there are two possible square-roots of the eigenvalues of \mathbf{R}_x leading to different $\mathbf{D}_x^{1/2}$ s. We may choose the positive square-roots for some eigenvalues and negative square-roots for the others. For each choice we get different $(\tilde{\mathbf{R}}_x)_p$. The choice also depends on the choice of basis vectors that span each subspace associated with the degenerate eigenvalue. The more we have degenerate eigenvalues, the more we can find matrices $(\tilde{\mathbf{R}}_x)_p$ satisfying $\mathbf{R}_x = (\tilde{\mathbf{R}}_x)_p (\tilde{\mathbf{R}}_x)_p^\dagger$. If we assume both \mathbf{R}_x and \mathbf{R}_y are of full rank, and have distinct eigenvalues and we choose only the positive square-roots of the eigenvalues, then we can find a unique $\tilde{\mathbf{R}}_x$ and $\tilde{\mathbf{R}}_y$, and hence a unique solution to the above procedure. (Here we exclude the possibility of different orderings of eigenvalues in the diagonal matrix \mathbf{D} and assume the conventional

practice of placing the eigenvalues in decreasing order. But this has no effect on the solution since the resulting matrix ($\tilde{\mathbf{R}}_x$) is unique and independent of how we place the eigenvalues, once we choose the eigenvectors.) But in general as discussed above we can find many solutions some of which may lead to more efficient implementations with fractional Fourier domain filtering. Nevertheless we will use this semi-definite root representation in order to reduce the quadratic mutual intensity synthesis problem to a linear one keeping in mind that it may have more than one solution.

Algorithm:

Overall the mutual intensity synthesis problem can be solved by the following algorithm:

- Given the desired mutual intensity function \mathbf{R}_y and the input mutual intensity function \mathbf{R}_x , find the square root representations using the singular-value-decomposition: $\tilde{\mathbf{R}}_x = \mathbf{U}_x \mathbf{D}_x^{1/2} \mathbf{U}_x^\dagger$ and $\tilde{\mathbf{R}}_y = \mathbf{U}_y \mathbf{D}_y^{1/2} \mathbf{U}_y^\dagger$ where $\mathbf{R}_x = \mathbf{U}_x \mathbf{D}_x \mathbf{U}_x^\dagger$ and $\mathbf{R}_y = \mathbf{U}_y \mathbf{D}_y \mathbf{U}_y^\dagger$.
- Form the equation $\tilde{\mathbf{R}}_y = \mathbf{H} \tilde{\mathbf{R}}_x$ and solve for \mathbf{H} using well known linear inverse problem solution techniques [93]. If there exists no solution (which means that required synthesis is in fact physically unrealizable), solve the problem in the least-squares sense. Synthesize the desired kernel in the form of fractional Fourier domain circuits using the algorithm discussed in section 4.1.1.

or

- Find the fractional Fourier domain circuit which minimizes the error $\|\tilde{\mathbf{R}}_y - \mathbf{T} \tilde{\mathbf{R}}_x\|_F^2$ where $\mathbf{T} \in (\mathbf{T}_{ss}, \mathbf{T}_{mc}, \mathbf{T}_{ms})$, using the similar procedures described in section 6.1.

In this section, we formulated the mutual intensity synthesis problem, proposed a solution that reduces this quadratic problem into a linear one and discussed some of the drawbacks of the method. The main point is that the system that satisfy (5.19) can be used to synthesize the desired mutual intensity function from an input mutual intensity function. However, there may be many such equations with different semi-definite roots. One solution may be implemented more efficiently by using fractional Fourier domain representations than other solutions. It is possible optimize over the set of possible solutions, but this is not undertaken in this thesis.

We may also try to directly solve the quadratic problem with iterative procedures.

One way is to assume an initial \mathbf{H}_0 in the form of a fractional Fourier filtering system and solve for the next \mathbf{H}_1 which minimizes the error by generalizing the method given in [58]. This approach is also not undertaken in this thesis.

A dual problem of synthesizing the desired mutual intensity function from a given light source is to synthesize the light source which after passing through an optical system results in a given output mutual intensity function. We may synthesize that source from another light source available or we may obtain it from the given (observed) output so the problem is essentially an inverse problem. Referring to Fig. 5.1, our aim is first to find the input mutual intensity function \mathbf{R}_x in the least squares sense, given the output mutual intensity function \mathbf{R}_y and the system \mathbf{H} . Mathematically this corresponds to finding the \mathbf{R}_x that minimizes the error defined as

$$\sigma_e^2 = \|\mathbf{R}_y - \mathbf{H}\mathbf{R}_x\mathbf{H}^\dagger\|_F^2 \quad (5.21)$$

where \mathbf{H} is the known system. Although interpreted from a different perspective here, the above problem is mathematically identical to the signal recovery problems to be discussed in the next chapter (there we interpret the above equation as to recover \mathbf{R}_x from \mathbf{R}_y). Here we only state that although not the most robust approach, \mathbf{R}_x can be found by using the left and right pseudo-inverses of \mathbf{H} and \mathbf{H}^\dagger respectively [93].

After we find the mutual intensity function \mathbf{R}_x , we can synthesize it from the output optical wave \mathbf{y} or from another optical source using the algorithm discussed in this section.

5.2 Examples

In this section we will give some computer simulations that show the applications of the mutual intensity synthesis problem.

First we will consider the synthesis of a Gaussian Schell-model (GSM) beam from an incoherent source. Then we will consider the synthesis of a Gaussian Schell-model beam from another Gaussian Schell-model beam. The mutual intensity function of this type of beam at the source can be represented by the superposition of Hermite-Gaussian modes [98, 99]:

$$R_y(u_1, u_2) = \sum_{n=0}^{\infty} \lambda_n \psi_n(u_1) \psi_n^*(u_2) \quad (5.22)$$

where $\psi_n(\cdot)$ is the n th order Hermite-Gaussian function discussed in chapter 2. For computer simulations, the above function is discretized using the definition of the discrete Hermite-Gaussian functions [21, 22]:

$$\mathbf{R}_y = \sum_{n=0}^{N-1} \lambda_n \underline{\psi}_n \underline{\psi}_n^\dagger. \quad (5.23)$$

Here $\underline{\psi}$ is the n th order discrete Hermite Gaussian vector of length N given in [22]. Since the discrete Hermite Gaussian vectors are orthonormal to each other,

$$\underline{\psi}_m^\dagger \underline{\psi}_n = \delta[n - m]$$

the expansion in equation 5.23 also corresponds to the coherent-mode representation of the beam (or the singular-value-decomposition of \mathbf{R}_y) with Hermite-Gaussians as coherent modes. We want to synthesize such a beam from an incoherent source whose mutual intensity function is given by

$$R_x(u_1, u_2) = p(u_1) \delta(u_1 - u_2) \quad (5.24)$$

in continuous time, and in discrete time

$$\mathbf{R}_x = \mathbf{D}_x \quad (5.25)$$

where \mathbf{D}_x is a diagonal matrix of full rank.

Example 1:

In our first example, the expansion coefficients λ_n in the equation 5.23 are chosen as plotted in Fig. 5.2 (a) with $N = 64$. With this choice the mutual intensity matrix \mathbf{R}_y is full rank, has no degenerate eigenvalues, and is shown in part (b) of the same figure. The mutual intensity of the incoherent source is taken to be the identity matrix, $\mathbf{R}_x = \mathbf{I}$. The semi-definite roots are then given by:

$$\begin{aligned} \tilde{\mathbf{R}}_x &= \mathbf{I} \\ \tilde{\mathbf{R}}_y &= \sum_{n=0}^{N-1} \lambda_n^{1/2} \underline{\psi}_n \underline{\psi}_n^\dagger \end{aligned} \quad (5.26)$$

The desired system kernel \mathbf{H} which satisfies $\tilde{\mathbf{R}}_y = \mathbf{H} \tilde{\mathbf{R}}_x$ is then simply given by $\mathbf{H} = \tilde{\mathbf{R}}_y$. When we synthesize this desired \mathbf{H} in the form of a single-stage filter, the normalized error, which is defined as

$$\epsilon_H = \frac{\|\mathbf{T}_{ss} - \mathbf{H}\|_F^2}{\|\mathbf{H}\|_F^2}, \quad (5.27)$$

turns out to be 22% in the optimum domain $a = 0.4$. For the multi-channel filtering configuration with $M = 4$ filters, the normalized error is 4%, and for the multi-stage configuration with $M = 4$ filters, it is 3% ($a_1 = 0.25$, $a_2 = 0.5$, $a_3 = 0.75$ and $a_4 = 1$ for both configurations). The normalized errors

$$\epsilon_{\text{mut}} = \frac{\|\mathbf{R}_y - \mathbf{T}\mathbf{R}_x\mathbf{T}^\dagger\|_F^2}{\|\mathbf{R}_y\|_F^2}, \quad \mathbf{T} \in (\mathbf{T}_{\text{ss}}, \mathbf{T}_{\text{mc}}, \mathbf{T}_{\text{ms}}) \quad (5.28)$$

in the synthesis of \mathbf{R}_y are then 34%, 7%, and 6% for the single-stage, multi-channel ($M = 4$), and multi-stage ($M = 4$) configurations respectively. The synthesized mutual intensity functions are plotted in Fig. 5.3

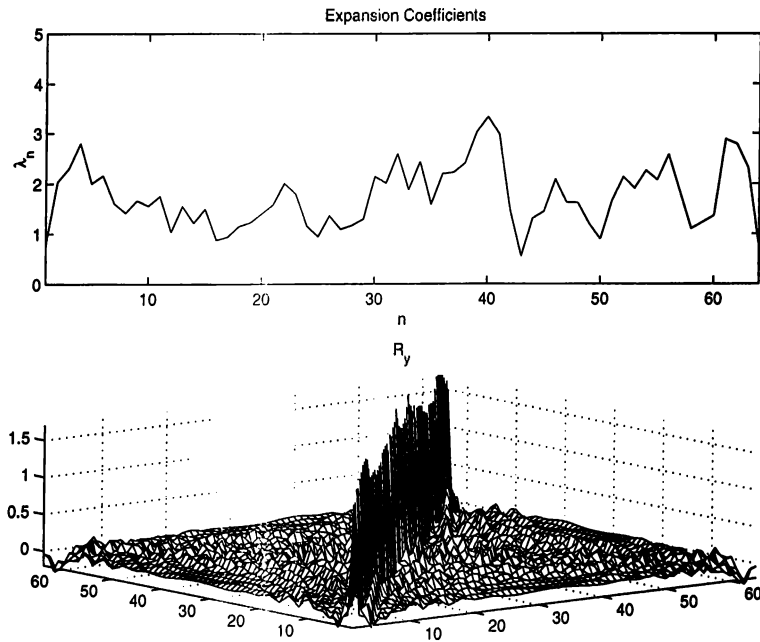


Figure 5.2: (a). The expansion coefficients of equation 5.23 used in the example 1. (b). The mesh plot of the resulting desired mutual intensity function \mathbf{R}_y .

We can also take approach (ii) and directly find the optimal fractional Fourier domain filtering configuration by minimizing the error $\|\tilde{\mathbf{R}}_y - \mathbf{T}\tilde{\mathbf{R}}_x\|_F^2$. But since \mathbf{R}_x is identity matrix, and $\mathbf{H} = \mathbf{R}_y$ this approach would yield the same result as above.

To illustrate the cost performance trade-off in this problem we have plotted the number of filters vs error plot for multi-stage (repeated) and multi-channel configurations in Fig. 5.4.

Example 2:

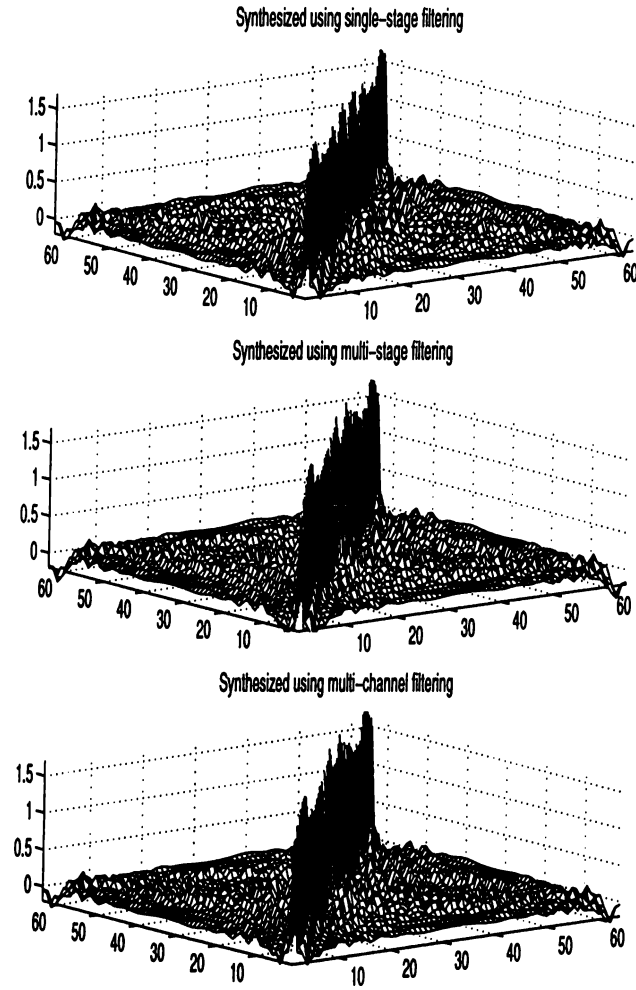


Figure 5.3: (a). Synthesized mutual intensity function using single-stage filtering (b). Synthesized mutual intensity function using multi-stage filtering ($M = 4$) (c). Synthesized mutual intensity function using multi-channel filtering ($M = 4$)

In the second example, the expansion coefficients in the equation 5.23 are chosen as plotted in Fig. 5.5 (a) with $N = 64$. With this choice the mutual intensity matrix \mathbf{R}_y is of rank $R = 52$, has 5 degenerate eigenvalues and is shown in part (b) of the same figure. The mutual intensity of the incoherent source is again taken to be the identity matrix, $\mathbf{R}_x = \mathbf{I}$. The semi-definite roots are then given by:

$$\begin{aligned} \tilde{\mathbf{R}}_x &= \mathbf{I} \\ \tilde{\mathbf{R}}_y &= \sum_{n=0}^{N-1} \lambda_n^{1/2} \underline{\psi}_n \underline{\psi}_n^\dagger \end{aligned} \quad (5.29)$$

The desired system kernel is then simply equal to $\tilde{\mathbf{R}}_y$. When we synthesize this desired

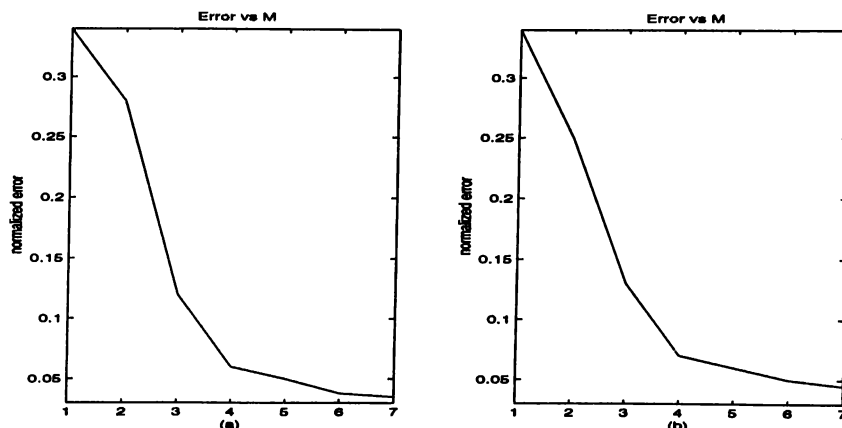


Figure 5.4: Normalized error in signal restoration example versus number of filters for (a) multi-stage (repeated) case, (b) multi-channel case.

\mathbf{H} in the form of a single-stage filter, the normalized error $\epsilon_{\mathbf{H}}$ turns out to be 20% in the optimum domain $a = 0.6$. For the multi-channel filtering configuration with $M = 5$ filters, the normalized error is 5% and for the multi-stage configuration with $M = 5$ filters it is 6%. The normalized errors ϵ_{mut} in the synthesis of \mathbf{R}_y are then 30%, 9%, and 11% for the single-stage, multi-channel ($M = 5$), and multi-stage ($M = 5$) configurations respectively. (In both of the multi-stage and multi-channel configurations we choose $a_1 = 0.2$, $a_2 = 0.4$, $a_3 = 0.6$, $a_4 = 0.8$, and $a_5 = 1$.)

Also in this example approach (ii) yields the same result as above.

Example 3:

In the last example, we consider the problem of synthesizing a GSM beam from another GSM beam. The expansion coefficients of the given GSM beam and desired (to be synthesized) beam are plotted in Fig. 5.6. With these choices of coefficients \mathbf{R}_x is of rank $R = 50$ and \mathbf{R}_y is of rank $R = 60$ and both have degenerate eigenvalues. Since \mathbf{R}_y has a rank greater than of \mathbf{R}_x , there exist no system \mathbf{H} exactly satisfies $\mathbf{R}_y = \mathbf{H}\mathbf{R}_x\mathbf{H}^\dagger$. We are seeking \mathbf{H} in the form of a fractional Fourier domain filter which minimizes the Frobenious norm between synthesized and desired mutual intensity functions. Since \mathbf{R}_x is of rank $R = 50$, we can at most achieve a synthesized mutual intensity function of rank $R = 50$. On the other hand, we know that the best rank 50 approximation of \mathbf{R}_y in the Frobenious norm criteria is achieved by keeping the largest 50 eigenvalues of \mathbf{R}_y and discarding the others. Thus our problem in this example reduces to synthesize $\hat{\mathbf{R}}_y$ from \mathbf{R}_x where $\hat{\mathbf{R}}_y$ is the rank 50 approximation of \mathbf{R}_y obtained by keeping the largest

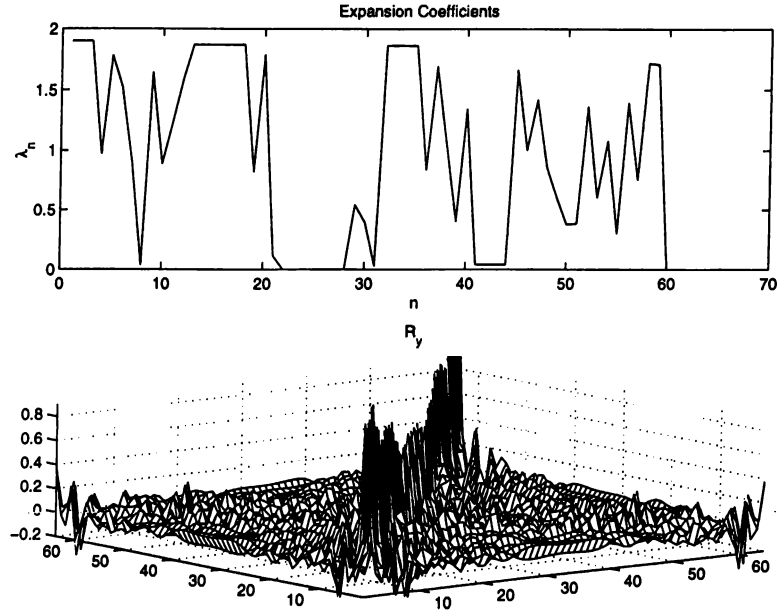


Figure 5.5: (a). The expansion coefficients of the desired GSM beam in example 2. (b). The mesh plot of the resulting desired mutual intensity function \mathbf{R}_y .

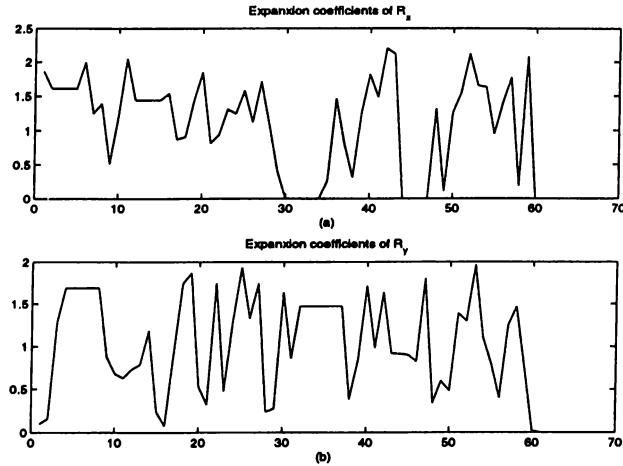


Figure 5.6: The expansion coefficients of (a). given GSM beam, \mathbf{R}_x , (b). desired GSM beam, \mathbf{R}_y .

50 expansion coefficients.

The desired system kernel \mathbf{H} which minimizes $\|\tilde{\mathbf{R}}_y - \mathbf{H}\tilde{\mathbf{R}}_x\|_F^2$ can be found by solving linear equations. When we synthesize this desired \mathbf{H} in the form of a single-stage filter, the normalized error, ϵ_H , turns out to be 27% in the optimum domain $a = -0.5$. For the multi-channel filtering configuration with $M = 5$ filters, the normalized error is 10% and

for the multi-stage configuration with $M = 5$ filters it is 13%. The normalized errors, ϵ_{mut} , in the synthesis of \mathbf{R}_y are then 48%, 18%, and 21% for the single-stage, multi-channel ($M = 5$), and multi-stage ($M = 5$) configurations respectively. (In both of the multi-stage and multi-channel configurations we choose $a_1 = 0.2$, $a_2 = 0.4$, $a_3 = 0.6$, $a_4 = 0.8$, and $a_5 = 1$.)

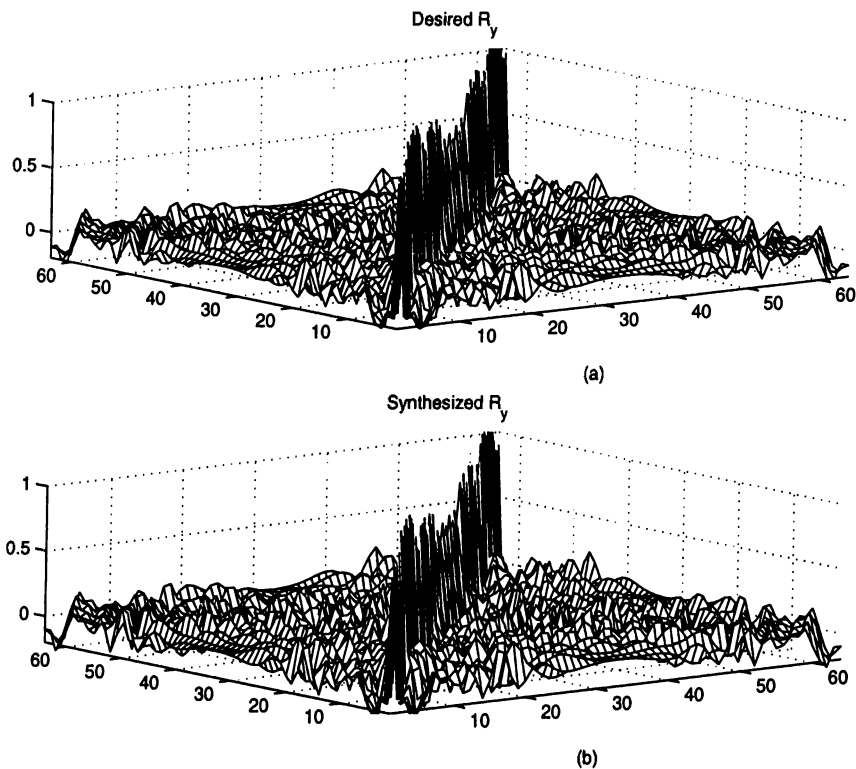


Figure 5.7: The mutual intensity functions of (a). the desired GSM beam (b). the synthesized GSM beam.

We can also take approach (ii) and directly find the optimal fractional Fourier domain filtering configuration minimizing the error $\sigma_e^2 = \|\tilde{\mathbf{R}}_y - \mathbf{T}\tilde{\mathbf{R}}_x\|_F^2$. For the single stage filtering, the normalized error in the synthesis of \mathbf{R}_y turns out to be $\epsilon_{\text{mut}} = 38\%$ and it is 15%, and 17% for the multi-channel and multi-stage filtering configurations respectively. $M = 4$ for both configurations. The mutual intensity function of the GSM beam synthesized by using multi-channel filtering is shown in Fig. 5.7 together with the desired GSM beam.

Chapter 6

Applications in Signal Recovery

In the previous chapters we discussed the applications of filtering circuits in signal and system synthesis problems. In this chapter we will concentrate on the signal recovery applications of filtering circuits.

In the recovery applications the aim is to recover the desired signal or system from the observed degraded data. This problem is well known to be an ill-posed problem. The general linear solution to this problem is known. However, the optical implementation of this direct solution would require very high space-bandwidth products. For this reason, fast methods such as conjugate gradient, LMS type algorithms are often employed. The problem with these iterative algorithms is that generally they can not be implemented optically. Thus we propose that filtering circuits which have efficient optical implementations may be used instead.

6.1 Signal Recovery and Restoration

In many signal processing and optical information processing applications, signals which we wish to recover are degraded by a known distortion and/or by noise. A simple example of this is the transmission of a signal through a channel or medium, yet another example is the degradation of optical images by the effects of imaging through a medium such as air and liquids. The problem is to reduce or eliminate these degradations to recover the original signal or some other desired signal which is obtained from the original

signal. Appropriate solutions to such problems depend on the observation model and the objectives, as well as the amount of prior knowledge available about the desired signal, degradation process and noise. A commonly used observation model is

$$g = \mathcal{G}x + n, \quad (6.1)$$

where \mathcal{G} is the linear system that degrades the desired signal (may be an image) x , and n is an possibly additive noise term (Fig. 6.1).

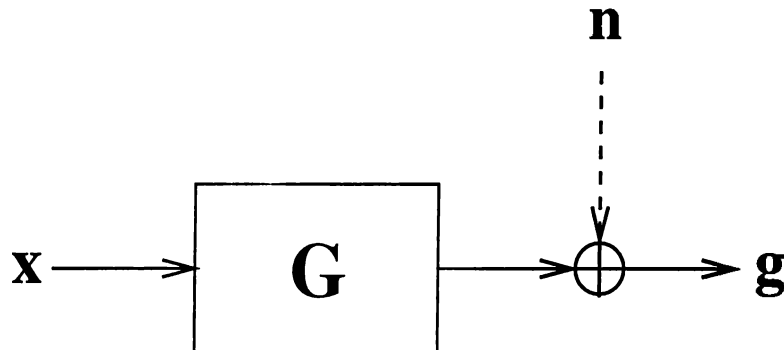


Figure 6.1: Observation model for the degraded signal

The problem is to recover the original signal or another desired signal obtained from the original signal by using a linear system. To achieve this goal, we can employ pre- or post-compensation filters depending on the application. The pre-compensation or reconstruction filter configuration is shown in Fig. 6.2. In this configuration, we apply the estimation filter \mathbf{H} before the transmission channel or medium which degrades the signal. Our aim is to obtain the signal \hat{y} which is as close as possible to the desired signal $y = \mathcal{G}_d x$ (shown in the lower part of the figure) at the receiver end. This type of configuration may be useful, for example, when there is one transmitter and it transmits a signal to many receivers. In this case we obviously don't want to implement many estimation filters for each receiver, since it will increase the cost of a receiver. Instead, we can use one pre-filter configuration at the transmitter to compensate the effects of the transmission medium.

There may be situations where we don't have access to the transmitter end. A simple example is ground-based astronomical imaging for which the quality of the optical image from the stars is degraded by the propagation media, such as atmospheric turbulence. In this case we can apply the post-compensation filter configuration shown in Fig. 6.3. Here the aim is to find the linear filter \mathcal{H} which yields the signal \hat{y} that is as close as possible to the desired signal $y = \mathcal{G}_d f$.

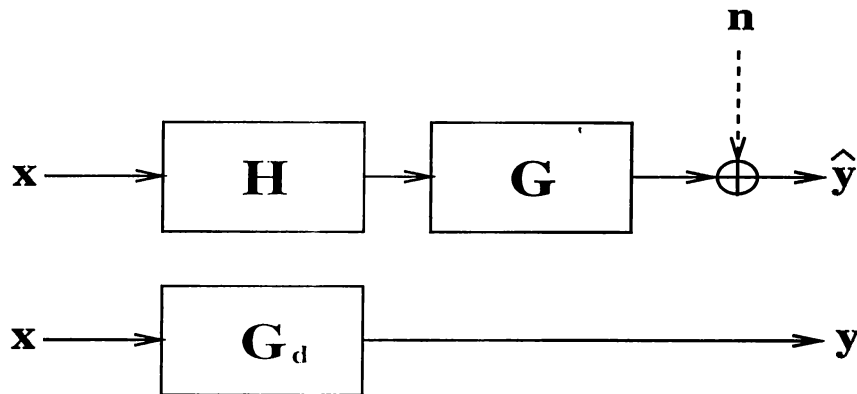


Figure 6.2: Pre-compensation filter configuration.

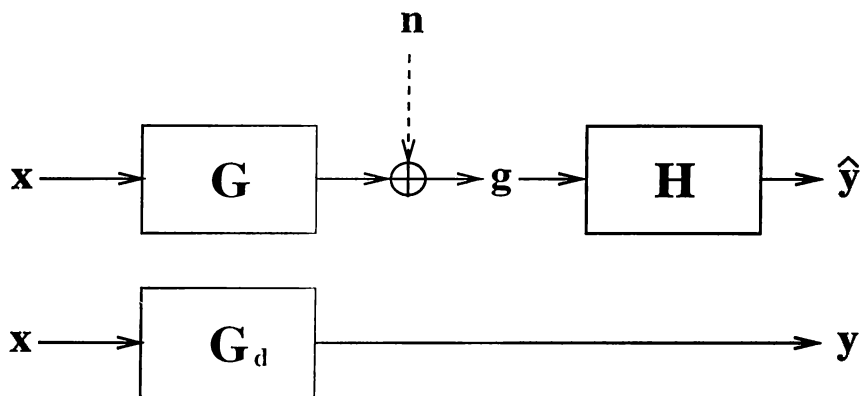


Figure 6.3: Post-compensation filter configuration.

The solutions to the above problems depend on the information available about the desired signal, degradation and noise. When there is no prior information available for input and if we concentrate on post-compensation configurations with $\mathcal{G}_d = \mathcal{I}$, the problem reduces to the well-known, ill-posed least squares problem which is to find x minimizing the error:

$$\min \| \mathcal{G}x - g \|^2 \quad (6.2)$$

whose discrete form is :

$$\min \| \mathbf{G}x - \mathbf{g} \|^2 \quad (6.3)$$

From now on, we will concentrate on the discrete formulation. There are many algorithms, some fast, proposed for the solution of this problem such as gradient methods, conjugate gradient methods and variational methods. In these methods, some form of regularization may also be introduced to overcome the ill-posed nature of the problem.

An example is the Tikhonov regularization for which the problem can be posed as:

$$\min \|\mathbf{G}\mathbf{x} - \mathbf{g}\|^2 + \epsilon J(\mathbf{x}) \quad (6.4)$$

where $J(\mathbf{x})$ serves the purpose of stabilizing the least-squares problem by penalizing undesirable artifacts. Another modification is the use of the weighted norm concept to benefit from the noise information if available [93].

If there is some information available for the input, (mostly in the form of second order statistics), we can then formulate the problem as a Wiener type statistical problem as in section 3.1 [94]. In this case we use the information available for both signal and noise in the solution of the problem. For the time- or space-invariant systems with stationary input and noise, the optimal solution turns out to be time- or space-invariant which can be implemented both digitally and optically in an efficient manner. For the time- or space-varying case, the general linear estimation operator can also be found but it has no longer efficient implementation algorithm. However, there are iterative algorithms for the solution of the post-filter configuration such as Kalman filtering.

The solution of the statistical problem can be shown to reduce to the solution of the least-squares problem given above when the auto-correlation matrices are taken to be the identity matrices (in fact, this corresponds to the no-information case). Also the above least-squares problem can be modified to include the input information by introducing the concept of weighted norm. Then we again have the similar solutions for both cases.

The discussed methods can be used to restore the digital signals, since implementing these algorithms on computers is straightforward although they may require high computation times. However for optical systems the problem is difficult. One can propose to measure the optical field and store it in a digital environment and process that data. However it is difficult to measure the optical signal completely; generally phase information is lost. In this case, we may prefer to work in an all optical environment. Or we may just want to process the optical signals by optical components. In this case implementing the above iterative algorithms which are useful on digital computers is difficult. Also implementing the general linear estimation systems requires optical components with space-bandwidth product of $O(N^2)$.

We can overcome these difficulties by introducing the concept of filtering in fractional Fourier domains. Given the degradation system and available information about input and noise, we can first find the optimal orders and filter coefficients for a given compensation and fractional Fourier filter configuration. We can then easily implement

that compensation filter optically since the optical implementation of fractional Fourier domain filters is known and easy.

We now discuss the use of fractional Fourier domain filtering configurations in the above introduced problems. In the following formulation we will assume square matrices, but extension to rectangular case is straightforward using the tools given in chapter 3.

Pre-compensation filter:

We consider the configuration in Fig. 6.2. We first assume that we know the correlation functions of input and noise (\mathbf{R}_{xx} and \mathbf{R}_{nn}), the undesired distorting channel \mathbf{G} and desired input-output relation \mathbf{G}_d . We want to obtain the pre-compensation filter \mathbf{H} in the form of fractional Fourier domain filter configurations (\mathbf{T}_{ss} , \mathbf{T}_{ms} , or \mathbf{T}_{mc}). We can employ both of the approaches (i) and (ii) discussed in the previous chapter.

To apply approach (i), we should first find the general linear pre-estimator \mathbf{H} . Then we can synthesize it in the form of \mathbf{T}_{ss} , \mathbf{T}_{ms} , or \mathbf{T}_{mc} as discussed in section 4.1.1. The problem can be stated as

$$\min E \left[\|\mathbf{G}_d \mathbf{x} - (\mathbf{G} \mathbf{H} \mathbf{x} + \mathbf{n})\|^2 \right] \equiv \min E \left[\|\mathbf{G}_d - \mathbf{G} \mathbf{H}\| \mathbf{x} - \mathbf{n} \|^2 \right] \quad (6.5)$$

It can be shown that the optimal general recovery operator \mathbf{H} satisfy the following equation:

$$\mathbf{G}^\dagger \mathbf{G}_d \mathbf{R}_{xx} = \mathbf{G}^\dagger \mathbf{G} \mathbf{H} \mathbf{R}_{xx} \quad (6.6)$$

This equation can be solved by using standard techniques. For example, we may use the SVD of \mathbf{R}_{xx} , \mathbf{G} and \mathbf{G}_d . We can then use the methods discussed in section 4.1.1 to synthesize the matrix \mathbf{H} in one of the fractional Fourier domain filtering configurations.

We can also apply approach (ii) to the above problem. In this case we directly plug the form of the filter \mathbf{G} in the formulation of the problem and solve for the filter coefficients and possibly for the orders. We first consider the single-stage case. The problem is then to find the optimal order a and filter coefficients that minimize the error:

$$\sigma_e^2 = E \left[\|\mathbf{G}_d - \mathbf{G} \mathbf{F}^{-a} \mathbf{\Lambda} \mathbf{F}^a\| \mathbf{x} - \mathbf{n} \|^2 \right] \quad (6.7)$$

Using the form of the single-stage filter \mathbf{T}_{ss} in equation 3.18, we can find the optimal filter coefficients for a given value a by solving the following linear equation for $h_1[l]$,

$$\text{diag} \left(\mathbf{F}^a \mathbf{G}^\dagger \mathbf{G}_d \mathbf{R}_{xx} \mathbf{F}^{-a} \right) = \text{diag} \left(\sum_{l=1}^N h_1[l] \mathbf{F}^a \mathbf{G}^\dagger \mathbf{G} \mathbf{f}_{1,l} \mathbf{f}_{1,l}^\dagger \mathbf{R}_{xx} \mathbf{F}^{-a} \right) \quad (6.8)$$

Here $\text{diag}(\mathbf{A})$ returns the vector whose elements are the elements on the main diagonal of \mathbf{A} and $\mathbf{f}_{1,l}$ denotes the l th column of the matrix \mathbf{F}^{-a} as defined before. This equation can be put in a standard linear equation form. The derivation is easy but lengthy so we don't give the details here.

We now consider the multi-channel case. We will assume that the orders are fixed and given by: $a_k = -1 + 2 * k/M$ $k = 1, \dots, M$. The problem is then to find the optimal filters for each channel that minimize the error:

$$\sigma_e^2 = E \left[\left\| (\mathbf{G}_d - \mathbf{G} \left(\sum_{k=1}^M \mathbf{F}^{-a_k} \Lambda_k \mathbf{F}^{a_k} \right)) \mathbf{x} - \mathbf{n} \right\|^2 \right] \quad (6.9)$$

Using equation 3.20, the filter coefficients $h_k[l]$ can be shown to satisfy the following linear equation:

$$\text{diag} \left(\hat{\mathbf{F}}^\dagger \mathbf{G}^\dagger \mathbf{G}_d \mathbf{R}_{xx} \hat{\mathbf{F}} \right) = \text{diag} \left(\sum_{k=1}^M \sum_{l=1}^N h_k[l] \hat{\mathbf{F}}^\dagger \mathbf{G}^\dagger \mathbf{G} \mathbf{f}_{k,l} \mathbf{f}_{k,l}^\dagger \mathbf{R}_{xx} \hat{\mathbf{F}} \right) \quad (6.10)$$

where we introduced the $MN \times N$ matrix $\hat{\mathbf{F}}$:

$$\hat{\mathbf{F}} = \left[\mathbf{F}^{-a_1} : \mathbf{F}^{-a_2} : \dots : \mathbf{F}^{-a_M} \right]$$

This equation can also be put in a standard linear equation form which is similar to equation 4.13 and it can be solved using linear algebra techniques discussed there [93].

If there is no information available about the input and noise processes, we may simplify the problem and pose it as a kernel synthesis problem. First, we consider the single-stage case. The problem is to minimize the Frobenious norm between the overall matrices of upper and lower channels in Fig. 6.2:

$$\min \|\mathbf{G}_d - \mathbf{G} \mathbf{F}^{-a} \Lambda \mathbf{F}^a\|_F^2 \quad (6.11)$$

If \mathbf{G}^{-1} exists, then we can rewrite the above equation as:

$$\min \|\mathbf{G}^{-1} \mathbf{G}_d - \mathbf{F}^{-a} \Lambda \mathbf{F}^a\|_F^2 \quad (6.12)$$

since $\|\mathbf{G}_d - \mathbf{G} \mathbf{F}^{-a} \Lambda \mathbf{F}^a\|_F^2 \leq \|\mathbf{G}^{-1} \mathbf{G}_d - \mathbf{F}^{-a} \Lambda \mathbf{F}^a\|_F^2 \|\mathbf{G}\|_F^2$. The problem defined in 6.12 is nothing but the kernel synthesis problem whose solution is discussed in section 4.1.1. We will consider the case where \mathbf{G}^{-1} does not exist, as a special case ($M = 1$) of the solution for multi-channel case which we will discuss next.

In the multi-channel case the problem discussed above take the form:

$$\min \|\mathbf{G}_d - \mathbf{G}(\sum_{k=1}^M \mathbf{F}^{-a_k} \mathbf{\Lambda}_k \mathbf{F}^{a_k})\|^2 \quad (6.13)$$

Given the domains a_k , the above problem can be exactly posed as a least-squares optimization problem leading to an associated set of normal equations which can be solved with other standard techniques, just like in section 4.1.1. In fact, we can solve the problem by slightly modifying the method discussed there. We can rewrite the equation 6.13, by plugging the form of \mathbf{T}_{mc} in equation 3.27,

$$\begin{aligned} \min \|\mathbf{G}_d - \mathbf{G}(\sum_{k=1}^M \sum_{j=1}^N h_k[j] \hat{\mathbf{T}}_{kj})\|_F^2 \\ \min \|\mathbf{G}_d - \sum_{k=1}^M \sum_{j=1}^N h_k[j] \mathbf{G} \hat{\mathbf{T}}_{kj}\|_F^2 \\ \min \|\mathbf{G}_d - \sum_{k=1}^M \sum_{j=1}^N h_k[j] \hat{\mathbf{T}}'_{kj}\|_F^2 \end{aligned} \quad (6.14)$$

where we have defined the matrix $\hat{\mathbf{T}}'_{kj} = \mathbf{G} \hat{\mathbf{T}}_{kj}$. Now we can follow the steps given in section 4.1.1 by just replacing the matrix $\hat{\mathbf{T}}_{kj}$ with $\hat{\mathbf{T}}'_{kj}$. The filter coefficients may be found by solving the following equation:

$$\hat{\mathbf{T}}'^{\dagger} \underline{\mathbf{G}}_d = \hat{\mathbf{T}}'^{\dagger} \hat{\mathbf{T}}' \underline{\mathbf{h}}, \quad (6.15)$$

where $\hat{\mathbf{T}}' = [\hat{\mathbf{T}}'_1 \hat{\mathbf{T}}'_2 \dots \hat{\mathbf{T}}'_{MN}]$ and underline denotes the column vectors obtained from the corresponding matrices by column ordering like in section 4.1.2.

Post compensation filter:

In this part, we consider the configuration in Fig. 6.3. Following the same order in pre-filter discussion, we first assume that we know the correlation functions of input and noise. We also assume that the systems \mathbf{G} and \mathbf{G}_{rmd} are known. We want to obtain the post-compensation filter \mathbf{H} in the form of fractional Fourier domain filter configurations (\mathbf{T}_{ss} , \mathbf{T}_{ms} , or \mathbf{T}_{mc}). We will employ both of the approaches (i) and (ii).

To apply approach (i), we should first find the general linear post estimator \mathbf{H} . Then we can synthesize it in the form of \mathbf{T}_{ss} , \mathbf{T}_{ms} , or \mathbf{T}_{mc} as discussed in section 4.1.1. The problem can be stated as

$$\min E [\|\mathbf{G}_d \mathbf{x} - \mathbf{H}(\mathbf{G} \mathbf{x} + \mathbf{n})\|^2] \equiv \min E [\|(\mathbf{G}_d - \mathbf{H} \mathbf{G}) \mathbf{x} - \mathbf{H} \mathbf{n}\|^2] \quad (6.16)$$

It can be shown that the optimal general recovery operator \mathbf{H} is the solution of the following equation:

$$\mathbf{G}_d \mathbf{R}_{xg} = \mathbf{H} \mathbf{R}_{gg} \quad (6.17)$$

where we used the correlation functions of the observed signal $\mathbf{g} = \mathbf{G}\mathbf{x} + \mathbf{n}$ which can be obtained by $\mathbf{R}_{xg} = \mathbf{R}_{xx} \mathbf{G}^\dagger$ and $\mathbf{R}_{gg} = \mathbf{G} \mathbf{R}_{xx} \mathbf{G}^\dagger + \mathbf{R}_{nn}$. After finding the optimal general linear filter \mathbf{H} , we can apply the kernel synthesis algorithm of section 4.1.1.

In order to apply approach (ii) to the above problem, we directly plug the form of the filter \mathbf{H} in the formulation of the problem and solve for the filter coefficients and possibly for the orders. In the single-stage case, the problem is to find the optimal order a and filter coefficients that minimize the error:

$$\sigma_e^2 = E \left[\left\| (\mathbf{G}_d - \mathbf{F}^{-a} \mathbf{\Lambda} \mathbf{F}^a \mathbf{G}) \mathbf{x} - \mathbf{F}^{-a} \mathbf{\Lambda} \mathbf{F}^a \mathbf{n} \right\|^2 \right] \quad (6.18)$$

The optimal filter that minimizes the above error is the solution of the following equation,

$$\text{diag} \left(\mathbf{F}^a \mathbf{G}_d \mathbf{R}_{xg} \mathbf{F}^{-a} \right) = \text{diag} \left(\mathbf{\Lambda} \mathbf{F}^a \mathbf{R}_{gg} \mathbf{F}^{-a} \right) \quad (6.19)$$

The filter coefficients are given by,

$$h[j] = \frac{(\mathbf{F}^a \mathbf{G}_d \mathbf{R}_{xg} \mathbf{F}^{-a})(j, j)}{(\mathbf{F}^a \mathbf{R}_{gg} \mathbf{F}^{-a})(j, j)}. \quad (6.20)$$

We now consider the multi-channel case. We again assume that the orders are fixed and given by: $a_k = -1 + 2k/M$ $k = 1, \dots, M$. The problem is then to find the optimal filters for each channel that minimize the error:

$$\sigma_e^2 = E \left[\left\| (\mathbf{G}_d - (\sum_{k=1}^M \mathbf{F}^{-a_k} \mathbf{\Lambda}_k \mathbf{F}^{a_k}) \mathbf{G}) \mathbf{x} - (\sum_{k=1}^M \mathbf{F}^{-a_k} \mathbf{\Lambda}_k \mathbf{F}^{a_k}) \mathbf{n} \right\|^2 \right] \quad (6.21)$$

Using equation 3.20, the filter coefficients $h_k[l]$ can be shown to satisfy the following linear equation:

$$\text{diag} \left(\hat{\mathbf{F}}^\dagger \mathbf{G}_d \mathbf{R}_{xg} \hat{\mathbf{F}} \right) = \text{diag} \left(\sum_{k=1}^M \sum_{l=1}^N h_k[l] \hat{\mathbf{F}}^\dagger \mathbf{f}_{k,l} \mathbf{f}_{k,l}^\dagger \mathbf{R}_{gg} \hat{\mathbf{F}} \right) \quad (6.22)$$

where $MN \times N$ matrix $\hat{\mathbf{F}}$ is as defined before. This equation can also be put in a standard linear equation form which is similar to equation 4.13 and it can be solved using linear algebra techniques [93].

If there is no information available about the input and noise processes, we may simplify the problem and pose it as a kernel synthesis. First, we consider the single-stage

case. The problem is to minimize the Frobenious norm between the overall matrices of upper and lower channels in Fig. 6.2:

$$\min \|\mathbf{G}_d - \mathbf{F}^{-a} \mathbf{\Lambda} \mathbf{F}^a \mathbf{G}\|_F^2 \quad (6.23)$$

If \mathbf{G}^{-1} exists, then we can rewrite the above equation as:

$$\min \|\mathbf{H}_d \mathbf{G}^{-1} - \mathbf{F}^{-a} \mathbf{\Lambda} \mathbf{F}^a\|_F^2 \quad (6.24)$$

since $\|\mathbf{G}_d - \mathbf{F}^{-a} \mathbf{\Lambda} \mathbf{F}^a \mathbf{G}\|_F^2 \leq \|\mathbf{H}_d \mathbf{G}^{-1} - \mathbf{F}^{-a} \mathbf{\Lambda} \mathbf{F}^a\|_F^2 \|\mathbf{G}\|_F^2$ The problem defined in 6.24 is nothing but the kernel synthesis problem whose solution is discussed in section 4.1.1. When \mathbf{G}^{-1} does not exist, we can again solve the problem. The solution is the special case ($M = 1$) of the solution for multi-channel case.

In the multi-channel case the problem discussed above take the form:

$$\min \|\mathbf{G}_d - \left(\sum_{k=1}^M \mathbf{F}^{-a_k} \mathbf{\Lambda}_k \mathbf{F}^{a_k}\right) \mathbf{G}\|^2 \quad (6.25)$$

Given the domains a_k , the above problem can be exactly posed as a least-squares optimization problem leading to an associated set of normal equations which can be solved with other standard techniques, just like in section 4.1.1. In fact, we can solve the problem by slightly modifying the method discussed there. We can rewrite the equation 6.25, by plugging the form of \mathbf{T}_{mc} in equation 3.27,

$$\begin{aligned} \min \|\mathbf{G}_d - \left(\sum_{k=1}^M \sum_{j=1}^N h_k[j] \hat{\mathbf{T}}_{kj}\right) \mathbf{G}\|_F^2 \\ \min \|\mathbf{G}_d - \sum_{k=1}^M h_k[j] \sum_{j=1}^N \hat{\mathbf{T}}_{kj} \mathbf{G}\|_F^2 \\ \min \|\mathbf{G}_d - \sum_{k=1}^M \sum_{j=1}^N h_k[j] \hat{\mathbf{T}}'_{kj}\|_F^2 \end{aligned} \quad (6.26)$$

where we have defined the matrix $\hat{\mathbf{T}}'_{kj} = \hat{\mathbf{T}}_{kj} \mathbf{G}$. Now we can follow the steps given in section 4.1.1 by just replacing the matrix $\hat{\mathbf{T}}_{kj}$ with $\hat{\mathbf{T}}'_{kj}$. The filter coefficients may be found by solving the following equation:

$$\hat{\mathbf{T}}'^{\dagger} \mathbf{G}_d = \hat{\mathbf{T}}'^{\dagger} \hat{\mathbf{T}}' \mathbf{h}, \quad (6.27)$$

where $\hat{\mathbf{T}}' = [\hat{\mathbf{T}}'_1 \hat{\mathbf{T}}'_2 \dots \hat{\mathbf{T}}'_{MN}]$ and \mathbf{h} denotes the column vectors obtained from the corresponding matrices by column ordering like in section 4.1.2.

We haven't considered the multi-stage case for all of the applications discussed above. The filter coefficients and orders cannot be found analytically for this case. However, as discussed before an iterative algorithm may be employed [13, 14, 15]. Also matching pursuit algorithm may be modified so that it can be used for multi-stage case as well. This topic requires further research.

6.2 Examples

In this section we present illustrative examples of the applications of the filtering configurations. In our first example, we consider restoration of images blurred by a space-variant point spread function characterized by \mathbf{G} . The point spread function is local and Gaussian in shape and its width changes slightly with position. We first consider post-filter case with no information about signal. In this case, the problem is to find the optimal recovery operator which is in the form of \mathbf{T}_{ss} , \mathbf{T}_{ms} , or \mathbf{T}_{mc} that minimizes the error:

$$\sigma_v^2 = \|\mathbf{HG} - \mathbf{I}\|_F^2$$

where $\mathbf{H} \in (\mathbf{T}_{ss}, \mathbf{T}_{ms}, \mathbf{T}_{mc})$. If we use single-stage filter ($\mathbf{H} = \mathbf{T}_{ss}$), the normalized error is 0.42. In the multi-stage case, the resulting error is 0.24 with $M = 3$ filters and 0.1 with 4 filters and 0.03 with 6 filters whereas for the multi-channel case it is 0.23, 0.12, 0.04 with 3, 4 and 6 filters respectively. ($a_k = k/M \quad k = 1, 2, \dots, M$) If we consider the pre-filter configuration the results changes slightly. The error would be 0.40, 0.04, and 0.04 for the single-stage, multi-stage ($M = 6$) and multi-channel ($M = 6$) filtering configurations respectively.

If we know the correlation of the input images, we can pose the problem as a statistical optimization problem discussed in section 6.1. We first consider the pre-filter case. The problem can be stated as:

$$\min E [\|\mathbf{x} - \mathbf{GHx}\|^2] \quad (6.28)$$

where \mathbf{H} is in the form of \mathbf{T}_{ss} , \mathbf{T}_{ms} , or \mathbf{T}_{mc} . For the single stage case the normalized error is 0.22. The multi-stage case results in error of 0.12, 0.06, 0.03 for $M = 3$, $M = 5$ and $M = 7$ filters respectively. The resulting error would be 0.11, 0.07, 0.03 for the multi-channel case with $M = 3$, $M = 5$ and $M = 7$ filters. Figure 6.4 shows the original, degraded and restored images.

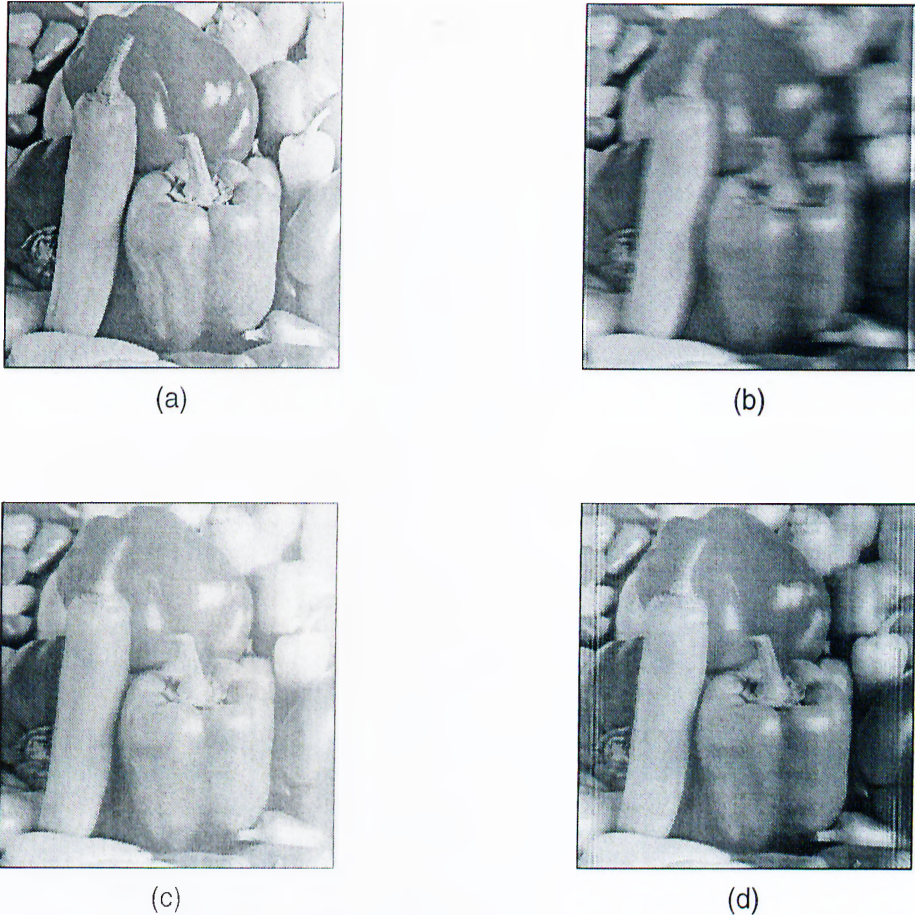


Figure 6.4: Original image (a). Blurred image (b). Restored by repeated filtering ($M = 5$) (c). Restored by multi-channel filtering ($M = 5$) (d).

We next consider the filter configuration of Fig. 6.3. In this case the aim is to minimize the error:

$$\min E [\|\mathbf{x} - \mathbf{H}\mathbf{G}\mathbf{x}\|^2] \quad (6.29)$$

where \mathbf{H} is again in the form of \mathbf{T}_{ss} , \mathbf{T}_{ms} , or \mathbf{T}_{mc} . The error in this case is 0.21, 0.03, and 0.05 for the single-stage, multi-stage ($M = 5$) and multi-channel ($M = 5$) filtering configurations respectively (Figure 6.5). To illustrate the cost performance trade-off consider the Fig. 6.6 where we have plotted the number of filters vs error plot for multi-stage (repeated) and multi-channel configurations.

The above error figures represent significant improvements with respect to single-stage ($M = 1$) filtering. Ordinary Fourier domain filtering gives very poor results. Although the errors obtained in both multi-stage and multi-channel configurations are

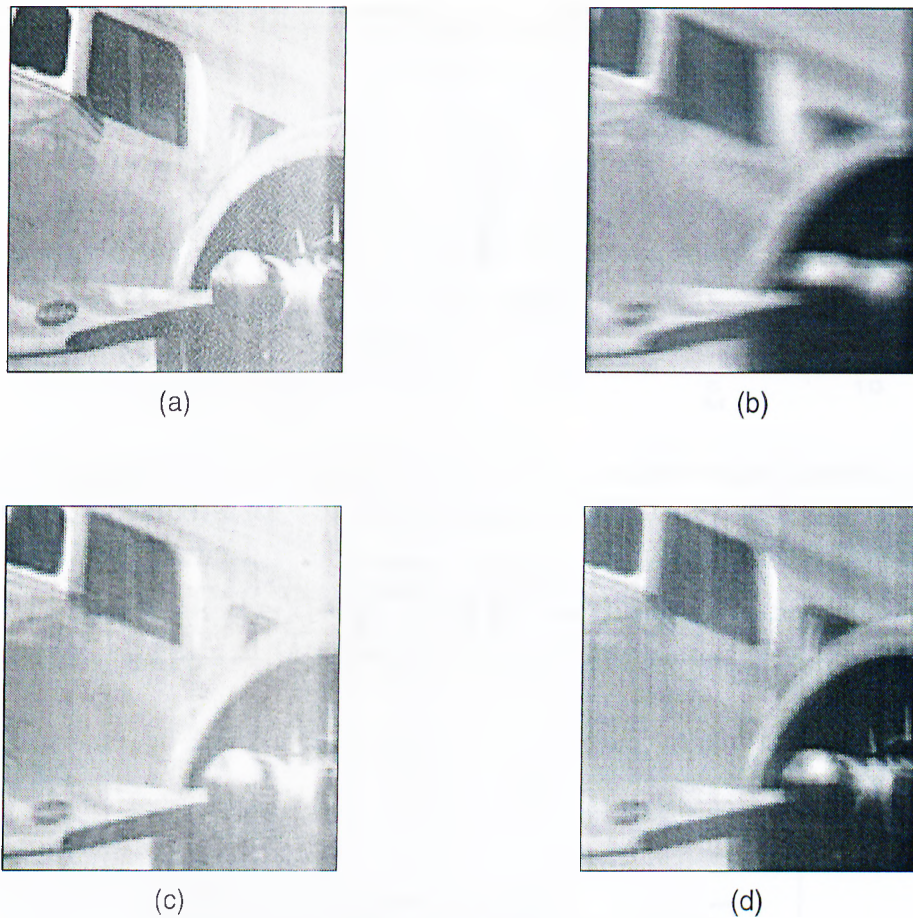


Figure 6.5: Original image (a). Blurred image (b). Restored by repeated filtering ($M = 5$) (c). Restored by multi-channel filtering ($M = 5$) (d).

close in this example, this is not always so. Often one or the other is clearly superior. Furthermore, repeated may be better for certain values of M and multi-channel for the other values of M .

We also investigate the use of fractional Fourier domain filtering circuit concept in the above image restoration example with the post-filtering configuration. We consider the filtering circuit shown in Fig. 6.7 which consists of two branches each with two repeated filters. The fractional domains are chosen as $a_1 = 0.25$, $a_2 = 0.5$ for the upper branch and $a_3 = 0.75$, $a_4 = 1$ for the lower branch. The overall operator representing this circuit is given by,

$$\mathbf{T}_{fc} = \sum_{k=1}^2 \mathbf{F}^{-a_{2k}} \mathbf{\Lambda}_{2k} \mathbf{F}^{a_{2k} - a_{2k-1}} \mathbf{\Lambda}_{2k-1} \mathbf{F}^{a_{2k-1}} \quad (6.30)$$

where $\mathbf{\Lambda}_l$ is a diagonal matrix whose diagonal consists of the filter vector \mathbf{h}_l as before. In

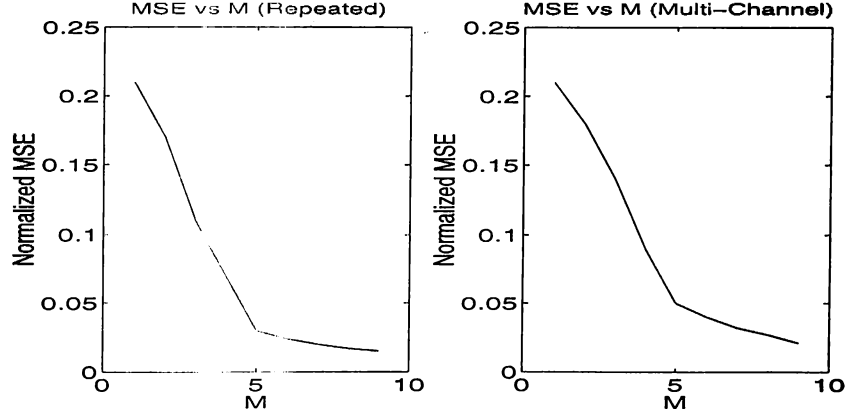


Figure 6.6: Normalized error in signal restoration example versus number of filters for (a) multi-stage (repeated) case, (b) multi-channel case.

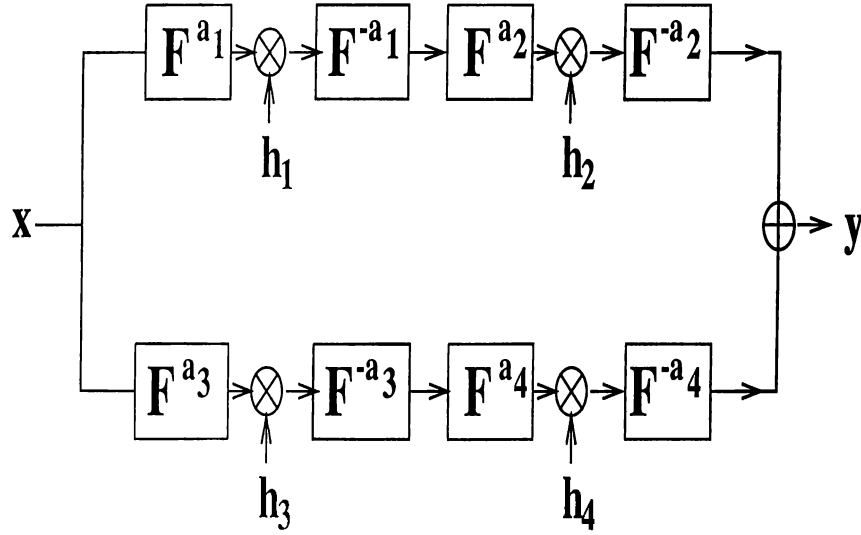


Figure 6.7: The structure of the filtering circuit used in the image restoration problem with post-filtering configuration.

order to solve for the optimal filter functions we modify the iterative algorithm suggested in [13] so that we first initialize the filters \mathbf{h}_1 and \mathbf{h}_3 to vectors consisting of 1s and then solve for the optimal filter vector \mathbf{h}_2 and \mathbf{h}_4 using an algorithm very similar to the one discussed in section 4.1.2. For instance, we replace the \mathbf{W}_k s in equation 4.21 with the initialized single-stage fractional Fourier domain filters: $\mathbf{W}_1 = \mathbf{F}^{-a_1} \mathbf{\Lambda}_1 \mathbf{F}^{a_1}$ and $\mathbf{W}_2 = \mathbf{F}^{-a_3} \mathbf{\Lambda}_3 \mathbf{F}^{a_3}$. With this replacement, equation 6.30 becomes identical to equation 4.21, and can be solved analytically as described there. We then take the solutions for \mathbf{h}_2 and \mathbf{h}_4 as constants and solve for the optimal filter vectors \mathbf{h}_1 and \mathbf{h}_3

again by using a similar approach. We continue to apply this procedure iteratively until the error does not change significantly as compared to the previous step. The normalized error turns out to be 0.02. This figure is slightly better than the figures obtained by the multi-stage and the multi-channel filtering configurations with 5 filters. We should here note that this need not always be the case. In some of the simulations we have tried we obtained less satisfactory results by using a filtering circuit with a total of M filters as compared to the multi-channel and the multi-stage configurations with same number of filters. In those simulations, we see that the results highly depend on the the choice of the filtering circuit structure.

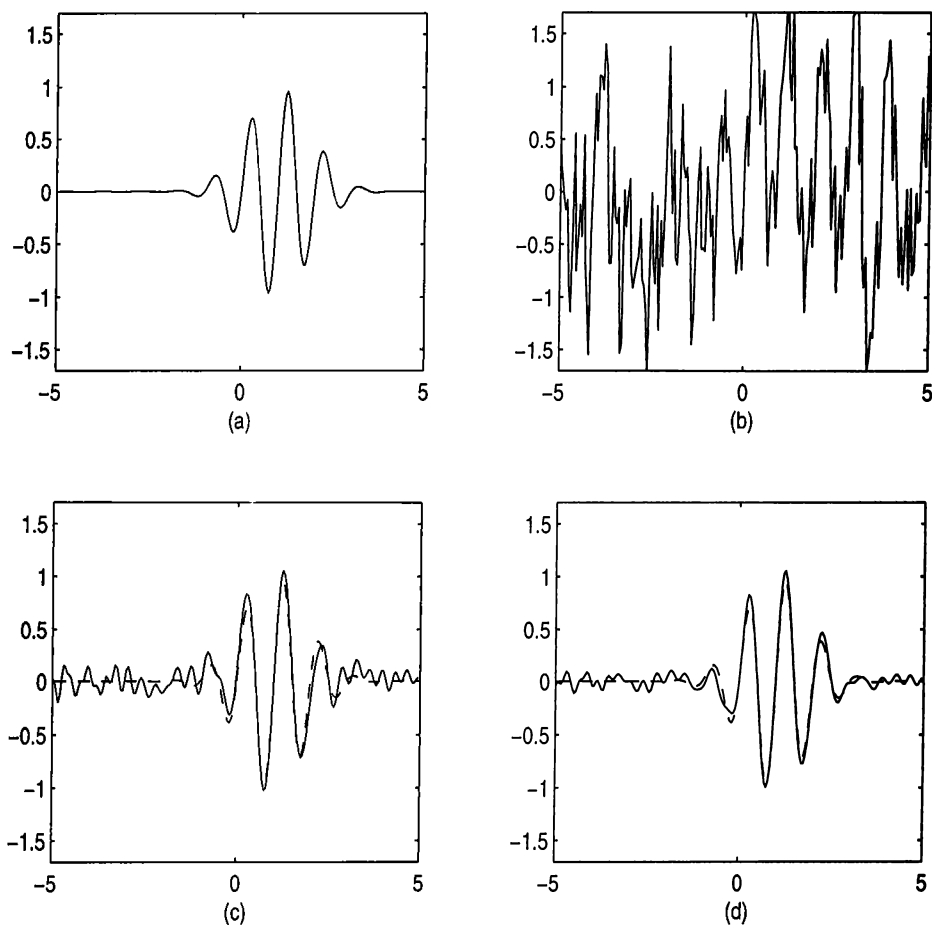


Figure 6.8: Original signal (modulated sinusoid) (a). Degraded signal (b). Restored signal by multi-stage with $M = 3$ filters (solid) and original (dashed) (c) and by multi-channel with $M = 3$ filters (d).

We next consider the problem of recovering a signal corrupted with several additive

chirp distortions with post-filter configuration (Fig. 6.8). We assume that the second-order statistics of the signal and chirp distortions are given. In our example, we assume that the Q chirps have uniformly distributed random amplitudes and time shifts, and their chirp rates are clustered around P (initially unknown) values. For $Q = 9$, $P = 3$ the multi-stage configuration with $M = 3$ (approach (i)) results in a mean-square error 2% and multi-channel configuration with $M = 3$ results in an error $< 1\%$.

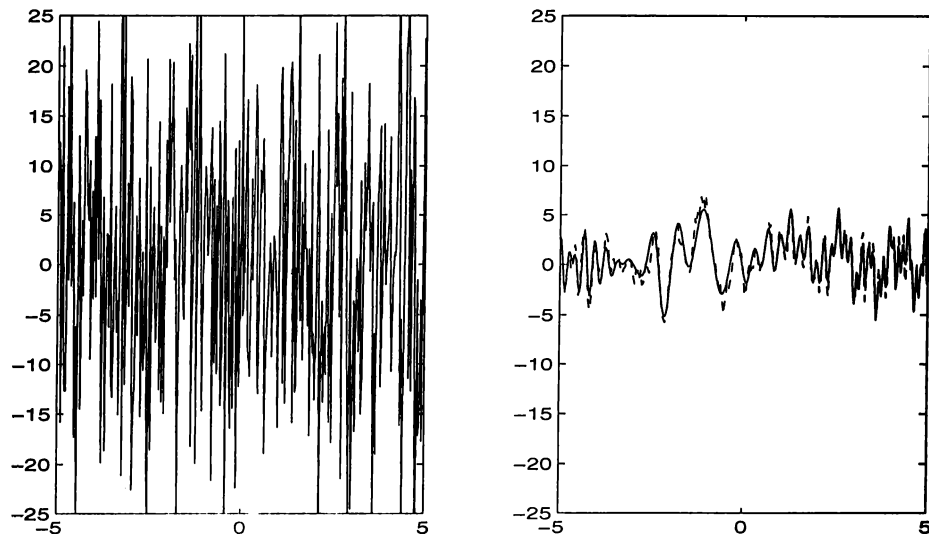


Figure 6.9: Degraded signal (a). Restored signal by multi-channel with $M = 6$ filters (solid) and original (dashed) (b).

We next consider the problem of recovering a signal consisting of multiple chirp-like components buried in white Gaussian noise with a signal-to-noise ratio = 0.1 (Fig. 6.9). We assume that the signal consists of 6 chirps with uniformly distributed random amplitudes and time shifts, and that the chirp rates are known with a $\pm 5\%$ accuracy. With approach (i), the multi-channel configuration results in a mean-square error of 5.2% with $M = 6$. With approach (ii), the same number of filters results in an estimation error of 2.6%.

In the final example, we show an application of the windowed fractional Fourier transform. We again consider the problem of recovering a signal buried in white Gaussian noise with a signal-to-noise ratio = 0.1. But this time, the signal is a chirp-like signal whose instantaneous frequency changes paraboloidally in time. Figure 6.10 shows the contour plot of the Wigner distribution of such a signal. We apply the windowed fractional Fourier transform introduced in section 3.6. The windows \mathbf{W}_k are taken to be shifted and overlapping Hanning windows of length 16, and there are 12 channels. We

obtain a normalized mean-square error of 6.8% with the above configuration. We have plotted the degraded and restored signals in Fig. 6.11.

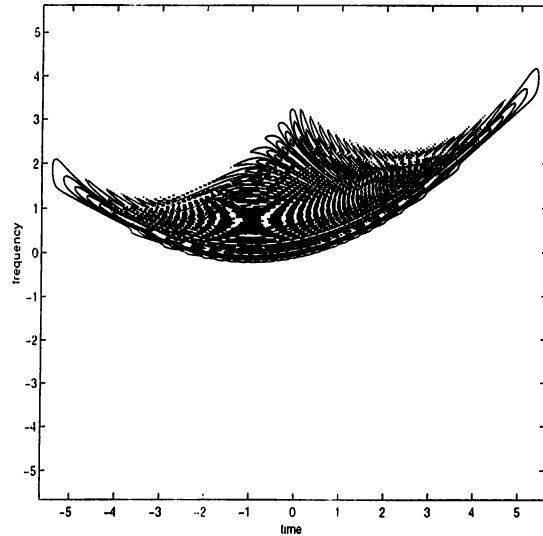


Figure 6.10: Wigner distribution of a signal with quadratic instantaneous frequency

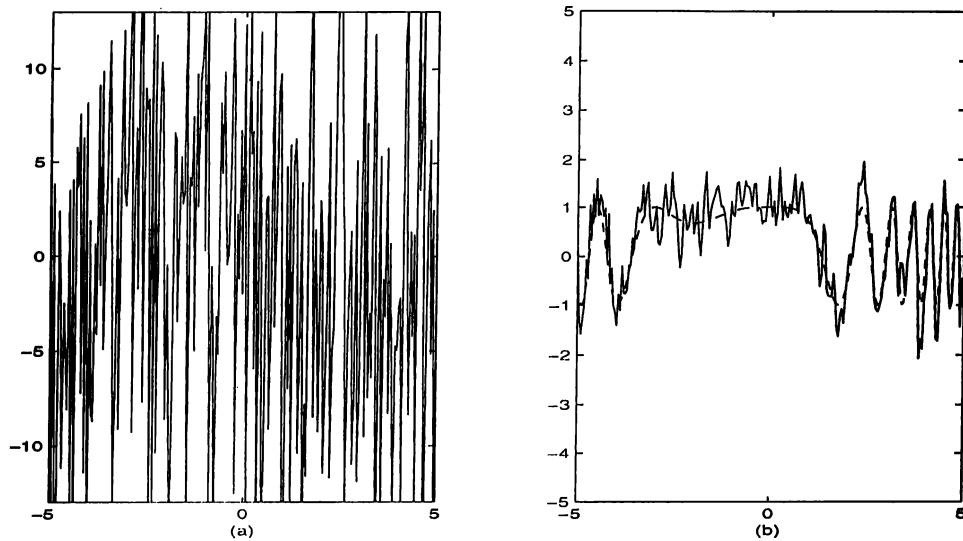


Figure 6.11: Degraded signal (a). Restored signal by the windowed fractional Fourier transform configuration (solid) and the original signal (dashed) (b).

The results obtained in all of the above examples represent significant improvements with respect to single domain filtering but are much cheaper to implement than general linear filtering.

Chapter 7

Conclusions and Future Work

The fractional Fourier transform is the generalization of the ordinary Fourier transform. Given this, every property and application of the common Fourier transform becomes a special case of that of the fractional transform. In every area in which Fourier transforms and frequency domain concepts are used, there exists the potential for generalization and improvement by using the fractional transform. It has many interesting properties that have important relations with well-known optical, physical and signal processing concepts. These properties also lead many interesting applications, some of which we discussed in this work. A comprehensive discussion, which we believe will lead many other applications, may be found in [17, 18].

In this thesis we introduced the concept of generalized filtering configurations (or filtering circuits) in fractional Fourier domains and discussed some of their applications. The single-stage configuration is obtained by generalizing the well-known ordinary Fourier filtering and was discussed before in [6, 8, 10, 12]. multi-stage (repeated) filtering, has been discussed in [13, 14, 15]. Here we introduced the dual configuration, multi-channel filtering, and unified all of the configurations under the concept of filtering circuits and proposed some interesting applications in an unified framework.

The filtering configurations discussed in this work allow a very flexible cost-accuracy trade-off. If we think of the single-stage filtering configuration and general linear systems as representing two extremes, then the multi-channel and multi-stage filtering configurations interpolate between these extremes. If we choose the number of filters M in the configuration to be small, cost and flexibility are both low; $M = 1$ corresponds

to single-stage filtering. If we choose M larger, cost and flexibility are both higher; as M approaches N , the number of degrees of freedom approaches that of a general linear system.

An interesting question is whether we can achieve the same performance offered by a general linear system by using exactly $M = N$ filters, or in other words if $M = N$ filters are necessary and sufficient to implement an arbitrary general linear system matrix exactly. The simulations show that this is most likely true but a rigorous treatment is not available.

We considered three main applications of generalized filtering configurations, namely system synthesis, signal synthesis and signal recovery. In the signal and system synthesis application, we use fractional Fourier domain filters to synthesize a desired signal or system. In the recovery applications we try to recover a degraded or noisy signal by use of fractional Fourier domain filters. In all of the applications we used one of the proposed solution methods (approach (i) or (ii)) to obtain the optimal filter coefficients. In approach (i) we first find the optimal linear system by applying some existing inverse method and then we synthesize that linear system in the form of a fractional Fourier domain filter. On the other hand in approach (ii), we directly constrain the system to be a fractional Fourier domain filter and find the optimal coefficients. In most of the examples we presented, general linear systems were approximated with a relatively small number of filters and thus a considerable amount of cost has been saved. These examples also illustrated the cost-accuracy trade-off offered by these configurations in a systematic manner. These results justify the use of these filtering configurations in optical and digital signal and image processing.

In chapter 5, we considered the problem of synthesizing the desired mutual intensity function from a given optical source. We proposed a semi-definite square-root representation to reduce this quadratic problem to a linear one. However, this representation turns out to be non-unique and we have not fully exploited this in our simulations. Thus, if a way of exploiting the many available choices for the square-root representation can be found, even better results than those presented can be obtained.

The multi-channel configuration possesses analytical solutions in all of the applications we discussed, whereas the multi-stage filtering requires iterative methods. Given the orders, we can find the optimal filter coefficients by solving linear equations. We can find the optimal orders by further optimization procedures. But this latter task is difficult and the determination of an efficient method requires further research. Presently,

we satisfy ourselves by choosing the orders uniformly in the interval $(-1, 1]$. This choice ensures that the linear equations such as given in section 4.1.1 are well-posed.

Another topic of future research is to find efficient algorithms for solving these equations. In image processing and optical applications, the size of the equations become very large and the cost of solving them is too high. Given the fact that degradation matrices in these applications are generally sparse, it may be possible to take advantage of sparse matrix notation together with the structured nature of the fractional Fourier matrices to propose an efficient algorithm for finding the optimal filter coefficients.

A practical solution to the above problem may be to process the images block by block. In this case, we can divide the large input images to blocks, and formulate the problem for that specific block and find the optimal configuration for each block. This method can be justified since degradations are generally assumed to be local. Although this assumption does not guarantee that the estimation filter should also be local, preliminary simulations show that reasonable results can be obtained in certain situations.

We also related the above method to the concept of windowed fractional Fourier transform which was introduced in section 3.6. We gave a simple simulation example in chapter 6 illustrating the potential application areas for this case. This structure may be useful in signal and image processing applications and requires further research.

Bibliography

- [1] H. M. Ozaktas and D. Mendlovic. Multistage optical interconnection architectures with the least possible growth of system size. *Opt. Lett.*, 18:296–298, 1993.
- [2] D. Mendlovic and H. M. Ozaktas. Optical-coordinate transformation methods and optical-interconnection architectures. *Appl. Opt.*, 32:5119–5124, 1993.
- [3] A. V. Oppenheim and R. W. Schaffer. *Digital signal processing*, Prentice-Hall, New Jersey, 1975.
- [4] A. K. Jain. *Fundamentals of Digital Image Processing*, Prentice Hall, New Jersey, 1989.
- [5] A. Vanderlugt. *Optical Signal Processing*, Wiley, New York, 1992.
- [6] H. M. Ozaktas, B. Barshan, D. Mendlovic, and L. Onural. Convolution, filtering, and multiplexing in fractional Fourier domains and their relation to chirp and wavelet transforms. *J. Opt. Soc. Am. A.*, 11:547–559, 1994.
- [7] M. A. Kutay, H. M. Ozaktas, L. Onural, and O. Arikan. Optimal filtering in fractional Fourier Domains. In *Proc. 1995 Int. Conf. Acoustics, Speech, and Signal Processing*, IEEE, Piscataway, New Jersey, 1995, pages 937-940.
- [8] M. A. Kutay, H. M. Ozaktas, O. Arikan, and L. Onural. Optimal Filtering in Fractional Fourier Domains. *IEEE Trans. Sig. Proc.*, 45:1129–1143, 1997.
- [9] M. F. Erden, H. M. Ozaktas, and D. Mendlovic. Synthesis of mutual intensity distributions using the fractional Fourier transform. *Opt. Commun.*, 125:288–301, 1996.
- [10] M. A. Kutay. Optimal filtering in fractional Fourier domains. M.S. Thesis. *Bilkent Univ., Dept. of Electrical and Electronics Eng.*, 1995.

- [11] Z. Zalevsky and D. Mendlovic. Fractional Wiener filter. *Appl. Opt.*, 35:3930–3936, 1996.
- [12] M. A. Kutay and H. M. Ozaktas. Optimal image restoration with the fractional Fourier transform. *J. Opt. Soc. Am. A*, 15:825–834, 1998.
- [13] M. F. Erden. *Repeated Filtering in Consecutive Fractional Fourier Domains*. Ph.D. Thesis, Bilkent Univ., Ankara, 1997.
- [14] M. F. Erden, M. A. Kutay, and H. M. Ozaktas. Repeated filtering in consecutive fractional Fourier domains and its application to signal restoration. To appear in *IEEE Trans. Sig. Proc.*, May 1999.
- [15] M. F. Erden, and H. M. Ozaktas. Synthesis of general linear systems with repeated filtering in consecutive fractional Fourier domains. *J. Opt. Soc. Am. A*, 15:1647–1657, 1998.
- [16] H. M. Ozaktas, M. F. Erden, and M. A. Kutay. Signal Processing with repeated filtering in fractional Fourier domains. *Journal of Optoelectronics Laser* (supplementary). 9:160–163, 1998.
- [17] Haldun M. Ozaktas, M. Alper Kutay and David Mendlovic. *Introduction to the fractional Fourier transform and its applications*. In *Advances in Imaging and Electron Physics*, Peter W. Hawkes, editor, Volume 109, pages 239–291 (chapter X). *Academic Press*, San Diego, California, 1999. Invited.
- [18] Haldun M. Ozaktas, David Mendlovic, M. Alper Kutay and Zeev Zalevsky. *The Fractional Fourier transform and Wigner distribution, with applications in optics and signal processing* (tentative). contract signed with John Wiley & Sons, expected completion in 1999
- [19] H. M. Ozaktas, N. Erkaya, and M. A. Kutay. Effect of fractional Fourier transformation on time-frequency distributions belonging to the Cohen class. *IEEE Signal Processing Lett*, 3:40–41, 1996.
- [20] H. M. Ozaktas, O. Arikan, M. A. Kutay, and G. Bozdagi. Digital computation of the fractional Fourier transform. *IEEE Trans. Signal Processing.*, 44:2141–2150, 1996.
- [21] Ç. Candan. *The discrete fractional Fourier Transformation*. M.S. Thesis, Bilkent Univ., Dept. of Electrical and Electronics Eng., 1998.

- [22] Ç. Candan, M. A. Kutay, and H. M. Ozaktas. The discrete fractional Fourier Transformation. Submitted for publication to *IEEE Trans. on Signal Processing*, September 1998.
- [23] Ç. Candan, M. A. Kutay, and H. M. Ozaktas. The discrete fractional Fourier Transformation. *Proceedings of IEEE International Conf. on Acoustic, Speech and Signal Processing (ICASSP'99)* Phoenix, March 15-18 1999.
- [24] A. Sahin, M. A. Kutay, and H. M. Ozaktas. Non-separable two-dimensional fractional Fourier transform. *Applied Optics*, 23:5444–5453, 1998.
- [25] M. A. Kutay, M. F. Erden, H. M. Ozaktas, O. Arikan, Ö. Güleriyüz, and Ç. Candan. Space-Bandwidth efficient realizations of linear systems. *Opt. Lett.*, 23:1069–1071, 1998.
- [26] M. A. Kutay, M. F. Erden, H. M. Ozaktas, O. Arikan, Ç. Candan, and Ö. Güleriyüz. Cost-Efficient approximation of linear systems with repeated and multi-channel filtering configurations. *Proceedings of IEEE International Conf. on Acoustic, Speech and Signal Processing (ICASSP'98)* , vol. 6, pp. 3433–3436, Seattle, May 12-15 1998.
- [27] M. A. Kutay, M. F. Erden, H. M. Ozaktas, O. Arikan, Ç. Candan, and Ö. Güleriyüz. Space-bandwidth efficient realizations of linear systems. *Proceedings of Optics in Computing - OC'98*, Brugge, June 17-20, 1998.
- [28] M. A. Kutay, H. Özaktas, M. F. Erden, H. M. Ozaktas, and O. Arikan. Solution and Cost Analysis of General Multi-Channel and Multi-Stage Filtering Circuits. *Proceedings of the IEEE Symp. on Time-Frequency and Time-Scale Analysis*, Pittsburgh PA, USA, October 6-9, 1998.
- [29] N. Wiener. Hermitian Polynomials and Fourier Analysis. *Journal of Mathematics Physics MIT*, 18:70-73, 1929.
- [30] E. U. Condon. Immersion of the Fourier transform in a continuous group of functional transformations. *Proc. Natl. Acad. Sci. USA*, 23:158–164, 1937.
- [31] V. Bargmann. On a Hilbert space of analytic functions and an associated integral transform, Part I. *Commun. Pure Appl. Math.* , 14:187–214, 1961.
- [32] N. G. De Bruijn. A theory of generalized functions, with applications to Wigner distribution and Weyl correspondence. *Nieuw Archief voor Wiskunde*, 21:205–280, 1973.

- [33] V. Namias. The fractional order Fourier transform and its application to quantum mechanics. *J. Inst. Maths. Applics.*, 25:241–265, 1980.
- [34] A. C. McBride and F. H. Kerr. On Namias’s fractional Fourier transform. *IMA J. Appl. Math.*, 39:159–175, 1987.
- [35] D.A. Mustard. Lie group imbeddings of the Fourier transform. *School of Mathematics Preprint AM87/13*, The University of New South Wales, Kensington, Australia, 1987.
- [36] D. A. Mustard. Uncertainty principles invariant under the fractional Fourier transform. *J. Australian Mathematical Society B*, 33:180–191, 1991.
- [37] H. M. Ozaktas and D. Mendlovic. Fourier transforms of fractional order and their optical interpretation. *Opt. Commun.*, 101:163–169, 1993.
- [38] D. Mendlovic and H. M. Ozaktas. Fractional Fourier transforms and their optical implementation, I. *J. Opt. Soc. Am. A.*, 10:1875–1881, 1993.
- [39] H. M. Ozaktas and D. Mendlovic. Fractional Fourier transforms and their optical implementation, II. *J. Opt. Soc. Am. A.*, 10:2522–2531, 1993.
- [40] A. W. Lohmann. Image rotation, Wigner rotation, and the fractional order Fourier transform. *J. Opt. Soc. Am. A.*, 10:2181–2186, 1993.
- [41] T. Alieva, V. Lopez, F. Agullo-Lopez, and L. B. Almeida. The fractional Fourier transform in optical propagation problems. *J. Mod. Opt.*, 41:1037–1044, 1994.
- [42] L. B. Almeida. The fractional Fourier transform and time-frequency representations. *IEEE Trans. Signal Processing*, 42:3084–3091, 1994.
- [43] K. B. Wolf. Construction and properties of canonical transforms. In *Integral Transforms in Science and Engineering*, Plenum Press, New York, 1979, chapter 9.
- [44] P. Pellat-Finet. Fresnel diffraction and the fractional-order Fourier transform. *Opt. Lett.*, 19:1388–1390, 1994.
- [45] H. M. Ozaktas and D. Mendlovic. Fractional Fourier optics. *J. Opt. Soc. Am. A.*, 12:743–751, 1995.

- [46] S. Abe and J. T. Sheridan. Optical operations on wave functions as the Abelian subgroups of the special affine Fourier transformation. *Opt. Lett.*, 19:1801–1803, 1994.
- [47] H. M. Ozaktas and M. F. Erden. Relationships among ray optical, Gaussian beam, and fractional Fourier transform descriptions of first-order optical systems. *Opt. Commun.* 143:75-86, 1997.
- [48] H. M. Ozaktas and D. Mendlovic. Fractional Fourier transform as a tool for analyzing beam propagation and spherical mirror resonators. *Opt. Lett.*, 19:1678–1680, 1994.
- [49] M. F. Erden and H. M. Ozaktas. Accumulated Gouy phase shift in Gaussian beam propagation through first-order optical systems. *J. Opt. Soc. Am. A.*, 14:2190–2194, 1997.
- [50] D. Mendlovic, H. M. Ozaktas, and A. W. Lohmann. Graded-index fibers, Wigner-distribution functions, and the fractional Fourier transform. *Appl. Opt.*, 33:6188–6193, 1994.
- [51] T. Alieva, and F. Agulló-López. Reconstruction of the optical correlation function in a quadratic refractive index medium. *Opt. Commun.*, 114:161–169, 1995.
- [52] S. Abe, and J. T. Sheridan. Comment on ‘The fractional Fourier transform in optical propagation problems.’ *J. Modern Optics*, 42:2373–2378, 1995.
- [53] L. M. Bernardo and O. D. D. Soares. Fractional Fourier transforms and imaging. *J. Opt. Soc. Am. A.*, 11:2622–2626, 1994.
- [54] L. M. Bernardo and O. D. D. Soares. Fractional Fourier transforms and optical systems. *Opt. Commun.*, 110:517–522, 1994.
- [55] P. Pellat-Finet and G. Bonnet. Fractional order Fourier transform and Fourier optics. *Opt. Commun.*, 111:141–154, 1994.
- [56] H. M. Ozaktas and D. Mendlovic. Every Fourier optical system is equivalent to consecutive fractional Fourier domain filtering. *J. Opt. Soc. Am. A.*, 35:3167–3170, 1996.

- [57] M. F. Erden, H. M. Ozaktas, and D. Mendlovic. Propagation of mutual intensity expressed in terms of the fractional Fourier transform. *J. Opt. Soc. Am. A.*, 13:1068–1071, 1996.
- [58] F. M. Erden, H. M. Ozaktas, and D. Mendlovic. Synthesis of mutual intensity distributions using the fractional Fourier transform. *Opt. Commun.*, 125:288–301, 1996.
- [59] R. G. Dorsch, and A. W. Lohmann. Fractional Fourier transform used for a lens design problem. *Applied Optics*, 34:4111–4112, 1995.
- [60] A. W. Lohmann. A fake zoom lens for fractional Fourier experiments. *Opt. Commun.*, 115:437–443, 1995.
- [61] B. Yurke, W. Schleich, and D. F. Walls. Quantum superpositions generated by quantum nondemolition measurements. *Phys. Rev. A.*, 42:1703–1711, 1990.
- [62] O. Aytur and H. M. Ozaktas. Non-orthogonal domains in phase space of quantum optics and their relation to fractional Fourier transforms. *Opt. Commun.*, 120:166–170, 1995.
- [63] M. G. Raymer, M. Beck, and D. F. Allister. Complex wave-field reconstruction using phase-space tomography. *Phys. Rev. Lett.*, 72:1137–1140, 1994.
- [64] D. T. Smithey, M. Beck, M. G. Raymer, and A., Faridani. Measurement of the Wigner distribution and the density matrix of a light mode using optical homodyne tomography: application to squeezed states and the vacuum. *Phys. Rev. Lett.*, 70:1244–1247, 1993.
- [65] A. W. Lohmann and B. H. Soffer. Relationships between the Radon-Wigner and fractional Fourier transforms. *J. Opt. Soc. Am. A.*, 11:1798–1801, 1994.
- [66] J. C. Wood and D. T. Barry. Linear signal synthesis using the Radon-Wigner transform. *IEEE Trans. Signal Processing*, 42:2105–2111, 1994.
- [67] D. Mendlovic, H. M. Ozaktas, and A. W. Lohmann. Fractional correlation. *Appl. Opt.*, 34:303–309, 1995.
- [68] A. W. Lohmann, D. Mendlovic, Z. Zalevsky, and R. G. Dorsch. Some important fractional transformations for signal processing. *Opt. Commun.*, 125:18–20, 1996.

- [69] Y. Bitran, Z. Zalevsky, A. W. Lohmann, and R. G. Dorsch. Fractional correlation operation: performance analysis. *Appl. Opt.*, 35:297–303, 1996.
- [70] D. Mendlovic, Z. Zalevsky, and H. M. Ozaktas. *The applications of the fractional Fourier transform to optical pattern recognition*. In F. T. S. Yu and S. Jutamulia editors, *Optical Pattern Recognition*, pages 89–125 (ch. 4), Cambridge University Press, Cambridge, 1998.
- [71] R. G. Dorsh, A. W. Lohmann, Y. Bitran, D. Mendlovic, and H. M. Ozaktas. Chirp filtering in the fractional Fourier domain. *Appl. Opt.*, 33:7599–7602, 1994.
- [72] S. Granieri, O. Trabocchi, and E. E. Sicre. Fractional Fourier transform applied to spatial filtering in the Fresnel domain. *Opt. Commun.*, 119:275–278, 1995.
- [73] D. Mendlovic, Z. Zalevsky, A. W. Lohmann, and R. G. Dorsch. Signal spatial-filtering using the localized fractional Fourier transform. *Opt. Commun.*, 126:14–18, 1996.
- [74] H. M. Ozaktas. Repeated fractional Fourier domain filtering is equivalent to repeated time and frequency domain filtering. *Signal Processing*, 54:81–84, 1996.
- [75] A. W. Lohmann, Z. Zalevsky, and D. Mendlovic. Synthesis of pattern recognition filters for fractional Fourier processing. *Opt. Commun.*, 128:199–204, 1996.
- [76] J. R. Fonollosa and C. L. Nikias. A new positive time-frequency distribution. In *Proc. 1994 Int. Conf. Acoustics, Speech, and Signal Processing*, IEEE, Piscataway, New Jersey, IV-301–IV-304.
- [77] W. F. G. Mecklenbrauker. *The Wigner Distribution: Theory and Applications in Signal Processing*. W. F. G. Mecklenbrauker, editor. Elsevier, Amsterdam, 1993.
- [78] F. Hlawatsch and G. F. Boudreaux-Bartels. Linear and Quadratic Time-Frequency Signal Representations. *IEEE Signal Proc. Magazine*, 21–67, April 1992.
- [79] H. O. Bartelt, K. H. Brenner and A. W. Lohmann. The Wigner Distribution Function and Its Optical Production. *Opt. Commun.*, 32:32–38, 1980.
- [80] L. Cohen. *Time-Frequency Analysis*. Prentice-Hall, Englewood Cliffs, New Jersey, 1995.

- [81] D. A. Mustard. The fractional Fourier transform and the Wigner distribution. School of Mathematics Preprint AM89/6, The University of New South Wales, Kensington, Australia, 1989.
- [82] H. M. Ozaktas. and O. Aytür. Fractional Fourier domains. *Signal Processing*, 46:119–124, 1995.
- [83] M. F. Erden, H. M. Ozaktas, A. Sahin and D. Mendlovic. Design of dynamically adjustable anamorphic fractional Fourier transformer. To appear in *Optics Commun.*
- [84] D. Mendlovic, Y. Bitran, C. Ferreira, J. Garcia, and H. M. Ozaktas. Anamorphic fractional Fourier transforming - optical implementation and applications. *Appl. Opt.*, 34:7451–7456, 1995.
- [85] A. Sahin, H. M. Ozaktas, and D. Mendlovic. Optical implementation of the two-dimensional fractional Fourier transform with different orders in the two dimensions. *Opt. Commun.*, 120:134–138, 1995.
- [86] A. Sahin. Two-dimensional fractional Fourier transform and its optical implementation. M.S. Thesis. *Bilkent Univ., Dept. of Electrical and Electronics Eng.*, 1996.
- [87] J. G. Nagy, V. P. Pauca. R. J. Plemmons, and T. C. Torgersen. Space-varying restoration of optical images. . *Opt. Soc. Am. A.*, 14:3162–3174, 1997.
- [88] B. Barshan, M. A. Kutay, and H. M. Ozaktas. Optimal filtering with linear canonical transforms. *Opt. Commun.*, 135:32–36, 1997.
- [89] M. A. Kutay, H. Özaktas, H. M. Ozaktas, and O. Arıkan. The fractional Fourier domain decomposition (FFDD). In preparaion for submission to *J. Opt. Soc. Am. A.*
- [90] D. Mendlovic, Z. Zalevsky, N. Konforti, R. G. Dorsch, and A. W. Lohmann. Incoherent fractional Fourier transform and its optical implementation. *Appl. Opt.*, 34:7615–7620, 1995.
- [91] M. J. Bastiaans. Wigner distribution function and its application to first-order optics. *J. Opt. Soc. Am. A.*, 69:1710–1716, 1979.
- [92] M. Nazarathy and J. Shamir. First-order optics—a canonical operator representation: lossless systems. *J. Opt. Soc. Am. A.*, 72:356–364, 1982.

- [93] G. Strang. *Linear algebra and its applications*, Harcourt Brace Jovanovich, San Diego, 1988.
- [94] L. L. Scharf. *Statistical Signal Processing*, Addison Wesley. New York, 1991.
- [95] B. E. A. Saleh and M. C. Teich. *Fundamentals of Photonics*, Wiley, New York, 1991.
- [96] J. W. Goodman. *Statistical Optics*, Wiley, New York, 1985.
- [97] J. W. Goodman. *Introduction to Fourier optics*, McGraw-Hill, New York, 1996.
- [98] T. Habashy, A. T. Friberg, and E. Wolf. Application of the coherent-mode representation to a class of inverse source problems. *Inverse Problems*, 13:47–61, 1997.
- [99] B. Zhang and B. Lu. Transformation of Gaussian schell-model beams and their coherent-mode representation. *Journal of Optics*, 27:99–103, 1996.
- [100] R. N. Bracewell, K. Y. Champ, A. K. Jha and Y. H. Wang. Affine theorem for two dimensional Fourier transform. *Electronics Lett.*, 29:304, 1993.
- [101] Z. Zalevsky and D. Mendlovic. Gerchberg-Saxton algorithm applied in the fractional Fourier or the Fresnel domain. *Opt. Lett.*, 21:842–844, 1996.
- [102] G. H. Golub and C. H. Van Loan. *Matrix Computations*, The Johns Hopkins University Press. Baltimore, 1991.
- [103] J. W. Goodman, A. R. Dias, and L. M. Woody. Fully parallel, high-speed incoherent optical method for performing discrete Fourier transforms. *Opt. Lett.*, 2:1–3, 1978.
- [104] S. K. Case, P. R. Haugen, and O. J. Løberge. Multifacet holographic optical elements for wave front transformations. *Appl. Opt.*, 20:2670–2675, 1981.

Vita

M. Alper Kutay was born in Konya, Turkey on January 25, 1972. He received both his B.S. and M.S. degrees from the Department of Electrical and Electronics Engineering at Bilkent University, Ankara, Turkey, in 1993 and 1995, respectively. He then pursued the Ph.D. in the same department. His research interests include signal restoration, reconstruction and enhancement, time-frequency analysis, optical information processing, and the fractional Fourier transform.